Development of a high temperature and high power PCM storage for standby operation

A thesis accepted by the Faculty of Energy-, Process- and Bio-Engineering

of the University of Stuttgart to fulfill the requirements for the degree of

Doctor of Engineering Sciences (Dr.-Ing.)

by

Maike Johnson

born in Nashville, TN, USA

Main examiner: Prof. Dr. André Thess

Co-examiner: Prof. Dr. Markus Eck

Chairperson: Prof. Dr. Günter Scheffknecht

Date of oral exam: December 19, 2023

Institute for Building Energetics, Thermotechnology and Energy Storage (IGTE)

at the University of Stuttgart

2024

Declaration

I hereby certify that this dissertation is entirely my own work except where otherwise indicated. Passages and ideas from other sources have been clearly indicated.

Stuttgart, _____   _____

Maike Johnson

Acknowledgments

Table of contents

Abstract

Thermal energy storages integrated in industrial processes allow for higher degrees of energy flexibility and reduction of fossil fuel use. The combination of latent heat thermal energy storage systems with water/steam processes can lead to optimized thermal gradients and therefore good system efficiencies. Storage units and systems have been proven at pilot scale. The integration in industrial processes remains a challenge, due to the size of the systems as well as the hurdles in design, permitting and build.

This thesis encompasses the parametrization, design, build, integration and initial operation of a megawatt-scale latent heat thermal energy storage unit, producing superheated steam for an operating cogeneration plant and industrial process customers. The storage unit can produce superheated steam at more than 300 °C and 25 bar at a mass flow rate of 8 t/h for at least 15 minutes. The data of the dispatchable production of superheated steam for more than 20 minutes show the thermal power and capacity at 5.5 MW and 1.9 MWh.

In order to develop this storage system and show the feasibility of the novel aspects of producing superheated steam in once-through operation, providing megawatt-scale thermal power and capacity, and integrating it into an operating system, various steps are involved. These steps are a combination of upscaling the thermal power and capacity, designing for a feasible build and for given system requirements, and system integration development. The upscaling in thermal power results in the development of a very dense fin structure and tight tube-spacing. The upscaling in capacity requires the development of a design model with capabilities for analysis of thermal losses and possible non-ideal flow through the headers, as well as more banal aspects such as transportability and weight considerations as well as physical filling capability with the pelleted salt during commissioning, and accessibility for permitting bodies. System integration in an operating system considers charging and discharging with the available components and maximization of benefits to the plant. This integration, requiring not just a design and optimization of the storage technology itself but of the whole system, is a novel point of view for the development of latent heat storage systems. It is not critical that the storage itself provide all of the parameters, but that the system integration makes this feasible.

x

Kurzfassung

Die Integration von thermischen Energiespeichern in Industrieprozesse trägt wesentlich zur Flexibilisierung des Energiesystems sowie zur Reduktion des Einsatzes fossiler Brennstoffe bei. Die Kombination von Latentwärmespeichern mit Wasser-/Dampfprozessen kann zur Optimierung von Temperaturgradienten und damit zu hohen Systemwirkungsgraden beitragen. Im Pilotmaßstab haben sich Speichereinheiten und -systeme bereits bewährt, die Integration in Industrieprozesse bleibt jedoch aufgrund der Größe der Systeme sowie der Hürden bei Entwurf, Genehmigung und Bau eine Herausforderung.

Diese Arbeit umfasst sowohl die Parametrisierung und den Entwurf, als auch den Bau, die Integration und den initialen Betrieb eines Latentwärmespeichers im Megawatt-Maßstab, der Dampf für einen industriellen Prozesskunden erzeugt. Der Speicher soll Dampf bei einer Temperatur oberhalb von 300 °C bei 25 bar und einem Massenstrom von 8 t/h für mindestens 15 Minuten erzeugen. Die Daten der bedarfsorientierten Erzeugung von überhitztem Dampf für mehr als 20 Minuten unter diesen Bedingungen zeigen eine thermische Leistung und Kapazität von 5,5 MW und 1,9 MWh.

Um dieses Speichersystem zu entwickeln, sind verschiedene Schritte nötig, die allesamt neue Aspekte abdecken: Sowohl die Erzeugung von überhitztem Dampf im Durchlaufbetrieb und die Bereitstellung von thermischer Leistung und Kapazität im Megawattbereich, als auch die Integration in ein bestehendes Betriebssystem. Dies erfordert eine Kombination aus der Hochskalierung der thermischen Leistung und Kapazität, der Konzeption eines realisierbaren Aufbaus sowie der Entwicklung der Systemintegration. Die Leistungssteigerung führt zur notwendigen Ausarbeitung einer sehr dichten Rippenstruktur und entsprechend engen Rohrabständen. Zudem ist eine Modellierung mit Analysemöglichkeiten von Wärmeverlusten und potentiell nicht idealer Strömungen der Wasser-/Dampfseite im Sammler erforderlich. Weiterhin werden Aspekte von der Transportfähigkeit über die Befüllbarkeit mit pelletiertem Salz während der Inbetriebnahme bis hin zur Zugänglichkeit für Zulassungsstellen behandelt. Die Entwicklung der Systemintegration in den laufenden Betrieb ermöglicht die Be- und Entladung mittels bestehender Komponenten und somit eine Optimierung der Anlagennutzung. Diese Integration, die nicht nur eine Auslegung und Optimierung der Speichertechnologie selbst, sondern eine Anpassung des gesamten Systems bedarf, eröffnet neue Blickwinkel für die Entwicklung von Latentwärmespeichern. Entscheidend für den Erfolg ist hierbei nicht nur die Betrachtung der Speicherkomponente, sondern die Betrachtung des gesamten Prozesses.

1. Introduction

With the climate change act of 2021 from the German Federal Government [1], a law was passed to commit Germany to greenhouse gas neutrality by 2045, reducing emissions by 65% of the 1990 levels by 2030. For industrial processes, this means reducing or eliminating fossil fuel use wherever possible. A possibility for the reduction of fossil fuel use in process steam applications is the integration of thermal energy storage systems. There are various options for this integration. One is to couple to-date separate processes, allowing for a transfer of heat between, for example, batch and continuous processes. Another is to provide peak energy by a storage system in a variable demand system, allowing for a smaller dimensioning or nominal load operation of a fossil-fuel burning unit. A third possibility is the provision of energy as a standby operation, providing energy to bridge between operation of different components. A fourth is to integrate electricity provided by renewable energies via a heat pump or directly converting this to heat, providing process steam directly through a thermal energy storage system. These are examples, but do not cover all of the decarbonization methods in process steam operation that are possible with thermal energy storage systems.

Each of these needs has two factors in common: the need is very dependent on the individual process being analyzed and, currently, thermal energy storages have not been developed to a commercially available state for such applications, allowing for an easy integration and adaptation. Within the work of this thesis, the world's largest high-temperature latent heat storage system for the production of superheated steam at the megawatt scale was developed, built and integrated into an operating cogeneration plant, raising the technology readiness level [2] of the technology from 4 to 5.

In the next two sections, first the industrial process decarbonization and the specific process considered in this work and then thermal energy storage development are discussed. This is followed by an outline of the research objectives and method, thereby presenting the publications that are the core of this thesis.

1.1. **Industrial process decarbonization**

Production processes relying on steam have been built and adapted to maximize product manufacturing. This results in greatly varying operating parameters, depending on duration of production, production equipment and the processes involved. The temperature ranges involved have been analyzed and detailed by several authors. Nägler et al. [3] differentiate the process heat demand in the European Union into four temperature categories – <100 °C, 100-500 °C, 500-1000 °C and >1000 °C – showing the different energy amounts needed in different industrial processes. Rehfeldt et al. [4] differentiate between <100 °C, 100-500 °C and >500 °C for the European Union plus Norway, Switzerland, Iceland, analyzing process heat as well as space heating and cooling demands. In a deliverable of Heat Roadmap Europe [5], the heating and cooling demand for 28 member-states of the European Union were analyzed regarding sub-sectors, end-use technologies and temperature levels. Here, it was concluded that process heat at temperatures above 200 °C accounts for about 50% of industrial heating and cooling demand.

In addition to temperature, the mass flows, pressures and variations in duration of demand are obvious differences in process steam requirements between industry types as well as specific sites. This makes the development of a standardized energy source or system for meeting demand essentially impossible. According to [4], natural gas accounts for 935 TWh or 39% of the total energy use for industrial heating and cooling in the European Union.

To attain the abovementioned goal of decarbonization, one of the building blocks can be the integration of thermal energy storage systems. Integration of energy storage systems is dominated by the variety of potential processes in which the storage technologies can be deployed as well as the various benefits they deliver. Therefore, the requirements for thermal energy storage systems vary greatly depending on the chosen application, just as the systems themselves have different capabilities depending on their technical principles. In **Paper I**, a systematic methodology that approaches the challenge of characterizing and evaluating thermal energy storage systems requirements in different industrial applications is presented. Key parameters from a system point of view are time-dependent mass flows, temperatures, pressures and working media. These in turn result in design criteria such as rate of heat transfer, necessary capacity, temperature range of operations, and working media.

Within this thesis work, a thermal energy storage unit was integrated into a heat- and power cogeneration plant in Neunkirchen-Wellesweiler, Germany. This plant provides process steam for industrial customers. The system and requirements for this storage system are discussed in **Paper III** and **Paper V**. These requirements are summarized here to detail

this process steam integration. The cogeneration plant consists of a gas turbine with 5.2 MW_{el} and 8.5 MW_{th} nominal powers connected to a downstream heat recovery steam generator, as shown in Figure 1. In parallel, two auxiliary boilers, each with a nominal power rating of 13 MW_{th}, also connect to the steam mains.
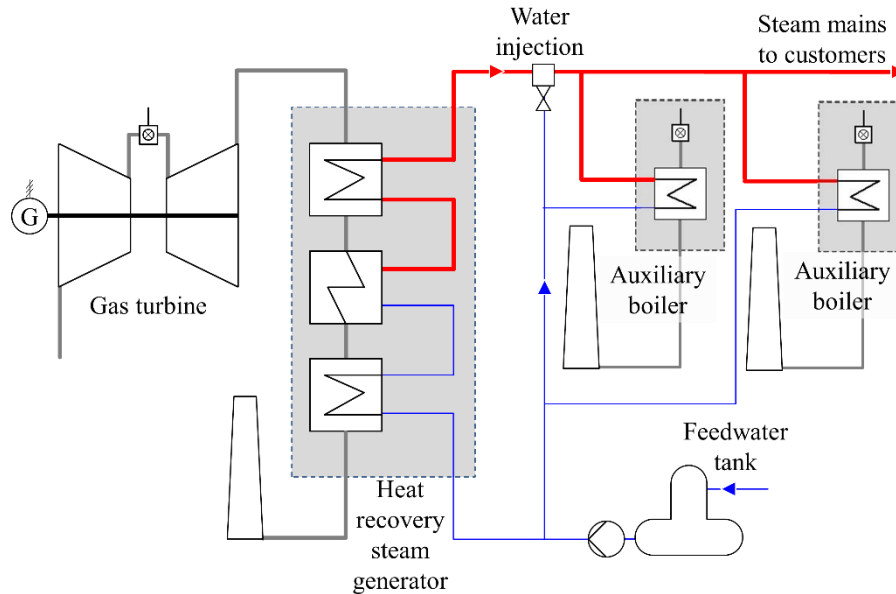
Figure 1: Simplified schematic of the cogeneration plant, showing the gas turbine with heat recovery steam generator in parallel to the two auxiliary boilers. These have main inlets from the feedwater tank and outlets to the steam mains.

The gas turbine solely burns mine damp; the auxiliary boilers can burn either light heating oil or mine damp, depending on the mine damp quality and availability. Mine damp is collected from previous coal mining sites and is distributed within a mine gas network in the state of Saarland. Due to the nature of the energy source, fluctuations in both quality and quantity of the mine damp occur. The burning of mine damp was classified within the Renewable Energy Sources act (Erneuerbare-Energien-Gesetz, EEG) to be beneficial to the climate. This was analyzed and discussed in an expert's report regarding the future of mine damp networks in the state of North Rhine-Westphalia [6]; the technical overview is also applicable to the state of Saarland, in which Neunkirchen-Wellesweiler is located. As detailed here, the amount of mine gas available will decrease in the future due to natural flooding of the abandoned mines; relevant methane quantities are, however, forecasted to be emitted through 2030.

To produce the necessary steam for customers, the steam mains are operated at a minimal temperature of 300 °C and a pressure of 25 bar. Condensate is returned to the plant from the customers and is stored in a feedwater container after the water quality is maintained.

The cogeneration plant is operated according to the demands of the steam customers, which vary according to production and weather. Due in part to the remuneration based on the

Renewable Energy Sources act classification, the gas turbine is the preferred primary load bearer. This results in several operating modes for the plant, that vary according to annual seasons. In the summer, process steam is produced for several industrial processes. In the winter, space heating energy is supplied as well. A mixed operation is necessary in spring and autumn. The main components of the cogeneration plant are operated accordingly in order to meet these varying demands.

Each component can be operated at full load or partial load, both of which produce steam and burn fossil fuels. Minimal load is the lowest load at which the component can be operated while burning fuel. For these auxiliary boilers, startup from minimal load to full load takes approximately two minutes. In addition, a further operating mode is possible in the auxiliary boilers: heat maintenance. In this mode, steam from an operating unit (in this case, either the heat recovery steam generator or the other auxiliary boiler) flows through the auxiliary boiler, maintaining a minimum temperature in the boiler components. This allows for a fast (here, about 15 minutes) return to full load compared to startup from ambient conditions, as well as less stress on the components due to load changes.

One of the customers of the cogeneration plant operates a process with very critical steam parameter demands, one of which is an uninterrupted supply. When the gas turbine trips due to fluctuations in mine gas supply, or for other reasons such as component failure, the steam emitted from the heat recovery steam generator has acceptable steam quality for the customer for about two minutes. In order to ensure uninterrupted supply, while one component is in operation, another is always kept at least at minimal load. This allows for a fast transition (<2 min., see above) when necessary. As minimal load requires a burning of fossil fuels, this operating scheme results in a constant burning of fossil fuels as a standby. The frequency of such supply transitions, according to the cogeneration plant operator, varies highly: between multiple times a week to once a month. Figure 2 shows a distribution of operating modes analyzed for the year 2021 for both auxiliary boilers and the gas turbine. The yellow bars show the summed times per month during which the gas turbine was not in operation and the auxiliary boilers assumed the primary steam production load. The summed times during which neither boiler was at minimal load – therefore either in heat maintenance or producing steam to augment overall production – are shown in blue. The times during which either auxiliary boiler was at minimal load are shown in green and indicate cases in which fossil fuel is burned to provide a standby for the steam production. As the cogeneration plant provides steam for heating purposes in the winter, the operating modes vary by season. In the year

4

analyzed here, discussed in [7], the gas turbine was repaired in January, resulting in a long shut-down time and therefore yellow bar in that month.
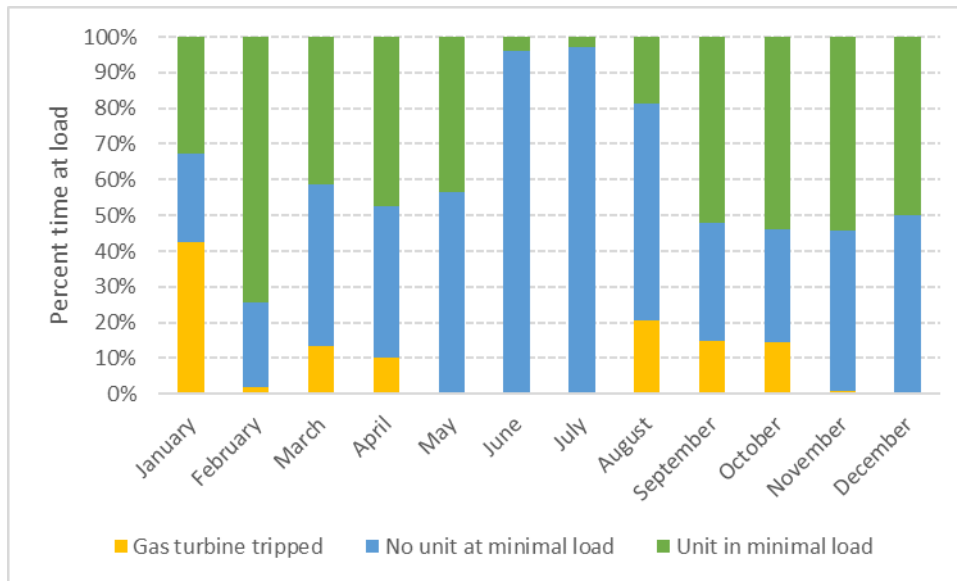
Figure 2: Operating modes at the cogeneration plant for the year 2021, cumulated per month, showing times during which the gas turbine is tripped, neither auxiliary boiler is at minimal load and the summed times a boiler is at minimal load. Based on [7]

A possibility for the reduction of carbon emissions from this cogeneration plant is the reduction of operation in minimal load through the replacement of the auxiliary boiler standby operation through a thermal energy storage system. This would reduce the times at minimal load by between 3 and 74%, depending on the season. Based on the analysis by Tawitpat [7], this would have resulted in a reduction of fuel use by about 8845 MWh/a in 2021.

1.2. Thermal energy storage

In this section, an overview of the state of research and development for thermal energy storages is discussed, in order to give a framework for the work in this dissertation.

1.2.1. Classification by energy storage principle

Thermal energy storage systems can be classified into sensible, latent and thermochemical concepts, listed in the order of technological maturity. This differentiation and categorization has been described by many authors, including Cabeza et al. [8] and Steinmann [9]; the classification is briefly summarized here.

In sensible systems, the energy is stored through an increase in temperature of the medium. This can be either a solid medium through or around which heat transfer fluid flows, as with packed bed or particle storage, or a liquid medium that is used either directly or via a heat exchanger, as in pit storages and molten salt storages in concentrating solar power applications, respectively. These types of systems are by far the most common type of storage

system [8], and today are used in industrial settings both in the form of heated solid media such as rocks or formed stones in regenerator storages [10] and as molten salt storage systems in concentrating solar power plant settings. In the future, these may also be viable as thermal energy storages for industrial processes [11]. Research in sensible heat storage has various aims. One is to expand system boundaries by increasing the operable temperature ranges through material research and monitoring, which would allow for higher power block efficiencies [12, 13, 14, 15]. Another is to optimize system design such as by applying thermoclines [16, 17]. Cost reduction through use of slag or other cheap materials [18] as well as adaptation for electrical charging [19] and integration into Carnot batteries [20] are further aims.

In latent heat storage, the storage is operated around a phase change temperature of the storage medium. This is typically for the phase change between solid and liquid states, due to lower volume changes from this state change as compared to liquid and gas. This technology has been developed for a wide range of applications and temperature ranges, as reviewed concisely by both Mehling et al. [21] and Du et al. [22]. These have partially been developed to commercial maturity, and some are still in research and development. This technology is the focus of this thesis, and relevant concepts and developments are discussed in the next section.

Thermochemical energy storage systems are based on reversible chemical reactions; energy is stored during endothermic reactions with a following separation of reactants. It can again be released during an exothermic reverse reaction. The energy release can be controlled by the temperatures and pressures required for reactions to occur. Research topics for thermochemical systems include stability and movement of the solid reactants, heat transfer through the solid reactant, system design and scalability and system integration [23].

1.2.2. Development and research topics in latent heat storage systems

In latent heat storage, heat is transferred to a phase change material, or PCM[1], during charging. This PCM is heated by the heat transfer fluid, or HTF[2], above the phase change temperature, thereby melting from the solid state to the liquid state. Barring thermal losses, this heat is stored until required, at which point the heat transfers back to the system. For such a system, both the PCM and the concept for heat transfer and containment are integral.

Nazir et al. [24] reviewed the work on phase change materials, providing a good summary of the goals and parameters. Ideally, the PCM has a high specific heat capacity as well as high

---

[1] PCM: phase change material
[2] HTF: heat transfer fluid

thermal conductivity, a good thermal stability, low flammability, no or controllable supercooling, low corrosivity and low volume change during phase change. When developing a storage for an application type or specific system, the phase change temperature needs to match the temperature demands of the system, and ideally be both cheap and available while being ecologically acceptable. Materials research on PCMs aims to synthesize such materials with specific phase change temperatures, apply coatings or encapsulations for a better heat transfer, as well as to enable a better characterization of the known materials. For the temperature range from 200 to 350 °C, Bauer et al. [25] determined the applicability of nitrate salts as PCMs. Specifically, sodium nitrate with a melting temperature of 306 °C has been well characterized [26].

The goals of the concept for heat transfer and containment of the PCM are multifold. On the one hand, the storage material simply needs to remain in place, regardless of its physically molten or solidified state and the volume change inherent to the change between states. This containment portion of the concept also needs to minimize or reduce, depending on system requirements, heat losses to the environment. On the other hand, the heat needs to be transferred into and out of the PCM at the desired rate over the desired time. This aspect has led to much research and development, leading to various latent heat storage concepts. Reviews and analyses of these have been conducted by several authors, including Steinmann [9], Du et al. [22], Tao and He [27], Elarem et al. [28] and Sharma et al. [29]. A brief overview is given here in order to show the level and breadth of development and research attained thus far. Differentiation in applications lead to differing developments. For this thesis, the term 'high temperatures' denotes temperatures greater than 100 °C, above which water cannot be stored at atmospheric pressure in the liquid state.

The main concepts that have been developed thus far are microencapsulation, addition of nanoparticles to the PCM, the creation of composite PCM/heat transfer materials, active removal of PCM from the heat transfer surface, insertion of foams or wire structures into the PCM, macroencapsulation of the PCM or use of extended fins.

In microencapsulation, the PCM is contained in capsules in order to contain the material while increasing the surface area for heat transfer. With this encapsulation, the PCM can be integrated in buildings, textiles or directly in an HTF to create a slurry. These concepts are reviewed by Huang et al. [30] and Giro-Paloma et al. [31]; it is a concept that has thus far not been developed for high temperature applications.

Nanoparticles added to a PCM aim to increase the thermal conductivity of the material, though these also, according to extensive reviews by Kibria et al. [32] Tariq et al. [33],

continue to entail materials research regarding material stability, as well as human and environmental safety considerations.

In composites, PCMs are combined with a structure material to increase thermal conductivity and, ideally, reduce corrosivity, as reviewed by Jiang et al. [34]. This publication discusses the work on composites, showing that the materials research on compatibility of components continues to be the main focus. Steinmann et al. [35] analyzed a composite of nitrate salts with graphite flakes for high temperature applications, determining that material separation occurs during thermal cycling. Zondag et al. [36] have analyzed composites of an organic PCM and graphite that show good thermal stability at temperatures between 150 and 250 °C.

In active removal concepts, the solidified PCM is physically removed from the heat transfer surface, allowing this surface to be continually used for further heat transfer. Various concepts have been developed and range from the movement of PCM, in a container, away from the HTF as developed by Pointner and Steinmann [37] to the removal of solidified PCM with a scraper as developed by in different setups by various researchers. Tombrink et al. [38] developed a horizontal rotating drum, from which the solidified PCM is removed. Maruoka et al. [39] and Egea et al. [40] developed vertical scraped cylinder storage concepts. Nepustil et al. [41] developed a flat-plate storage unit, whereby the solidified PCM is scraped from the flat plates. Zipf et al. [42] researched a scraped auger screw-type heat transfer concept. All of these concepts have in common that they are as yet in an early stage of research, developing solutions to problems with stability of moving parts with HTF and PCM contact, system design and scaling. The potential of active concepts with the possibility for separation in design of the heat transfer area and the thermal energy storage capacity makes these attractive for very large-scale integrations. Several of these concepts were analyzed for system development by Alario et al. [43] in 1980, underlining the difficulties in developing these concepts to high technology readiness levels. As yet, they have not been developed for use outside of the laboratory environment, and have been operated at limited pressure and temperature ranges.

Macroencapsulation aims to increase the surface area for heat exchange. Some designs for macroencapsulation are open to the atmosphere [37], while others are fully enclosed and can be immersed in the HTF [44, 45]. According to Liu et al. [46], concepts have been well developed for building applications. For process steam and other high temperature applications, two problems remain difficult to manage. One the one hand, if the HTF is a pressurized medium, in a macroencapsulated concept, both the containment for the HTF is a

pressure vessel and the macroencapsulation itself must withstand the higher pressures as well. The second difficulty is allowing for the volume change of the PCM during phase change while maintaining capsule leak integrity, as discussed by Steinmann et al. [35].

Another method for enhancing the thermal conductivity of PCM is to integrate structures with high surface-area-to-mass ratios – foams, wools, wire structures. These have been approached at low temperatures for copper foams numerically by Lei et al. [47] and experimentally by Martinelli et al. [48], aluminum fibers experimentally and numerically by Klemm et al. [49], copper wire structures numerically by Schlott et al. [50] and steel wool experimentally by Gasia et al. [51]. Prieto et al. [52] analyzed the combination of stainless-steel wool with a porosity of 98.6% and sodium nitrate as the PCM for high temperature applications, showing promising but early results. This development for reducing the heat transfer structure mass in a storage design should be continued. The feasibility of having a good thermal connection between the fibers, wool, etc. in a physical build needs to be determined.

Heat transfer structures have been used to enhance the overall thermal conductivity of the PCM. This method has been applied to flat plate concepts of latent heat storage concepts [53, 54, 55], which have thus far been tested in lab-scale environments, as well as tube-and-shell storage concepts. In the tube-and-shell storage concepts, the PCM can be on the inside of the tubes and the HTF outside, as analyzed by Zondag et al. [36]. With this concept, the entire storage system is a pressure vessel as in macroencapsulated systems. If the PCM is on the shell side, only the tube register is a pressure vessel, but increased attention needs to be paid to the enhancement of thermal conductivity to attain necessary process-steam heat transfer levels. As this is the concept focused on within this dissertation, it is discussed in more detail in the next section.

1.2.3. Finned-tube latent heat storage concepts

One of the concepts being developed for high temperature latent heat storages is an extended finned tube in a shell-and-tube assembly. This concept can be used at high pressures for steam applications. Several authors have reviewed the current state of research on finned-tube latent heat storage concepts, including Dhaidan et al. [56], Ibrahim et al. [57], Lin et al. [58], Li et al. [59] and Eslami et al. [60]. These reviews show that although there is extensive research on optimizing and understanding fin design and optimal arrangement, including experimental, analytical and numerical work, experience in scale-up and with real processes remains extremely limited. The design of the extended fins allowing for

independent thermal expansion of the tubes and fins with a physically possible assembly has not thus far been optimized.

In order to have a large amount of storage material between heat transfer tubes, a large tube spacing is needed. This in turn requires long fins or structures, in order to enhance the heat transfer throughout the PCM. The overall aim of the fin is to transmit heat from the HTF and the tube to the PCM. Hübner [61] analyzed the effect of a gap between the fin material and the tube material, showing that it is critical to minimize gaps. Pizzolato et al. [62] have shown that a gap is only critical for higher power levels. A common finned-tube concept is extended fins, as discussed in the review papers mentioned above. A further method, as discussed and tested by Garcia et al. [63], is the use of standard finned tubes with metal inserts in the PCM between the finned tubes. This is a promising concept for reducing costs in feasible large-scale units. This method overcomes the aspect of attachment of the fins to the tubes.

Laing et al. [64] compare the effects on heat transfer due to the use of four different materials as the fin structure: graphite, carbon steel, stainless steel and aluminum, concluding that, for operating temperatures above 250 °C, aluminum is the optimal material for heat transfer structures.

Aluminum has a higher coefficient of thermal expansion (for example, 23.4x10^{-6}/K for Aluminum 6060 (3.3206) [65]) than steel (for example, 10x10^{-6}/K for 16Mo3 [66]). For a feasible thermal cycling, this differential needs to be considered in the design. One method for attachment is tested by Urschitz et al. [67], using a hinge clamp on the outside of the fin geometry to hold the fin segments to the tube, centered between several segments. In **Paper II**, two attachment methods for aluminum fins on steel tubes were analyzed, determining that a method of clipping the fins to the tubes [68] is feasible from a manufacturing point of view as well as operationally stable. A second method of clamping the fins to the tubes was found to be unsatisfactory as a standalone solution. Pairing this with the clipping method [69] could lead to reduced costs.

Hübner et al. [70] focused on a techno-economic analysis, designing a fin and storage concept that is a combined optimization of the thermodynamic ideal and is technically feasible and attractive at large scale builds. This design was tested at a lab-scale with the design application being direct steam generating concentrating solar power plants, as discussed in [61]. The aim in this application is a high-power application for long periods of time, resulting in a large fin design, with a large storage volume between the fins.

Laing et al. [71] developed a latent heat storage using plate-like aluminum fins for direct steam generating concentrating solar power plants, combining the operation of the latent heat storage system with a sensible heat system based on concrete. This storage design was tested to have a heat transfer rate of 480 kW and a capacity of 700 kWh [72], producing about 0.3 kg/s (or 1.1 t/h) saturated steam in recirculation mode. This storage unit had 152 tubes, each 6 m long, and contained about 14 t of sodium nitrate as the PCM.

Vuillerme [73] similarly combined sensible heat storages with a latent heat storage, using the finned-tubes with inserts [63]. This allowed for a storage capacity of 852 kWh with 8.6 m³ (about 19.4 t [26]) of sodium nitrate as the PCM, using 61 tubes, each 4.5 m long. With a sensible storage unit located as a preheater and superheater (from a discharging perspective), this system produces superheated steam directly from a concentrating solar power test site; the latent heat storage system alone produces saturated steam.

1.3.   Research objectives and method

This thesis focuses on the development and analysis of a thermal energy storage system for a cogeneration plant providing process steam with critical parameters for industrial customers. The idea behind the storage integration is to reduce the use of minimal load operation of the auxiliary boilers, as discussed in section 1.1. In order to act as a standby, the storage system needs to assume full steam load within two minutes. The steam production needs to meet the minimal parameters for the critical customer: 8 t/h, 25 bar, at least 300 °C. The saturation temperature of steam at 25 bar is 226 °C. Steam production needs to be upheld for at least fifteen minutes, during which time the auxiliary boiler can be ramped up from heat maintenance to full load operation. With a feedwater temperature of 103 °C, this results in a required heat transfer rate of 5.72 MW_{th} and a capacity of at least 1.43 MWh_{th}.

A two-tank thermal energy storage system was analyzed for integration in this cogeneration plant [74]. It was determined that the trace heating requirements and volume of necessary molten salt or thermal oil were not acceptable for the plant operation.

As discussed in section 1.2.3, current development of latent heat thermal energy storages has analyzed very many concepts, tested many, but has resulted in an upscaling to above 200 kWh capacity for only finned-tube designs. These have produced either saturated steam at maximum mass flow rates of just over 1 t/h, with a maximum capacity under 1000 kWh.

Within this thesis, research for the development, build, integration and testing of a high-power large-scale latent heat storage system was conducted to produce superheated steam for an industrial customer with fixed steam quality parameters at a large scale, thereby raising the technology readiness level from 4 to 5. The main novel aspects are:

- designing for specific retrofit process requirements,
- producing superheated steam in once-through operation,
- providing megawatt-scale thermal power and capacity and
- integrating in an operating system.

A method for systematically determining the requirements for integration into systems was developed (**Paper I**), systemizing the determination and analysis of process requirements for a retrofit integration. For a storage of this size, a realistic, scalable and feasible method for increasing the heat transfer surface is necessary. Concepts for the attachment of fins to tubes were compared, varied and experimentally tested (**Paper II**). In order to design an upscaled storage system for a specific set of parameters, a method for designing and analyzing fin structures to thermodynamically design a black-box storage unit was developed (**Paper III**). As the storage unit is integrated into an operating system, the overall system integration was developed, including both physical aspects as well as process engineering aspects. Physical aspects such as the foundation, thermal insulation, connection to the existing system, and detailed aspects in the storage unit design from transportability and weight considerations to physical filling capability with the pelleted salt during commissioning and accessibility for permitting bodies were analyzed (**Paper IV**). The process engineering of the system integration in an operating system was developed to allow for charging and discharging with the available components while maximizing benefits to the plant. Simulations for both charging and discharging of the process integration of the storage system and the detailed design of the storage unit are discussed in **Paper V**. This integration, requiring not just a design and optimization of the storage technology itself but of the whole system, is a novel point of view for the development of latent heat storage systems. It is not necessarily critical that the storage itself meet all of the system requirements, but that the overall integration makes this feasible. Following the integration of the storage system, it was commissioned. The results of the commissioning are discussed in **Paper VI**.

2. Publications

A list of publications that form the core of this thesis and to which it is related are shown in section 2.1. The following sections 2.2 to 2.7 give a brief summary and detail the responsibility of the author according to CRediT [75] before presenting each paper.

2.1. List of publications

2.1.1. Core publications

Paper I: Determination of process and storage requirements

D. Gibb, M. Johnson, J. Romaní, J. Gasia, L.F. Cabeza, and A. Seitz. "Process integration of thermal energy storage systems – evaluation methodology and case studies," *Applied Energy*, vol. 230, pp. 750-760, 2018. doi: 10.1016/j.apenergy.2018.09.001.

Paper II: Finned-tube attachment methods

M. Johnson, S. Hübner, M. Braun, M. Schönberger, C. Martin, M. Fiß, B. Hachmann and M. Eck. "Assembly and attachment methods for extended aluminum fins onto steel tubes for high temperature latent heat storage units," *Applied Thermal Engineering*, vol. 144, pp. 96-105, 2018. doi: 10.1016/j.applthermaleng.2018.08.035.

Paper III: Thermal storage design

M. Johnson, J. Vogel, M. Hempel, B. Hachmann and A. Dengel. "Design of High Temperature Thermal Energy Storage for High Power Levels," presented at Greenstock, Beijing, China, May 2015, *Sustainable Cities and Society*, vol. 35 (November), pp. 758-763, 2017. doi: 10.1016/j.scs.2017.09.007.

Paper IV: Physical storage integration

M. Johnson, B. Hachmann, A. Dengel, M. Fiß, M. Hempel and D. Bauer. "Design and Integration of High Temperature Latent Heat Thermal Energy Storage for High Power

Levels," presented at ASME IMECE in Pittsburgh, USA, Nov. 2018, *Proceedings of the ASME IMECE*, IMECE2018-86281, copyright ASME, 2018. doi: 10.1115/IMECE2018-86281.

Paper V: Process integration

M. Johnson, J. Vogel, M. Hempel, A. Dengel, M. Seitz, and B. Hachmann. "High temperature latent heat thermal energy storage integration in a co-gen plant," presented at 9th IRES in Düsseldorf, Germany, Mar. 2015, *Energy Procedia*, vol. 73 (June), pp. 281-288, 2018. doi: 10.1016/j.egypro.2015.07.689.

Paper VI: Experimental results

M. Johnson and M. Fiss. "Superheated steam production from a large-scale latent heat storage system within a cogeneration plant," *Communications Engineering*, 2023. doi: 10.1038/s44172-023-00120-0.

2.1.2. Further relevant publications

Further parts of the research presented in this dissertation have been published in the following references.

Journal Articles

J. Vogel, M. Keller, and M. Johnson. (2020) Numerical modeling of large-scale finned tube latent thermal energy storage systems. *Journal of Energy Storage*, vol. 29, ISSN 2352-152X, doi: 10.1016/j.est.2020.101389.

J. Vogel and M. Johnson. (2019) Natural convection during the melting process in vertical shell-and-tube latent heat thermal energy storage systems with extended fins. *Applied Energy*, vol. 246, pp. 38-52. doi: 10.1016/j.apenergy.2019.04.011.

M. Seitz, M. Johnson and S. Hübner. (2017) Economic impact of latent heat thermal energy storage systems within direct steam generating solar thermal power plants with parabolic troughs. *Energy Conversion and Management*, vol. 143 (July), pp. 286-294. doi: 10.1016/ j.enconman.2017.03.084.

D. Laing, T. Bauer, N. Breidenbach, B. Hachmann and M. Johnson. (2013) Development of high temperature phase-change-material storages. *Applied Energy*, vol. 109, pp. 497-504. doi: 10.1016/j.apenergy.2012.11.063.

Conference Proceedings

M. Johnson, S. Hübner, C. Reichmann, M. Schönberger and M. Fiß. (2017) Experimental analysis of the performance of optimized fin structures in a latent heat energy storage test rig. *AIP Conference Proceedings*, vol. 1850(1), 080013. doi: 10.1063/1.4984434. Presented at SolarPACES 2016, Abu Dhabi, UAE, Oct. 2016.

M. Johnson, A. Dengel, B. Hachmann, J. Vogel, M. Seitz, M. Hempel and M. Fiß. (2016) Integration eines Latentwärmespeichers im Heizkraftwerk Wellesweiler. *Chemie Ingenieur Technik*, vol. 88(9), pp. 1265-1265. Presented at ProcessNet Jahrestagung, Aachen, Germany, Sep. 2016.

M. Johnson, A. Dengel, B. Hachmann, J. Vogel, M. Seitz, and M. Hempel. (2015) Integration eines Latentwärmespeichers im Heizkraftwerk Wellesweiler. Presented at *OTTI Fachforum*, Neumarkt, Germany, Jul. 2015.

M. Johnson, N. Breidenbach, D. Laing, and B. Hachmann. (2013) Experimental and numerical analyses of a phase change storage unit. Presented at *42nd ASES Annual Conference - SOLAR 2013*, Baltimore, USA, Apr. 2013.

Patents

M. Johnson and M. Fiß. Wärmeübertragungsrohranordnung sowie Wärmespeicher mit einer solchen, German patent nr DE 10 2017 114 141.3, Date of publication of grant: 09.12.2021.

M. Johnson and M. Fiß. Wärmespeichervorrichtung und Verfahren zum Speichern oder Bereitstellen von Wärme mittels einer Wärmespeichervorrichtung, German patent nr DE 10 2017 213 718.5, Date of publication of grant: 01.06.2023.

M. Johnson and M. Fiß. Wärmespeichervorrichtung und Verfahren zur Bestimmung eines thermischen Ladezustands einer Wärmespeichervorrichtung, German patent nr DE 10 2017 219 593.2, Date of publication: 09.05.2019.

M. Johnson, M. Fiß and D. Bauer. Wärmespeichervorrichtung und Verfahren zum Speichern oder Bereitstellen von Wärme mittels einer Wärmespeichervorrichtung, German patent nr DE 10 2019 102 955.4, Date of publication of grant:13.02.2020.

2.2. Paper I: Determination of process and storage requirements

This article, entitled "Process integration of thermal energy storage systems – Evaluation methodology and case studies", was published in *Applied Energy*, vol. 230, pp. 750-760, copyright Elsevier, 2018. It was co-authored by Duncan Gibb, Joaquim Romaní, Luisa F. Cabeza and Antje Seitz and this author is the second author.

The requirements for thermal energy storage systems vary greatly depending on the chosen application, just as the systems themselves have different capabilities depending on their technical principles. This paper addresses this issue by developing a systematic methodology that approaches the challenge of characterizing and evaluating thermal energy storage systems in different applications in three concrete steps. The methodology is applied to two case studies of high-temperature storage: concentrating solar power and cogeneration plants. Also introduced are the concepts of retrofit and greenfield applications, which are used to clarify differences between integrated storage systems. The paper shows how such a systematic approach can be used to consistently analyze processes for storage integration, facilitate comparison between thermal energy storage systems integrated into processes across applications and finally grasp how the benefits of the integrated storage system are perceived by different interests. This will assist other researchers making the leap from the lab to the industrial environment.

The author is responsible for the development of the process analysis guidelines described in section 3.1 as well as the case study detailed in section 4.1.2, the cogeneration power plant case study. Following CRediT, the author is responsible for the conceptualization, funding acquisition, investigation, methodology, project administration, visualization and writing of these sections. These process analysis guidelines were also published by the IEA ECES Annex 30 [76], through which the collaboration took place.

In addition, the author collaborated in the IEA ECES Annex 30 work, in which the definitions of the described key performance indicators were set, the differences between retrofit and greenfield integrations discussed, and the system boundaries defined for various system levels. Following CRediT, the author is co-responsible for the conceptualization, funding acquisition, investigation, methodology, and review and editing of these sections.
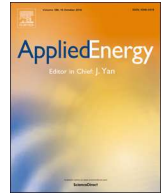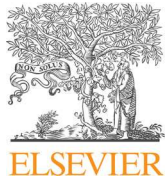
Process integration of thermal energy storage systems – Evaluation methodology and case studies

Duncan Gibb[a],[*], Maike Johnson[a], Joaquim Romaní[b], Jaume Gasia[b], Luisa F. Cabeza[b], Antje Seitz[a]

[a] Institute of Engineering Thermodynamics, German Aerospace Center (DLR), Pfaffenwaldring 38-40, 70569 Stuttgart, Germany
[b] GREiA Research Group, INSPIRES Research Centre, University of Lleida, Pere de Cabrera s/n, 25001 Lleida, Spain

HIGHLIGHTS

- A methodology has been developed for evaluating thermal energy storage systems integrated in processes.
- The work defines process analysis guidelines and the thermal energy storage system boundary.
- A definition for key performance indicators based on a stakeholder perspective is developed.
- The methodology was benchmarked using real case studies in concentrated solar power and cogeneration.

ARTICLE INFO

ABSTRACT

As a key tool for decarbonization, thermal energy storage systems integrated into processes can address issues related to energy efficiency and process flexibility, improve utilization of renewable energy resources and thus reduce greenhouse gas emissions. However, integration of these systems is dominated by the variety of potential processes in which the storage technologies can be deployed as well as the various benefits they deliver. Therefore, the requirements for thermal energy storage systems vary greatly depending on the chosen application, just as the systems themselves have different capabilities depending on their technical principles. This paper addresses this issue by developing a systematic methodology that approaches the challenge of characterizing and evaluating thermal energy storage systems in different applications in three concrete steps. To begin, a set of guidelines for process analysis has been created to disclose process requirements for storage integration. The methodology continues by explicitly defining the system boundary of a thermal energy storage system, as well as addressing technical and economic parameters. Finally, the approach concludes by determining the benefit of an integrated thermal energy storage system to an application and examines how key performance indicators vary based on the perspectives of different stakeholders. Within this work, the methodology is then applied to two case studies of high-temperature storage in concentrating solar power and cogeneration plants. Also introduced are the concepts of retrofit and greenfield applications, which are used to clarify differences between integrated storage systems. The paper shows how such a systematic approach can be used to consistently analyse processes for storage integration, facilitate comparison between thermal energy storage systems integrated into processes across applications and finally grasp how different interests perceive the benefits of the integrated storage system. This type of systematic methodology for technology integration has not been previously developed and as such, is a novel and important contribution to the thermal energy storage community. In the long term, this work builds the basis for a discussion on benefits of thermal energy storage system integration with diverse stakeholders including storage system designers, process owners and policy makers.

1. Introduction

For the first time in history, in the 2015 Paris Climate Accord, over 130 countries agreed that current levels of CO_2 emissions are leading to potentially catastrophic global warming events [1]. Three years later, a global stabilization of emissions has nevertheless resulted in a still-rising concentration of atmospheric CO_2, outlining the increasing urgency for a reduction of future emissions. Displacement of fossil-fuel technologies and an overall reduction in energy consumption through energy efficiency methods are key solutions to this crisis. Nevertheless, the increasing shares of renewable energy and available options for boosting energy efficiency pose important energy management problems that must be addressed through a variety of measures [2]. One of these possibilities is the efficient management of heat. Due to the abundance of waste heat and heat demand in industrial processes [3,4], a critical need for increased flexibility in all types of power plants [2], the demand for low-temperature heating and cooling solutions in buildings [5], as well as the emergence of new technologies for enabling the coupling of energy-intensive sectors, the storage of thermal energy is more relevant than ever [4,6]. Integration of these systems into processes is thus an important step towards reducing CO_2 emissions and advancing the integration of variable renewable energy [7].

Thermal energy storage (TES) systems are diverse technologies that are suitable for deployment in a wide variety of applications. There is, however, no 'one-size-fits-all' version of a TES system. Each storage concept has its own advantages and disadvantages that make it more or less appropriate for a specific application. A challenge is in identifying these factors and subsequently matching the most beneficial storage system(s) with an appropriate process. Processes are similarly variable and complex, usually with a series of interdependent steps and often with significant variations in the sectors themselves. The type of energy available or required can be inconsistent. A process can provide heat, cold, or electricity as a source, or can require any of these as a sink. Most importantly, there is no standard process, even within specific sectors or industries. These aspects make the integration of a TES unit quite complex. It is therefore important to characterize both the process and available TES systems independently, before joining them in an application.

Furthermore, integration of a TES system into a process can be categorized into one of two types: retrofit and greenfield. Retrofit applications examine an existing process where the storage system must be designed to fit the needs of an already dimensioned and built process. The challenge is in designing a storage system that fulfils the process requirements. In a greenfield analysis, the storage parameters are designed from the very beginning in parallel with the rest of the process. While no two greenfield projects are the same, it is noteworthy that the fundamental principles of the integration remain consistent and as such, a ground-up engineering of the system is not required and best practices can be employed.

Within this paper, processes are considered to be an organized collection of operations that engage in the transmission (e.g. district heating), use (e.g. steelmaking) or transformation (e.g. steam production in a power plant) of energy. An important point is that the boundaries of a process can be inexplicit, thus process definition is a major step addressed in this work. Two processes are detailed here: steam production in a cogeneration power plant and electricity production in a concentrating solar power plant.

As introduced in Fig. 1, the TES system and the process are interlinked with each other. Shown on the right, the process has requirements that must be fulfilled by the TES system. These are conditions that must be met in order for the integration to be considered at all. Shown on the left, the TES has system parameters that indicate the specifications for which the storage is appropriate. These dictate the technical and economic boundaries of the storage and the basic connection between process and TES system that should be further characterized.
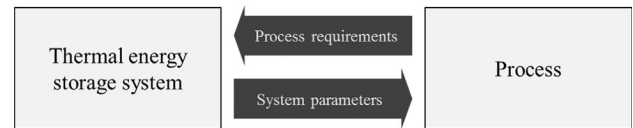

Fig. 1. Linking of process and TES system by process requirements and system parameters.

Following this characterization step, the benefit delivered by storage integration should be identified and the TES system and process evaluated for the specific application. This can be done by determining the key performance indicators (KPI) of the integrated technology.

Developed in Annex 30 of the IEA technology collaboration programme Energy Conservation through Energy Storage (ECES) [8], the methodology presented in this paper is a first step towards a systematic evaluation procedure for TES systems integrated in different applications. Through such novel technology assessment methods, the potential of an integrated TES system can be properly evaluated and the deployment of these systems can be advanced.

2. Existing methodologies for process integration of thermal energy storage systems

A complete methodology for the evaluation of TES systems integrated in processes is not known. Nevertheless, there exists literature regarding process analysis, TES system characterization and KPI across a wide selection of fields in the energy sector.

Regarding process analysis, Wallerland et al. [9] reported on the development of a methodology for the integration of heat pumps into processes. This technical methodology focused on a computational mathematical approach, however, they did not take on a holistic view of the process itself nor recommend generalized measures for process analysis. On a larger scale, Zhang et al. looked at a waste heat recovery network that dealt with the identification of waste heat source and sink plants. This methodology then set up a waste heat transportation system and engaged in optimization procedures [10]. Furthermore, certain optimization strategies have been investigated that include process design and techniques for storage integration. Olsen et al. [11] developed software tools for optimization of heat recovery based on process integration techniques while Fazlollahi et al. [12] created a heat storage optimization model that demonstrates the utility of integrating thermal storage.

Concerning the methodology to describe the TES system itself, the focus of this paper is laid on the boundary of the storage system. Even within literature regarding a specific application, there is little consensus on where the system boundary should be placed. In some studies on indirect TES systems integrated into concentrating solar power (CSP) plants, the boundary is considered to contain the storage module and selected components of the power block [13,14]. In others, no power block components are considered in the economic evaluation of the storage system [15–17]. Furthermore, Kapila et al. [18] found that many earlier studies with technology assessments on large-scale energy storage relied primarily on vendor data or a top-down approach that did not take a consistent definition of system boundary into account. This inconsistency and ambiguity underscores the need for a precise definition for the TES system boundary. Though not covered in this paper, it is important to note that research work has also been conducted in economic considerations regarding thermal energy storage integration. Rathgeber et al. [19] developed a methodology for determining an acceptable storage price for integrated TES systems and Welsch et al. [20] performed an LCA assessment for district heating systems with borehole TES that outlines additional possibilities for economic assessment.

The necessity of a clear and methodical approach for identification of key performance indicators has been investigated by Giacone and

Mancò, who found that the complexity and variety of definitions for several energetic properties makes a structured KPI framework necessary [21]. Lindberg et al. also admit that the KPI themselves are too complex to define uniformly across industrial processes, yet offer suggestions on how to proceed with the KPI identification process [22]. The need for a comprehensive and flexible framework is clear.

Key performance indicators have been previously addressed in only one study involving TES systems. Cabeza et al. looked at prior efforts to benchmark KPI for TES systems, specifically focusing on work in CSP plants and the building sector [23]. In this case, specific metrics for performance evaluation were defined, quantified, and presented as future benchmarks. This type of approach has also been used in several other academic studies that present a version of KPI identification focusing on numerical targets [24–27]. One example is the study by Portillo et al. that developed a parametric model for evaluating performance of TES in CSP plants in which the model gave numerical values for TES integration that can help optimize technical choices [27]. In these cases, the KPI represent values of parameters that would already demonstrate the success of a particular technology, instead of providing a framework for KPI identification, as suggested by Giacone and Mancò [21]. The latter is an approach more appropriate to technology integration and performance assessment.

There are many examples of identification processes for specific KPI in which the studies explicitly identify the KPI for their particular fields [28–37]. These chosen indicators address a similarly broad selection of decision-making criteria, encompassing sustainability for manufacturing, production reliability, energy efficiency, delivery of industrial services, general energy management, and flexibility in building energy systems. In some cases, the indicators were weighted and an overall value was assigned [28], while other studies defined a hierarchy or grouped the indicators that supported the explicit selection of KPI [30,33,34,38]. In three publications, the final selection was validated in one or more case studies [30,31,33]. Wang et al. compared performance indicators between a hot water storage tank and a molten salt storage tank that laid the basis for comparison, but still explicitly defined its own indicators [39].

It is clear that the inherent variety of processes in which TES can be integrated requires flexibility in KPI identification. Therefore, it is necessary to create a basic methodology that will assist in determining the most relevant indicators for integrated TES systems in order to properly perform a technology evaluation for the diverse list of applications.

This approach can be seen foremost in May et al. [40], in which KPI for energy efficiency are defined as reference parameters that must be taken into consideration. In Cassettari et al. [41], a decision tool rooted in KPI was developed for sustainability in industrial manufacturing and applied to a case in a tannery. This study was an in-depth analysis into the industrial manufacturing process to derive a method in which both CO_2 emissions and production costs were minimized. Toor et al. [42] developed a method for ranking KPI in construction projects through the use of a survey. In that study, the authors remarked on discrepancies between stakeholder KPI that were largely caused by differing viewpoints on what constitutes project success. A study by Matino et al. [28] also developed a decision support tool with the aim of identifying process-related KPI that were ultimately normalized, scored and aggregated into a unique, global indicator. The study most relevant to the work presented in this paper is that of Li et al. [43], which focused on KPI in building performance. Here, the authors identified stakeholders and KPI, used a bi-index method to select the KPI that underlie stakeholder performance and finally validated the method using a case study. These works from literature highlight the importance of the stakeholder perspective, as well as support the idea that KPI are always application-dependent and a comprehensive framework for their identification in a case-by-case basis is required.

In order to advance the use of TES systems, it is necessary to better characterize the benefit that the technology brings to the processes. Due to the variability and diversity of processes and storage integration

strategies, KPI for TES systems should not be uniformly defined without paying detailed consideration to the application. However, there are sufficient similarities between technologies and processes to pursue the development of a comprehensive and flexible framework for analyzing and evaluating an integrated TES system. This framework is useful for evaluating the potential of an integrated TES system in a specific application. Furthermore, it is widely recognized that studies on stakeholder analysis for technology integration and assessment are limited [43]. As such, the stakeholder perspective forms a fundamental element of the analysis methodology.

3. Developed methodology for process integration of thermal energy storage systems

Evaluating processes with integrated TES systems requires a detailed characterization of three features: the process, the storage system, and the benefits of storage integration within an application. The methodology is structured around these ideas. Expanding on the theoretical background from Fig. 1, the suitability of the TES system is dictated through the process requirements and subsequently the TES performance in an application, as shown in Fig. 2. It is important because the application recontextualizes the TES system integration; now, its performance is established via the application.

In the following subsections, the stages of the analysis methodology are described in detail before being applied to two case studies in Section 4.
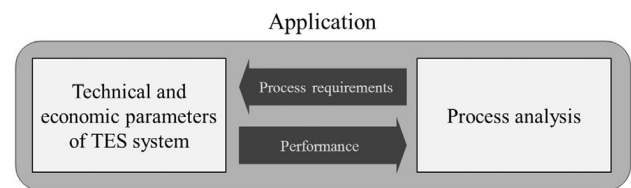

Fig. 2. Interaction between the process analysis and the TES system parameters for a successful integration.

3.1. Process analysis guidelines

The goal of the process analysis step is to address all information relevant to the integration of a TES system in order to provide a comprehensive overview of the critical process information. The complexity of the relation between the process and the TES system can thusly be simplified. As such, a set of guidelines has been developed to provide a clear and comprehensive overview of both technical and non-technical issues regarding the integration of a TES system into a process. The main step in this procedure is the structured collection and analysis of process information. Following that, a storage concept can be evaluated and roughly planned, while the aspects of detailed engineering become relevant after this first step. Fig. 3 shows a flowchart of the process analysis guidelines while the following paragraphs describe the goals of and issues addressed in each step.

In the first step, the overall goal of integration is determined and the functionality of the TES system within the process broadly outlined. Secondly, an important step in process analysis for the possible integration of a TES system is to determine and delineate which process is being analyzed, and where the boundaries of that process are. This addresses what factors can and need to be analyzed. For example, in the context of a power plant it has to be distinguished whether the process consists of the whole power plant or just one functional unit within the overall plant.

With the process defined, the thermal sink(s) and source(s) available within and at the boundaries of the process should be determined. This can be done via discussions with specialists, analysis of piping and instrumentation diagrams, process database analysis, estimation via
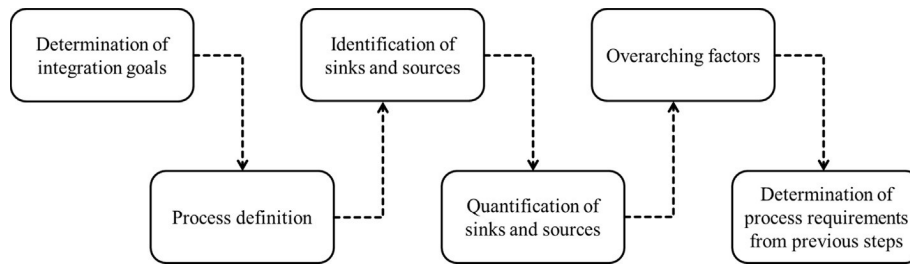
Fig. 3. Flowchart of process analysis guidelines.

extrapolation of fuel usage or measurement, among other information sources. There is a wide range of thermal sinks and sources normally under consideration, with sinks such as a steam turbine, a heat pump, process heat (direct integration), water or steam main, or an organic Rankine cycle. Sources investigated within Annex 30 include waste heat, direct combustion, heat provided directly for charging (e.g. from heat recovery steam generator), solar radiation e.g. in concentrating solar power, cooling water, and many others. Sources that are not directly within the existing process, such as electricity, as well as sinks such as a neighbouring process, should also be considered.

The sink(s) and source(s) must be quantified in order to evaluate the potential applicability for TES integration. Here there are two major groups of parameters: thermodynamics and spatial properties. Thermodynamic parameters can initially be analyzed independently of the physical environment. The three most important aspects of the thermodynamic properties that must be expanded upon are heat transfer medium, temperature levels and transient profiles. The heat transfer medium of the sink or source influences the heat transfer rate, types of containment and materials used and applicable storage concepts. The temperature levels and transient profiles of the sink and/or source are key for the development of a TES concept, especially regarding power level and capacity. Furthermore, mass flow rates and pressure levels have an important role in determining power, capacity, phase of heat transfer fluid, and heat transfer characteristics. A section on spatial properties addresses problems or opportunities regarding available or usable space, obstacles and distances between process parts, and already-existing infrastructure.

Once the source(s) and sink(s) have been quantified, non-technical issues regarding the process including the recurrence of the process, company targets, and any environmental aspects need to be addressed. Finally, the last step of the process analysis is a summary and initial estimation of the integration possibilities for TES systems in the analyzed process. Ultimately these steps result in an identification of the process requirements for a TES system to be integrated that can be applied to both retrofit and greenfield integrations. This results in a differing viewpoint while applying the process analysis guidelines that will be further considered in the discussion.

3.2. Thermal energy storage system: system boundary

One of the most important aspects of evaluating TES integration is the placement of the system boundary. It has previously been shown that boundary placement can influence calculated parameters significantly [44], so consistency between analyzed cases is crucial for comparability. Despite this, there is an disagreement as to what constitutes the system boundary and perspectives vary significantly as to

where the limit of the thermal energy storage system should be set. Thus, it is highly important that there be a robust and applicable definition for proper comparison of integrated systems to be undertaken.

Before doing so, it is necessary to clarify the lower analysis levels of a TES system – component and module. Components are the smallest parts of the TES, which in combination form the overall system. A module is a set of components that fulfils a distinct and specific task within the TES system.

The definition is proposed as follows:

The TES system boundary is the point of contact between the fluid streams and the thermal sink and thermal source. The system contains all the components and modules exclusively used by it and those necessary to deliver heat to the sink and to retrieve heat from the source.

Included in this definition are all components required for linking the storage system to the process, i.e. components for connecting to the source or sink of thermal energy. As such, a system refers to all the materials, components and modules that allow the TES device to perform its purpose of absorbing, storing, and delivering heat.

An example of the system boundary applied to a concentrating solar power plant can be seen in Fig. 4, in which a two-tank molten salt TES system is integrated. The entire process is the CSP plant, the objective of which is to produce electricity using solar irradiation as the primary energy source. Therefore, it only has one thermal source (the solar field) and one thermal sink (the power block). The TES system is connected in parallel to the thermal source and sink. This means that the process can operate by providing thermal energy directly from the thermal source to the thermal sink to produce electricity. In this example, the boundary comprises the units 4, 5, 6 and 7, because they are the necessary components to connect the TES system to the process. Here the heat exchanger (4) is included because it is required for transferring energy from the source to the storage unit and from the storage unit to the sink. This is an example of indirect storage; the heat exchanger is considered as part of the TES system. In Section 4, an example of direct storage is used where the heat exchanger is external to the TES system.

In addition to the boundary, a TES system is characterized by a selection of parameters. These include technical properties such as storage capacity, nominal thermal power, temperature levels, and response time, as well as economic parameters including capital expenditures and operating expenditures. While discussing these in detail is beyond the scope of this paper, it is important to note that they are highly relevant in the KPI identification step discussed in the following subsection.
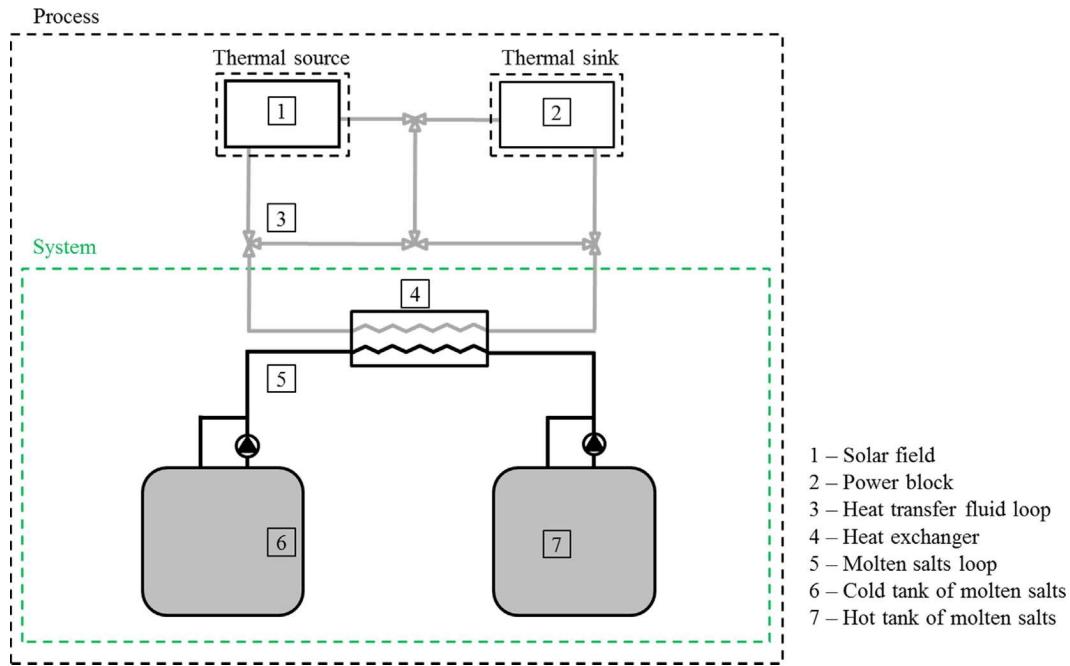
Fig. 4. Definition of the system boundary as applied to an example of indirect storage in concentrating solar power.

3.3. Key performance indicators in an application

The next step in the analysis methodology is the examination of the benefits that a TES system brings to an application. Determination of KPI revolves around the concept of performance. An isolated TES system cannot be evaluated in terms of its performance, as it is still a process unit with a purpose that is unclear – there are not yet any requirements to fulfil. Once it is integrated in an application, its performance in terms of meeting the process requirements can be assessed. Additionally, aspects external to the TES system (e.g. effect on CO_2 emissions) that also characterize the integration are considered. The KPI are then determined by taking different stakeholder perspectives on the integration to determine the most relevant TES system parameters and external factors. This is shown graphically in Fig. 5 and explained in the following subsections.

3.3.1. Performance indicators

To judge performance, the TES system must be evaluated with a process in an application for which there are specific requirements. In this case, the performance indicators denote the identified TES system parameters that are relevant to the process requirements. For example, a particular process may require a response time or a minimum power to be delivered from the TES system.

Nevertheless, the complete impact that a TES system may have on an application does not necessarily emerge from only the technical and economic parameters. As such, the definition also considers external factors that arise from outside the TES system, for which an understanding of the broader effects of the storage integration are necessary. This consideration could range from qualitative, process-specific factors such as process flexibility, to factors relevant to the local or regional energy system, such as dispatchability or grid flexibility. Further
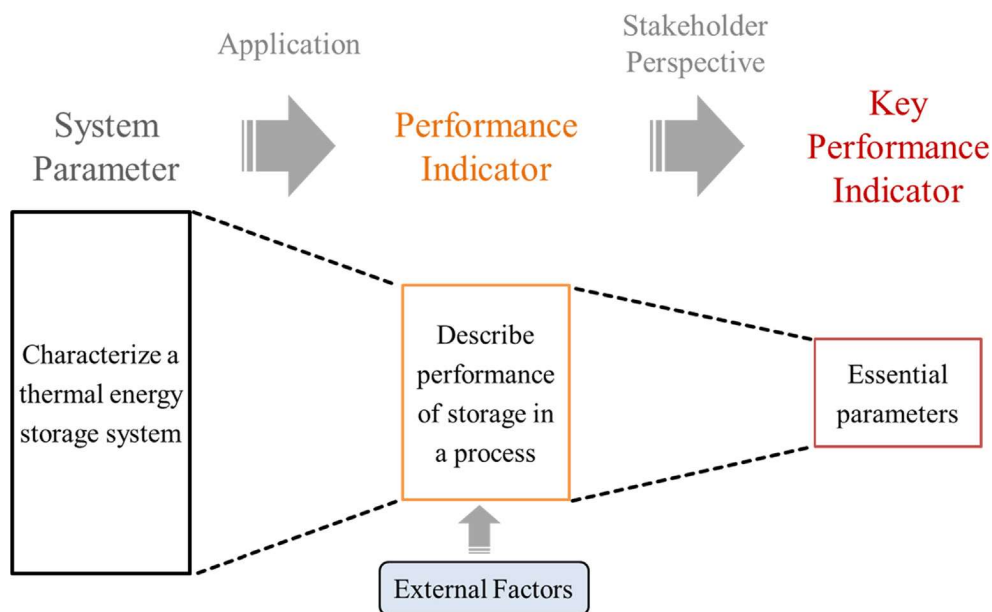

Fig. 5. The KPI funnel showing the transition from system parameter to KPI.

prospects for the category of external factors include a reduction in greenhouse gas emissions and increased renewable energy utilization, both of which are generally favorable from a policy maker perspective. External factors are the overarching impacts of TES integration to the process and the overall energy system that are not directly connected to storage system parameters.

3.3.2. Stakeholder perspective and key performance indicators

Performance of a technology can be defined by its ability to satisfy a specific need [45], however, the performance indicators are prioritized differently depending on the viewpoints of parties interested in the integration of the TES system. The final step in determining the key performance indicators is thus an analysis from various stakeholder perspectives. By introducing the concept of a stakeholder, it becomes possible to determine the most relevant performance indicators. The stakeholders selection process identifies the interests with the most potential to influence the integration or operation of the integrated TES system. They are the parties with the most invested in the integration. With these KPI identified, a stakeholder-based assessment can establish the benefits a specific TES system brings to an application.

The transition from system parameter to performance indicator to key performance indicator tightens the perspective from step to step, as shown in Fig. 5. At each step of the evaluation, a unique assessment of the TES system occurs. It follows that a KPI for technology assessment of TES is an internal (i.e. TES system-related parameter) or external (e.g. process benefits) property that demonstrates its ability to meet external needs as defined by stakeholders. With such a framework for KPI identification created, it is possible to assess the integration of TES systems from a selection of perspectives to form a comprehensive and dynamic view on the integration of the technology.

4. Application of developed methodology to case studies

Two case studies were evaluated using the methodology presented in this paper. These were selected to highlight the diversity of applications of high-temperature TES technologies and to facilitate distinction between the integration examples that will be further elaborated in the discussion.

A prominent application of high-temperature TES systems is in concentrating solar power plants. Most often installed in a two-tank molten salt storage configuration, this system allows the plant to provide dispatchable power that complies with an intermediate load profile [46]. These integrated systems are commercially available and well-known. They are to be considered "greenfield" cases according to the logic explained in the introduction.

In contrast, a first-of-its-kind example of an integrated TES system was selected as a second case study. A high-temperature latent heat storage unit has been developed for the integration in a cogeneration plant in Saarland, Germany [47]. The TES system produces steam for an

industrial customer in case a turbine trips. It will be integrated into an existing process and therefore reflects the "retrofit" situation.

The following sections begin by describing the purposes of TES integration in each application, followed by the implementation of the method from Section 3. Ultimately, a process analysis is performed, the system boundary is determined, and KPI are derived and prioritized based on the perspectives of three relevant stakeholders.

4.1. Case descriptions

4.1.1. Concentrating solar power case study

The specific CSP case analyzed is the solar tower power plant in Crescent Dunes, Nevada, USA. This is an example of direct thermal energy storage, where the solar salt comprises both sensible storage medium and heat transfer fluid, as shown in Fig. 6. The storage medium has a temperature range of 288 °C to 566 °C and the plant has a storage duration of 10 h. With a turbine power of 110 MW$_e$, this corresponds to approximately 3.3 GWh$_{th}$ storage capacity [48].

To proceed with the analysis, it is important to understand the role TES plays in CSP plants. Of primary importance is an increase in the plant capacity factor, which is the ratio of the plant nominal power to its rated power [51]. This occurs largely due to two effects. For one, the turbine is able to operate when the solar receiver has no direct insolation, i.e. during the night. The second effect is buffering by the storage system during cloudy periods or other weather-related disturbances. During these times, the storage provides enough thermal power to stop the turbine from entering transient mode or in the worst case, shutting down completely [49]. Use of the storage also minimizes a need for back-up capacity or start-up buffering, both of which are often provided by natural gas combustion turbines [52,53].

TES also improves the overall energy efficiency of the plant by lowering turbine start-up losses and by reducing curtailment during times of high generation [49]. Furthermore, the now-dispatchable electricity allows the plant to align its generation with peaks in power demand, creating a direct economic benefit as well as ancillary economic incentives through arbitrage, culminating in a decrease in the levelized cost of electricity (LCOE) of the plant [52]. Dispatchable power also provides flexible generation for the power system, which is a critical aspect for the integration of variable renewable energy [2]. Another grid-relevant effect is the potential for the power plant to act as a frequency regulator by balancing generation and supply with inertia provided by the turbine [54].

Further impacting the LCOE is a reduction of the solar multiple, thereby lowering the required solar field size or allowing for an increased solar field size (i.e. higher capacity factor) without considerable cost escalation [52]. Capacity factor and LCOE are closely related. However, it is important to highlight the direct impacts on both, so that the integration benefits may be fully characterized.

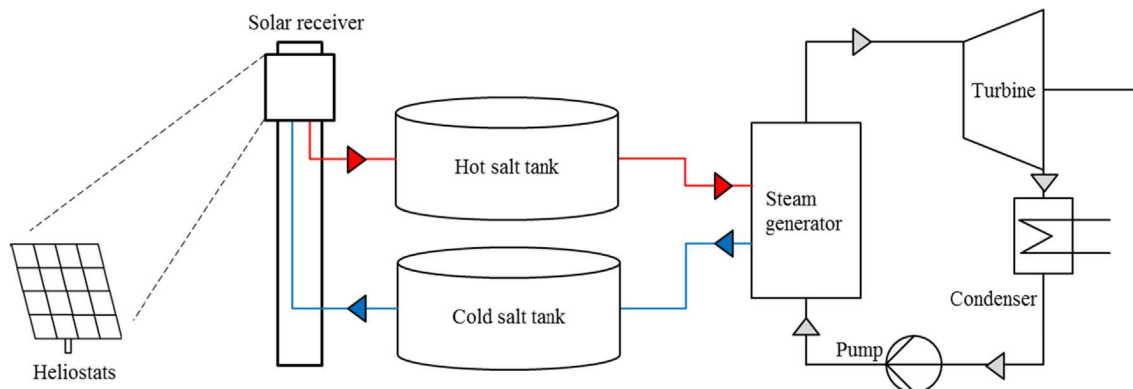These main motivators are summarized in Table 1.

Fig. 6. Schematic of the CSP plant with direct molten salt storage in Nevada, USA (adapted from [49;50]).

Table 1
Outcomes of TES integration into CSP plants.

Outcome of TES integration	Description
Increased plant capacity factor	- Night-time generation
	- Buffering during weather events
Improvements in energy efficiency	- Less curtailment during periods of high generation
	- Lowering turbine start-up losses
Dispatchable power	- Economic incentives
	- Improved grid flexibility
Reduced LCOE	- Maximized generation at peak demand
	- Reduction in solar multiple (i.e. smaller solar field)
Ancillary benefits	- Start-up buffering & minimizing back-up capacity
	- Frequency regulator for power grid

4.1.2. Cogeneration power plant case study

A TES unit is currently in development and build for the integration in a cogeneration plant in Saarland, Germany [55]. The plant supplies steam to several customers, with a minimal load being a constant supply of superheated steam at 6 MW$_{th}$ and 300 °C. Under normal operating conditions, the steam is generated by delivering the exhaust air from a mine-gas-fired turbine to a heat recovery steam generator (HRSG). The steam produced by this HRSG is then temperature-controlled and sent to the customers through the steam main. If the turbine trips due to fluctuations in the mine-gas network and supply, an additional boiler serves as back-up and ensures the steam meets the required specifications until the turbine can be brought back to full load. In order to ensure continuous steam quality, a back-up solution must ramp up to full load within the two minutes that the HRSG is still producing a rest-steam amount. Therefore, a back-up boiler runs on 'warm load', meaning that it is constantly burning fossil fuels so that it can be transitioned to full load within two minutes [55].

The latent heat TES system is designed to be integrated in parallel to both the HRSG and the existing back-up boiler. The critical advantage following integration is that the back-up boiler is run on 'cold load', meaning that it burns fewer fossil fuels to satisfy a prolonged transition time of 15 min [55]. The TES system provides the steam for the industrial customer while the boiler undergoes the transition to full load. The process diagrams before and after TES integration are shown in Fig. 7.

The TES system is directly enhancing the functionality of a currently-operational process unit and must meet precise specifications for the industrial steam client. There are therefore specific TES system properties that are critical to storage operation, especially related to the discharging procedure. On the one hand, the storage must meet the two minute ramp-up time for producing the full load of steam. On the other,

it must discharge for 15 min while the back-up boiler transitions from warm to full load [47]. Finally, it must produce steam that meets the required steam parameters from the industrial client. In other words, the steam must be delivered at the required temperature of at least 300 °C, pressure of minimum 21 bar at a flow rate of 8 t/h, which corresponds to a thermal power of 6 MW. These three factors form the main process requirements that characterize the integration.

4.2. Process analysis

As described in Section 3.1, the process analysis is a structured guideline for identifying critical information that directly concerns the integration procedure and suitability of the storage. For the purposes of this paper, an abridged version of the process analysis results, shown in Table 2, illuminate the contrast between the different processes.

4.3. System boundary

Figs. 8 and 9 show the system boundaries of the CSP and cogeneration case studies, respectively, based on the definition from Section 3.2. As according the definition, in Fig. 8 only the storage tanks are considered within the boundary. The steam generator (heat exchanger) is not included because it is not a component used exclusively by the TES system and belongs primarily to the power block. This direct storage configuration can be distinguished from Fig. 4, in which the heat exchanger was included due to its necessary role in transferring energy between the source, storage unit and sink. In Fig. 9, the TES system boundary is similarly restricted to the storage tank and surrounding piping because the HRSG and other process components were present before the retrofit integration. These components are not used exclusively by the TES and as such, are not within the system boundary.

4.4. Key performance indicators

The performance indicators and key performance indicators were determined for both cases following the method described in Section 3.3.

4.4.1. Concentrating solar power case study

The performance indicators are derived from Table 2 by associating the TES advantages with system parameters or external factors. The most important system parameters are selected based on required storage performance in a CSP application; the external factors that TES integration delivers to the solar power plant and its electric system are added to this list. The list of these performance indicators and an explanation of their importance is shown in Table 3.

Allocation of the KPI depends on a stakeholder perspective. In this case, three relevant stakeholders were identified (CSP plant operator,
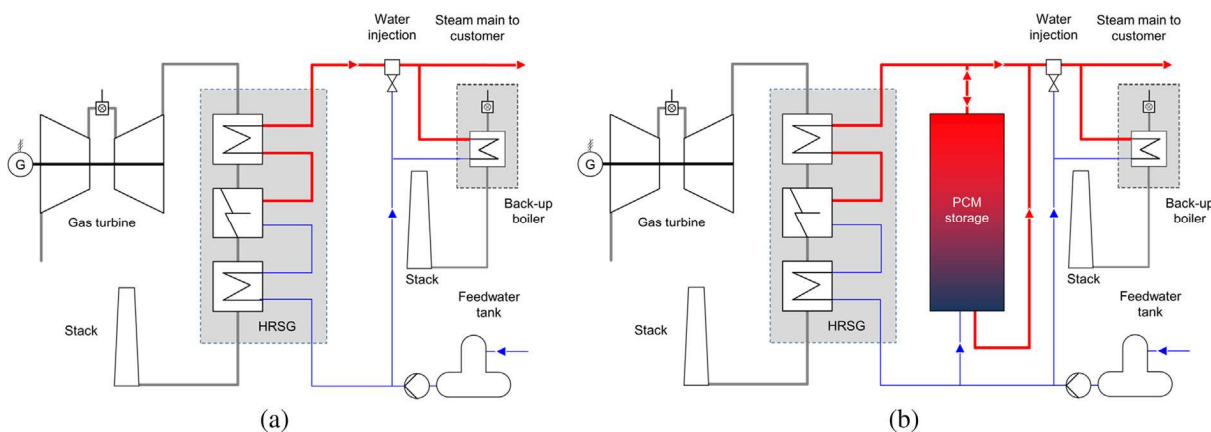

Fig. 7. Process diagrams of cogeneration plant (a) prior to and (b) following TES integration (adapted from [55]).

Table 2
Abridged results of process analysis of the two evaluated cases.

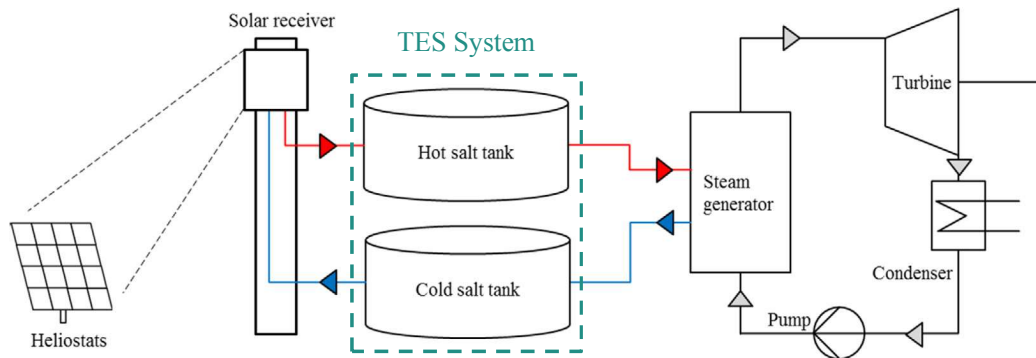| Process variable	Concentrating solar power ("greenfield process")	Cogeneration power plant ("retrofit process")
Integration goal	Increase capacity factor, reduce LCOE, reduce back-up utilization and improve efficiency	Decrease fossil fuel use by reducing combustion in back-up boiler
Process definition	Solar tower power plant with molten salt as heat transfer fluid	Cogeneration plant consisting of a gas turbine, steam generator, two back-up boilers and steam main
Thermal source(s)	Solar insolation	HRSG outlet steam
Thermal sink(s)	Power block (steam generator)	Steam customer
Medium of thermal source(s) and sink(s)	Molten salt	Steam
Cycle length	24 h	15 h
Acceptable TRL for TES	8–9	5–6

Fig. 8. System boundary for the concentrating solar power case study (diagram adapted from [49;50]).
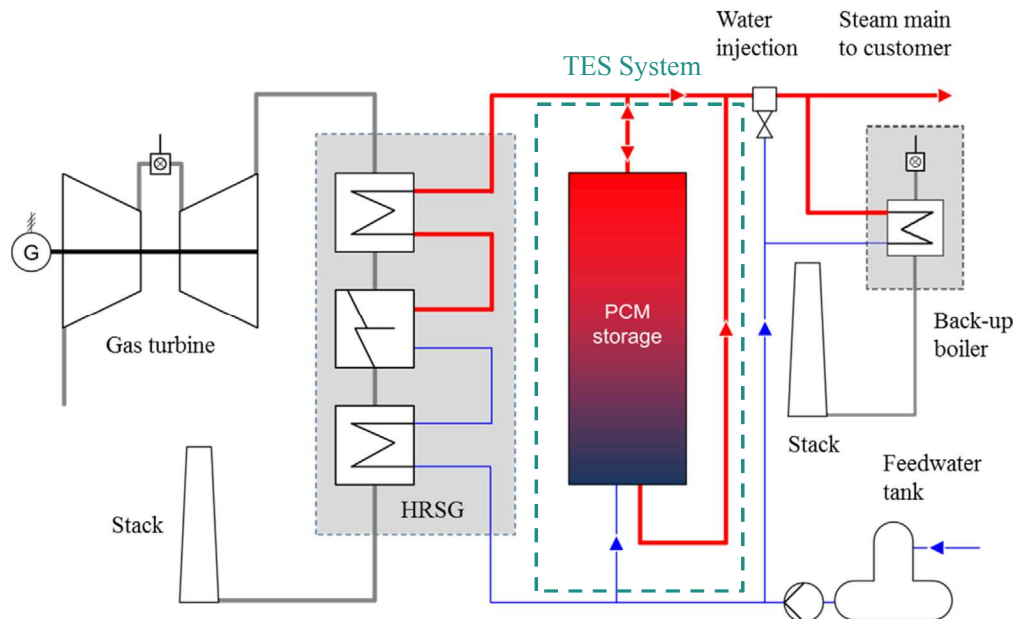

Fig. 9. System boundary for the cogeneration power plant case study.

electric utility, and policy maker) and the performance indicators were considered from their perspectives. The results are shown in Table 4.

4.4.2. Cogeneration power plant case study

The main process requirements outline the storage integration in terms of its TES system parameters, thus forming the basis for a derivation of performance indicators. In addition, there are external factors that arise due to the storage integration. These results for the cogeneration case study are shown in Table 5.

Through the implementation of three stakeholder perspectives (process operator, industrial customer, and policy maker), the importance of the performance indicators can be prioritized into KPI, as shown in Table 6.

5. Discussion

The results provide key insights on the methodological steps of process analysis, TES system boundary determination and KPI selection. Focus of the discussion is on how the methodology differentiates between greenfield and retrofit applications, how the boundary of the storage system varies depending on the application, and how KPI change significantly for different stakeholders.

Table 3

Performance indicators and their justification for TES integration in CSP plants.

Performance indicator	Justification of importance (Crescent Dunes requirements)
TES system-related factors	
Storage capacity of TES system	Increased plant capacity factor, (3.3 GWh$_{th}$)
Power delivered by TES system	Required to meet turbine design power, (110 MW)
Response time of TES system	Response to weather events or other disruptions, (< 1 min)
Lifetime of TES system	Critical to economic viability of the plant, (> 20 years)
External factors	
Dispatchable power	Reduced dependence on intermittent nature of solar thermal resources
Reduced LCOE	Optimization of economic potential through generation at peak demand, increased capacity factor, avoided back-up capacity and reduction in solar field.
CO_2 mitigation	Further displacement of fossil-fuel generation, especially relevant due to flexible dispatch. Reduced natural gas combustion during buffering and start-up.
Increased use of renewable energy	Expanded generation from solar thermal resources
Improved grid stability and flexibility	Potential to serve as frequency regulator by reducing imbalances between generation
Boosted energy efficiency	Start-up buffering and reduced curtailment

Table 4

KPI for stakeholders in CSP application.

CSP plant operator	Electric utility	Policy maker
Storage capacity	Dispatchable power	CO_2 mitigation
Power	Response time	Increased use of renewable energy
Lifetime		Grid stability
Reduced LCOE		
Boosted energy efficiency		

Table 5

Performance indicators for TES integration in a cogeneration plant.

Performance indicator	Justification of importance
TES system-related factors	
Response time of TES system	Must ramp to 6 MW$_{th}$ within two minutes
Steam quality (temperature, pressure)	Generated steam must meet process requirements
Discharge time	Must provide 6 MW$_{th}$ for 15 min
Lifetime of TES system	Critical to economic viability of the integration and permitting procedure
External factors	
Reduced fossil fuel use	Fewer fossil fuels burned during 'warm load' of backup boiler
Reliability	TES delivers process services that improve reliability
Increased process flexibility	Delivered by TES in several ways beyond the scope of this paper
CO_2 mitigation	Reduced combustion of fossil fuels

Table 6

KPI for stakeholders in cogeneration case study.

Process operator	Industrial customer	Policy maker
Response time	Steam quality	Reduced fossil fuel use
Discharge time	Reliability	CO_2 mitigation
Lifetime		
Reliability		
Increased process flexibility		

5.1. Greenfield vs. retrofit applications

The process analysis guidelines highlight an important difference between greenfield and retrofit applications. In the CSP example, with the case being a greenfield installation, it can be seen that the emphasis is laid on the integration benefits. The fundamental question is determining what the storage delivers to the application itself, with the process analysis guidelines used to identify the integration goal as a first step. This is necessary because the process will be designed from the ground up and it is important to know precisely what function the storage will serve. An adjustment of this function could have profound implications on the design of the process itself, e.g. on temperature levels, mass flows, etc.

In the cogeneration example, the power plant itself already exists with the storage being integrated as a supplementary process unit; it is thus a retrofit integration. For these processes, a specific engineering design is required that fully grasps the potentially novel aspects of the integration. Here, the emphasis is placed on the process requirements, i.e. what does the process require from the storage? There is little flexibility in these cases and for retrofit, the integration goal may only be quantitatively understood once the process analysis has been completed. This shows the key difference in how the process analysis guidelines are applied.

Such variations can be seen in the results, wherein the discussion in CSP revolves around the services the TES provides to the power plant. Dispatchable power, reduced LCOE and improved energy efficiency are the desired benefits of this storage. In the cogeneration example, the stakeholders place a higher emphasis on technical performance and reliability. Here, the focus is on maintaining steam quality and responding effectively to any disruptions. The key point is that these integrated systems are currently considered differently, yet through the use of this technology assessment methodology, they can be compared more tangibly with one another.

5.2. Boundary of the thermal energy storage system

There are key elements in the two cases that underscore the importance of a consistent system boundary definition. To begin, it can be seen that both system boundaries contain all the components necessary to retrieve heat from the source and deliver it to the sink, as well as those used only for the purpose of storing heat. This means that in the case of direct two-tank molten salt storage within a solar tower CSP plant, the steam generator is not included as is shown in the definition itself in Fig. 4. In a case of indirect TES, when the heat transfer medium is not identical with the heat storage medium, the heat exchanger used to transfer thermal energy from the solar field HTF (e.g. thermal oil) to the storage medium (e.g. molten salt) would be included as part of the storage system and taken into consideration in the technical and economic evaluation.

It is also significant that the placement of the system boundary differs for concentrating solar power with indirect storage as in e.g. Thaker et al. [8], which considers the heat exchanger within the power block to be part of the TES system. This diverges from the definition in this paper and indeed the results as without storage, the heat exchanger would already be a necessary component.

The boundary of the TES system in the cogeneration case is a typical

example of a retrofit process. In this instance, the system is integrated into a process with previously existing components that are not used exclusively by the storage, as required from the definition. As such, the TES system boundary remains clearly distinguishable from the HRSG, water injection line and back-up boiler that had already been present in the process.

5.3. Performance indicators and stakeholder perspective

There are some key performance distinctions between the two cases that ultimately define the selection of KPI. In CSP, the storage capacity defines the ability for the power plant to continue producing electricity overnight, for example. In the cogeneration case, the technical suitability is ultimately laid out by the power of the TES system that provides the necessary steam parameters, with pure storage capacity taking secondary importance. Storage reliability is also more pronounced in the cogeneration case, as the TES system constitutes a process unit that is essential to the process. These differences are crucial in the storage design phase and the distinction can be described simply through the use of the KPI results.

Key similarities between the cases are also present. Foremost is the importance of the storage response time, that is distinctive in both the greenfield and retrofit cases. This shows that when a storage is required, it is crucial that it deliver punctually, otherwise the integration is unsuccessful. The storage lifetime is also relevant in both cases, which emphasizes that process components are long-term investments and is related to long-term reliability, which in both cases constitutes an important KPI.

Regarding the stakeholders, it can be seen particularly in the cogeneration example that certain stakeholders are interested purely in a specific product from the process. As such, the industrial steam client is focused on reliably obtaining the steam with the proper quality. The integration of the TES storage system is not relevant for this stakeholder, as long as the steam is delivered. In cases such as these, the TES technology must compete with any alternative solutions.

6. Conclusions

Thermal energy storage systems integrated in processes have been lacking a clear and concise evaluation method that will help exploit their full potential. Until now, no detailed process analysis method has been proposed and there has been significant ambiguity regarding where the thermal energy storage system boundary is placed. Furthermore, previous uses of key performance indicators have either been target-focused, entirely non-technical, or over-specified.

The novelty of this paper is in the methodology, which takes a first step in addressing issues related to further deployment of thermal energy storage technologies in promising applications. The inclusion of both technical and economic storage parameters and external factors of integration present an opportunity to comprehensively and differentially evaluate the application. Through implementation of the methodology to two case studies in high-temperature storage, it has been shown how different applications prioritize different requirements from storage systems. The proposed methodology can also be applied to cases in low- and medium-temperature thermal storage. Moreover, the greenfield and retrofit approaches can be compared through the use of this systematic methodology and the benefits of a thermal energy storage system to an application can be highlighted and discussed more tangibly. In the end, this methodology is highly applicable to real applications and can be used from the very beginnings of process design to the final evaluation of tangible benefits of the storage integration.

Following this work, it is recommended to further expand the methodology by addressing more explicit economic concerns in the process analysis guidelines, e.g. local subsidies, tax benefits, renewable heat incentives. Also suggested is incorporating a ranking function that allows for a weighing of the different key performance indicators based

on the stakeholder. This will increase the precision and nuance of the key performance indicator identification. Furthermore, providing the users of the methodology with a suggested list of key performance indicators could help avoid any oversight or bias. Additional stakeholder involvement should be pursued as some thermal energy storage benefits are well-understood, yet others are less evident when first considering an integrated system. Engagement with the research community, industry, and policy makers is a critical step in addressing this gap. Finally, for validation and continued development, the application of the methodology by independent parties to differing cases will be needed, in order to better understand the strengths, weaknesses as well as development potential of these tools.

References

[1] UNFCCC. Paris agreement. Conf parties its twenty-first Sess; 2015. p. 32. <FCCC/CP/2015/L.9/Rev.1>.
[2] IEA. Getting wind and sun onto the grid; 2017. <https://www.iea.org/publications/insights/insightpublications/Getting_Wind_and_Sun.pdf>.
[3] Naegler T, Simon S, Klein M, Christian Gils H. Quantification of the European industrial heat demand by branch and temperature level. Int J Energy Res 2015;39. https://doi.org/10.1000/er.3436.
[4] Miró L, Brueckner S, Cabeza LF. Mapping and discussing Industrial Waste Heat (IWH) potentials for different countries. Renew Sustain Energy Rev 2015;51:847–55.
[5] REN21. Renewables 2018 global status report. Paris: REN21 Secretariat; 2018.
[6] Alva G, Lin Y, Fang G. An overview of thermal energy storage systems. Energy 2017;144:341–78. https://doi.org/10.1016/j.energy.2017.12.037.
[7] IEA. The power of transformation 2014. https://doi.org/10.1787/9789264208032-en.
[8] IEA. Energy conservation through energy storage; 2018. <https://iea-eces.org/> [accessed May 22, 2018].
[9] Wallerand AS, Kermani M, Kantor I, Maréchal F. Optimal heat pump integration in industrial processes. Appl Energy 2018;219:68–92. https://doi.org/10.1016/j.apenergy.2018.02.114.
[10] Zhang C, Zhou L, Chhabra P, Garud SS, Aditya K, Romagnoli A, et al. A novel methodology for the design of waste heat recovery network in eco-industrial park using techno-economic analysis and multi-objective optimization. Appl Energy 2016;184:88–102. https://doi.org/10.1016/j.apenergy.2016.10.016.
[11] Olsen D, Liem P, Abdelouadoud Y, Wellig B. Thermal energy storage integration based on pinch analysis – methodology and application. Chemie Ing Tech 2017;89:598–606. https://doi.org/10.1002/cite.201600103.
[12] Fazlollahi S, Becker G, Maréchal F. Multi-objectives, multi-period optimization of district energy systems: II – daily thermal storage. Comput Chem Eng 2014;71:648–62. https://doi.org/10.1016/j.compchemeng.2013.10.016.
[13] Thaker S, Olufemi Oni A, Kumar A. Techno-economic evaluation of solar-based thermal energy storage systems. Energy Convers Manage 2017;153:423–34. https://doi.org/10.1016/j.enconman.2017.10.004.
[14] Montes MJ, Abánades A, Martínez-Val JM. Performance of a direct steam generation solar thermal power plant for electricity production as a function of the solar multiple. Sol Energy 2009;83:679–89. https://doi.org/10.1016/j.solener.2008.10.015.
[15] Heller L, Gauché P. Modeling of the rock bed thermal energy storage system of a combined cycle solar thermal power plant in South Africa. Sol Energy

2013;93:345–56. https://doi.org/10.1016/j.solener.2013.04.018.

[16] Feldhoff JF, Schmitz K, Eck M, Schnatbaum-Laumann L, Laing D, Ortiz-Vives F, et al. Comparative system analysis of direct steam generation and synthetic oil parabolic trough power plants with integrated thermal storage. Sol Energy 2012;86:520–30. https://doi.org/10.1016/j.solener.2011.10.026.

[17] Seitz M, Johnson M, Hübner S. Economic impact of latent heat thermal energy storage systems within direct steam generating solar thermal power plants with parabolic troughs. Energy Convers Manage 2017;143:286–94. https://doi.org/10.1016/j.enconman.2017.03.084.

[18] Kapila S, Oni AO, Kumar A. The development of techno-economic models for large-scale energy storage systems. Energy 2017;140:656–72. https://doi.org/10.1016/j.energy.2017.08.117.

[19] Rathgeber C, Lävemann E, Hauer A. Economic top-down evaluation of the costs of energy storages – a simple economic truth in two equations. J Energy Storage 2015;2:43–6. https://doi.org/10.1016/j.est.2015.06.001.

[20] Welsch B, Göllner-Völker L, Schulte DO, Bär K, Sass I, Schebek L. Environmental and economic assessment of borehole thermal energy storage in district heating systems. Appl Energy 2018;216:73–90. https://doi.org/10.1016/j.apenergy.2018.02.011.

[21] Giacone E, Mancò S. Energy efficiency measurement in industrial processes. Energy 2012;38:331–45. https://doi.org/10.1016/j.energy.2011.11.054.

[22] Lindberg CF, Tan S, Yan J, Starfelt F. Key performance indicators improve industrial performance. Energy Procedia 2015;75:1785–90. https://doi.org/10.1016/j.egypro.2015.07.474.

[23] Cabeza LF, Galindo E, Prieto C, Barreneche C, Inés Fernández A. Key performance indicators in thermal energy storage: survey and assessment. Renew Energy 2015;83:820–7. https://doi.org/10.1016/j.renene.2015.05.019.

[24] Personal E, Guerrero JI, Garcia A, Peña M, Leon C. Key performance indicators: a useful tool to assess Smart Grid goals. Energy 2014;76:976–88. https://doi.org/10.1016/j.energy.2014.09.015.

[25] RHC. Cross-cutting technology roadmap; 2014. p. 1–56. <http://www.rhc-platform.org/fileadmin/user_upload/members/Downloads/2014-Brochure-Crosscutting-light.pdf>.

[26] Vilanova MRN, Magalhães Filho P, Balestieri JAP. Performance measurement and indicators for water supply management: review and international cases. Renew Sustain Energy Rev 2015;43:1–12. https://doi.org/10.1016/j.rser.2014.11.043.

[27] González-Portillo LF, Muñoz-Antón J, Martínez-Val JM. An analytical optimization of thermal energy storage for electricity cost reduction in solar thermal electric plants. Appl Energy 2017;185:531–46. https://doi.org/10.1016/j.apenergy.2016.10.134.

[28] Matino I, Colla V, Baragiola S. Quantification of energy and environmental impacts in uncommon electric steelmaking scenarios to improve process sustainability. Appl Energy 2017;207:543–52. https://doi.org/10.1016/j.apenergy.2017.06.088.

[29] Amrina E, Vilsi AL. Key performance indicators for sustainable manufacturing evaluation in cement industry. Procedia CIRP 2015;26:19–23. https://doi.org/10.1016/j.procir.2014.07.173.

[30] Gonzalez-Gil A, Palacin R, Batty P. Optimal energy management of urban rail systems: key performance indicators. Energy Convers Manage 2015;90:282–91. https://doi.org/10.1016/j.enconman.2014.11.035.

[31] Schmidt C, Li W, Thiede S, Kornfeld B, Kara S, Herrmann C. Implementing key performance indicators for energy efficiency in manufacturing. Procedia CIRP 2016;57:758–63. https://doi.org/10.1016/j.procir.2016.11.131.

[32] Kylili A, Fokaides PA, Lopez Jimenez PA. Key Performance Indicators (KPIs) approach in buildings renovation for the sustainability of the built environment: a review. Renew Sustain Energy Rev 2016;56:906–15. https://doi.org/10.1016/j.rser.2015.11.096.

[33] Lourenço P, Pinheiro MD, Heitor T. From indicators to strategies: Key Performance Strategies for sustainable energy use in Portuguese school buildings. Energy Build 2014;85:212–24. https://doi.org/10.1016/j.enbuild.2014.09.025.

[34] Samuel B, Agamuthu VP, Hashim MA. Indicators for assessment of sustainable production: a case study of the petrochemical industry in Malaysia. Ecol Ind 2013;24:392–402.

[35] Vestly Bergh LI, Hinna S, Leka S, Jain A. Developing a performance indicator for psychosocial risk in the oil and gas industry. Saf Sci 2014;62:98–106. https://doi.org/10.1016/j.ssci.2013.08.005.

[36] Drouineau M, Maïzi N, Mazauric V. Impacts of intermittent sources on the quality of power supply: the key role of reliability indicators. Appl Energy 2014;116:333–43. https://doi.org/10.1016/j.apenergy.2013.11.069.

[37] Stinner S, Huchtemann K, Müller D. Quantifying the operational flexibility of building energy systems with thermal energy storages. Appl Energy 2016;181:140–54. https://doi.org/10.1016/j.apenergy.2016.08.055.

[38] Xu P, Chan EHW, Qian QK. Success factors of energy performance contracting (EPC) for sustainable building energy efficiency retrofit (BEER) of hotel buildings in China. Energy Policy 2011;39:7389–98. https://doi.org/10.1016/j.enpol.2011.09.001.

[39] Wang J, Xie X, Lu Y, Liu B, Li X. Thermodynamic performance analysis and comparison of a combined cooling heating and power system integrated with two types of thermal energy storage. Appl Energy 2018;219:114–22. https://doi.org/10.1016/j.apenergy.2018.03.029.

[40] May G, Barletta I, Stahl B, Taisch M. Energy management in production: a novel method to develop key performance indicators for improving energy efficiency. Appl Energy 2015;149:46–61. https://doi.org/10.1016/j.apenergy.2015.03.065.

[41] Cassettari L, Bendato I, Mosca M, Mosca R. Energy Resources Intelligent Management using on line real-time simulation: a decision support tool for sustainable manufacturing. Appl Energy 2017;190:841–51. https://doi.org/10.1016/j.apenergy.2017.01.009.

[42] Toor SuR, Ogunlana SO. Beyond the "iron triangle": stakeholder perception of key performance indicators (KPIs) for large-scale public sector development projects. Int J Proj Manage 2010;28:228–36. https://doi.org/10.1016/j.ijproman.2009.05.005.

[43] Li Y, O'Donnell J, García-Castro R, Vega-Sánchez S. Identifying stakeholders and key performance indicators for district and building energy performance analysis. Energy Build 2017;155:1–15. https://doi.org/10.1016/j.enbuild.2017.09.003.

[44] Tanaka K. Assessment of energy efficiency performance measures in industry and their application for policy. Energy Policy 2008;36:2877–92. https://doi.org/10.1016/j.enpol.2008.03.032.

[45] Meier H, Lagemann H, Morlock F, Rathmann C. Key performance indicators for assessing the planning and delivery of industrial services. Procedia CIRP 2013;11:99–104. https://doi.org/10.1016/j.procir.2013.07.056.

[46] Bauer T, Breidenbach N, Pfleger N, Laing D, Eck M. Overview of molten salt storage systems and material development for solar thermal power plants. In: World renew. energy forum 2012, Denver, Colorado; 2012. p. 1–8. 234.

[47] Johnson M, Vogel J, Hempel M, Dengel A, Seitz M, Hachmann B. High temperature latent heat thermal energy storage integration in a co-gen plant. Energy Procedia 2015;73:281–8. https://doi.org/10.1016/j.egypro.2015.07.689.

[48] SolarReserve. Crescent Dunes; 2017. <http://www.solarreserve.com/en/global-projects/csp/crescent-dunes> [accessed April 10, 2018].

[49] Kuravi S, Trahan J, Goswami DY, Rahman MM, Stefanakos EK. Thermal energy storage technologies and systems for concentrating solar power plants. Prog Energy Combust Sci 2013;39:285–319. https://doi.org/10.1016/j.pecs.2013.02.001.

[50] Pelay U, Luo L, Fan Y, Stitou D, Rood M. Thermal energy storage systems for concentrated solar power plants. Renew Sustain Energy Rev 2017;79:82–100. https://doi.org/10.1016/j.rser.2017.03.139.

[51] Masters GM. Renewable and efficient electric power system. Hoboken, New Jersey: John Wiley & Sons, Inc.; 2004.

[52] Kuravi S, Goswami Y, Stefanakos EK, Ram M, Jotshi C, Pendyala S, et al. Thermal energy storage for concentrating solar power plants. Technol Innov 2012;14:81–91. https://doi.org/10.3727/194982412X13462021397570.

[53] Bauer T, Steinmann W, Laing D, Tamme R. Thermal energy storage materials and systems. Annu Rev Heat Transf 2012;15:131–77. https://doi.org/10.1615/AnnualRevHeatTransfer.2012004651.

[54] Banjaree B, Jayaweera D, Islam S. Smart power systems and renewable energy integration. Cambridge, United Kingdom: Springer International Publishing; 2016.

[55] Johnson M, Vogel J, Hempel M, Hachmann B, Dengel A. Design of high temperature thermal energy storage for high power levels. Sustain Cities Soc 2017;35:758–63. https://doi.org/10.1016/j.scs.2017.09.007.
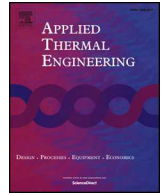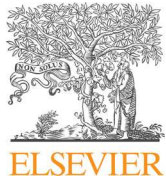
2.3.   Paper II: Finned-tube attachment methods

This article, entitled "Assembly and attachment methods for extended aluminum fins onto steel tubes for high temperature latent heat storage units," was published in *Applied Thermal Engineering*, vol. 144, pp. 96-105, copyright Elsevier, 2018. It was co-authored by Stefan Hübner, Markus Braun, Manfred Schönberger, Claudia Martin, Michael Fiß, Bernd Hachmann and Markus Eck and this author is the first author.

One of the concepts being developed for high temperature latent heat storages is an extended finned-tube in a shell-and-tube assembly. This concept can be used at high pressures for steam applications and can be built at a large scale. The design of the extended fins allowing for independent thermal expansion of the steel tubes and the aluminum fins with a physically possible assembly has not thus far been optimized. Due to the large fin surfaces necessary for transferring and storing large amounts of thermal energy, conventional finned-tube assemblies have to-date not been applicable for thermal energy storage systems.

Designs using spring steel clips on axial fins have been proven [72], using conservatively high numbers of clips. In this paper, this "clip" and a "crimp" mounting method are compared. Experiments were conducted to analyze the mechanical strength of the assembly; these are described and the results discussed. The results can be used for reducing costs and optimizing design of upscaled high temperature latent heat storages.

The author is responsible for the conceptualization, data curation, investigation, methodology, project administration, visualization and writing, as well as partially for the funding acquisition. Analysis of the two different attachment methods ("crimp" developed by Manfred Schönberger, "clip" developed at DLR), analysis of the experimental tests conducted in the mechanical removal testing and oversight hereof (carried out by Claudia Martin and Markus Braun), analysis of the experimental tests conducted in the cycling and movement measurement tests and oversight hereof (carried out by Michael Fiß) as well as data curation in collaboration with Stefan Hübner and Michael Fiß on the tests under operating conditions was also carried out by the author. Stefan Hübner assisted in the writing of the article and was the main reviewer of the article, as well as responsible for the conceptualization and formal analysis of the testing under operating conditions. The fins analyzed here were designed in collaboration with Bernd Hachmann. One fin was designed in collaboration with Stefan Hübner, the other two with the author. Markus Eck supervised the work and reviewed the article.

Research Paper

Assembly and attachment methods for extended aluminum fins onto steel tubes for high temperature latent heat storage units

Maike Johnson[a,*], Stefan Hübner[b], Markus Braun[a], Claudia Martin[a], Michael Fiß[a], Bernd Hachmann[c], Manfred Schönberger[d], Markus Eck[a,1]

[a] German Aerospace Center (DLR), Institute of Engineering Thermodynamics, Pfaffenwaldring 38-40, 70569 Stuttgart, Germany
[b] Linde AG, Seitnerstraße 70, 82049 Pullach, Germany
[c] F.W. Brökelmann GmbH & Co. KG, Oesterweg 14, 59469 Ense, Germany
[d] Linde AG, Carl-von-Linde-Straße 15, 83342 Tacherting, Germany

HIGHLIGHTS

- Clipping, crimping and heat shrinking of longitudinal fins onto tubes tested.
- Testing with thermal cycling in air and in salt conducted.
- Heat shrinking not stable under thermal cycling.
- Clipping maintains good thermal contact but is weaker than crimping.
- Crimping is a very strong bond but does not maintain contact over the fin length.

ARTICLE INFO

ABSTRACT

High temperature latent heat storages are being developed for both concentrating solar thermal power applications as well as integration in industrial processes. One of the concepts being developed is an extended finned-tube in a shell-and-tube assembly. This concept can be used at high pressures for steam applications and be built at a large scale. The design of the extended fins allowing for independent thermal expansion of the steel tubes and the aluminum fins with a physically possible assembly has not thus far been optimized. Due to the large fin surfaces necessary for storing large amounts of heat, conventional finned-tube assemblies have to date not been applicable for thermal energy storage systems.

Designs using spring steel clips on axial fins have been proven, using conservatively high numbers of clips. In this paper, various fin and tube diameters with spring steel clips as well as other mounting methods are compared. Experiments were conducted to analyze the mechanical strength of the assembly; these are described and the results discussed. In addition, two assembly methods were tested using the same fin geometry and testing environment, allowing for a thermodynamic comparison of the assemblies. The tests have shown that while the steel clips allow for the best heat transfer, the crimping method has a higher bond strength. These results can be used for reducing costs and optimizing design of high temperature latent heat storages.

1. Introduction

High temperature (> 100 °C) latent heat storages are in development for concentrating solar power as well as industrial applications [1–7]. Due to the varying integration requirements of the different systems, as well as research development of new technologies, several latent heat storage concepts have been developed such as micro/macro particle [8], metal foam [9], encapsulated phase change materials (PCM) [10] and moving PCM based systems [11,12]. The concept that has been researched at the greatest depth is a shell-and-finned-tube design. Finned-tube designs offer significant advantages with regard to heat transfer enhancement at low amounts of additional material and

---

are therefore the focus of this paper. These concepts have been researched by, among many others, Garcia et al. [13,14], Walter et al. [15], and Laing et al. [16].

One of the reasons for the variety of concepts in development is the relatively low thermal conductivity of PCMs. Nitrate salts can be used in the temperature range between 130 °C and 350 °C and have a thermal conductivity below 1 W/m K [17]. In finned-tubes in a shell-and-tube concept, the fins are designed to increase heat transfer to the storage medium on the shell side by extending the surface area for heat transfer using a highly conductive material. The shell-and-tube concept can be used at high pressures for steam applications. Large-scale shell-and-tube heat exchangers are built for power plants and industrial processes. An adaptation of these shell-and-tube heat exchangers for thermal energy storages is in testing or has been tested at a large scale by Garcia et al. [14] and Laing et al. [16].

Due to a pressurized heat transfer fluid (HTF), steel is the preferred tube material in finned-tube storage concepts. The fin material and design, on the other hand, are selected for very good thermal conduction and low storage material displacement. Various fin materials have been researched, including aluminum, graphite and steel, as discussed by Steinmann et al. in [10,18]. Aluminum has been shown to be a very good choice for temperatures up to 350 °C, due to its high thermal conductivity, malleability, availability and corrosion properties [19]. Aluminum has a higher coefficient of thermal expansion in comparison to steel, which can result in elevated stresses, dismantling of the fin-tube bond or a disconnection between the fin and tube materials, if the mounting type is not designed correctly. Therefore, this needs to be considered in the bi-metal finned-tube configuration for the thermal cycling operation of a thermal energy storage unit.

As the aim of the fins is to conduct heat between the HTF and the PCM, it is generally considered necessary to have a good thermal contact between the fins and the HTF containment (i.e. tubing). Recent theoretical research by Pizzolato et al. [20] has shown, however, that this may not be the case for storages with longer discharge times and lower power levels. This contact necessity needs to be further researched for various application requirements.

All of the above discussed factors result in the need for an extended fin (EF) with a bi-metal mounting method that withstands differing thermal expansion in thermal cycling. As discussed in Section 3, there are thus far no commercially available methods for assembling steel tubes with long/high aluminum fins, which are necessary for large energy capacities in latent heat thermal energy storage systems. The fin manufacturing and assembly also needs to be technically and economically feasible for a storage unit or system to be realized for large numbers of finned-tubes.

Thus far in the development of high temperature latent heat storages, the focus has been on concept development, geometry optimization, proof-of-concept testing and analysis of application integration. The analysis of specifics such as the feasibility and the economics of mounting fins onto tubes has not been the published research and development focus. With the build of larger scale storage units, this factor becomes more critical. These aspects were therefore analyzed and compared with large-scale realizable storages in mind, with a focus on longitudinal fin concepts. In this paper, three mounting methods are experimentally analyzed for their applicability in large scale high temperature latent heat storage units.

2. Description of extended finned-tube assemblies

In order to better discuss the differences in mounting methods, first the requirements and aspects of the fins and tubes in the EF tube assemblies are discussed. In EF tube assemblies for high temperature applications, steel tubing is used due to its strength at both higher temperatures and under pressure. Fins are used to increase the heat transfer surface area, thereby transferring the thermal energy more directly from the pressurized HTF into a greater portion of the PCM,

which is contained at or near atmospheric pressures. Since fin and tubing material displace PCM, a minimal volume should be introduced into the system in order to maximize the PCM volume and thereby storage capacity per volume of storage unit. The requirements of the tube and fin are detailed here, including brief information about three fin designs that were tested with the clipping mounting method.

2.1. Steel tubing

In an EF shell-and-tube latent heat storage unit, the tubing has to fulfill various requirements. It needs to withstand the pressure requirements of the HTF and temperature gradients between this fluid and the PCM during both charging and discharging. In order to assemble the pressure vessel, the material must be welded together and have acceptable corrosion properties with both the HTF (water/steam) and the PCM, in these cases nitrate salts. In addition, the tubing must transmit heat between the HTF and the PCM. For these requirements, the materials 16Mo3 or P265GH were used in the discussed work, depending on the temperatures and pressures operated. There are various manufacturing methods for seamless cold rolled steel tubes [21], resulting in outside diameters varying within either ± 1% or ± 0.5 mm, standardized in DIN EN 10216-2 (for tubes with < 210.1 mm outer diameter). This variation in outside diameter can lead to variations in the physical contact between fins and tubes.

2.2. Fin designs and considerations

The fin material in EF tube assemblies needs to have a high thermal conductivity, have good corrosion characteristics with the other materials and be both malleable or be able to be manufactured in a required and desired geometry as well as be affixed to the tube.

In this analysis, mounting methods for extruded aluminum axial fins are analyzed. The alloy EN AW 6060-T6 is used for the extrusion. The T6 heat treatment results in a considerably higher strength, which allows for less sensitive handling during the assembly process. Later, during operation above the precipitation hardening temperature (ca. 120 °C) [22], the strength drops again.

Three extruded aluminum fin designs have been developed and analyzed for differing applications within work done by the authors. Due to the application differences, the storage units have differing tube materials, wall thicknesses, tube diameters and tube pitches. The fin labeled 'A' is discussed in more detail by Seitz et al. [1] as well as in [23–26]. The fin labeled 'B' is discussed in more detail by Johnson et al. in [27] and [7] and the fin labeled 'C' is discussed in more depth by Laing et al. [13]. In this article, the focus is not on the geometry or design of the fins, as this has been discussed elsewhere.

The A-fins have been mounted both with clipping and with crimping. The B- and C-fins have been mounted using the clipping method.

3. Mounting methods of aluminum extended fins

Aluminum EF need to be attached to the steel tube to allow for both the differential thermal expansions of the metals as well as maintaining good thermal contact during thermal cycling. The mounting method needs to withstand corrosion between the steel, aluminum, nitrate salts and the mounting material itself. The method needs to be practical in terms of assembly methods and economically feasible for larger scale deployment. In this paper, the authors differentiate in terminology between the mounting method – how the fins are attached to the tube – and the assembly method – how this mounting method can be assembled to produce the mounted finned-tube.

3.1. State of the art

Finned-tubes are a common design feature in heat exchangers, and

as such have been widely developed and are commercially available from many companies. Methods for wrapping, extruding or shrinking the fins in various dimensions are available, among many others from [28–30]. Wrapping is a common method, resulting in a helical fin that can be welded, soldered or only affixed at the ends to the tubes. The fin material can also be wrapped into a pre-cut groove. The resulting fin can be serrated to allow for increased fin height at larger diameters, or can be crunched for increased turbulence on the fin side of the heat exchanger. In extruded fins, the fin material is mechanically rolled and pulled out of the tube material. This results in a uniform contact between fins and base, as it is one material. This base can be the tube itself or a second material attached to the tube. The fin height is, however, limited to a couple of centimeters. Fins can also be shrunk onto a tube by heating the fins and cooling the tube and then assembling the two. This method was analyzed for large fin heights in this work.

These existing methods are applicable for small fin spacings (< 5 mm) and small fin heights (< 20 mm), and only some of which can be used at temperatures up to 350 °C. The fin assembly methods have been developed for round fin cross-sections, which, in the case of a latent heat storage unit, lead to low packing densities of finned-tubes in the storage material and therefore would lead to large volumes of poorly used PCM. Due to these limitations in existing fin designs, EF with a higher fin height of 100 mm and more have been developed for latent heat storages.

Some of the analysis that has been done has been only theoretical in nature, analyzing which fin geometries would ideally be applicable under a variety of parameters. The methods applied in these works are, to some degree, purely mathematical and do not attempt to analyze the feasibility of the designs [31–33]. Fin designs analyzed theoretically as well as experimentally have been developed by, among others, Garcia et al. [13,14], Walter et al. [15], Laing et al. [16], as mentioned in the discussion of storage concepts. The focusses in these published works were on the analysis of the fins themselves or the storage components as a whole, and not on analyzing or optimizing the mounting method. Mounting methods have been tested by Urschitz et al. for longitudinal fin structures in [34], using hose clamps or so-called expansion-ears to hold the fins onto the tube. Both results were promising, with the bending ear likely being most applicable for large-scale design. However, further development work is necessary in terms of design and manufacturability. Other published analyses of bi-metal EF mounting methods are not known to the authors.

Three different mounting methods were developed and are analyzed here – heat shrinking the materials together, using plumber's crimps [35], and clipping of the fins to the tubes [36] – as shown in Fig. 1 (a), (b), and (c) respectively.

3.1.1. Heat shrinking

Heat shrinking was analyzed as a mounting method based on the thermal expansion of the fin material at higher temperatures prior to assembly onto a colder steel tube. This method has the benefits that it is well studied and known and that it introduces no new materials into the corrosion system.

The samples, shown in Fig. 1 (a) use a tube of 21.3 mm in diameter and an aluminum sheath with an outer diameter of 27.5 mm.

3.1.2. Crimping

In the crimping mounting method analyzed thus far, a so-called plumber's crimp was used to mount the fins onto the tube [35]. In this method, a part of the fins are removed from the fin bases, so that the crimp can be slid over both the tube and the fin bases. Samples used in one of the testing methods used an aluminum sheath instead of re-worked fins. One of these crimp sheath samples is shown in Fig. 1 (b).

This novel mounting method has been analyzed for its strength after thermal cycling (Section 4.1) and in a large lab-scale latent heat storage unit (Section 4.3). In this unit, a crimp was affixed around the tube and the inner fin layer using a Viega® press gun 5 with a constant pressure of 32 kN at the top of the fin length. At the bottom of the fin length, an overlapping crimp was mounted on an additional sheath, such that the fins were affixed radially but could move axially. The goal of this assembly technique was to allow for an axial expansion of the fin material during cycling, while maintaining a radial contact between fin and tube.

The development of an assembly method for this mounting style on a larger scale has not yet been conducted. As plumber's crimps are commercially available and standardized, these do not cost very much, and the strength of the crimping tool can be set as necessary. Three crimp sample types were analyzed, as shown in Table 1.

3.1.3. Clipping

The third mounting method analyzed uses spring-steel clips to hold the aluminum fins onto the steel tubing, as shown in Fig. 1 (c) [36]. The clips hold the fin, which is separated into segments, to the outer tube wall. Attachment nubs for the clips are designed into the fin geometry. The tube, fin, and clip parameters are shown in Table 2. Fig. 2 shows these parameters on the A-fin using a clipped fin/tube assembly for clarification of the terms.

The spring-steel type used in the clips, type 1.4310, maintains its shape and strength through the operable temperature ranges of aluminum. Therefore, this mounting method should allow for the differing thermal expansion of the aluminum and steel parts, while maintaining sufficient contact between fin and tube to have good heat transfer by conduction. Under pressure, at higher temperatures and during thermal expansion, the soft aluminum is pressed onto the steel tube, improving the contact.

Longitudinal EF using clips (with the C-fin design) have been tested in a lab-scale storage module operated up to 330 °C for approximately 200 cycles using sodium nitrate as the PCM [13], proving their feasibility.
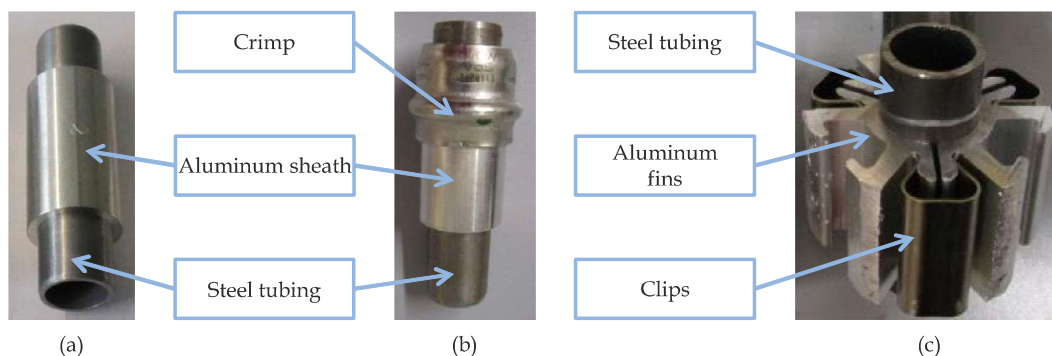

Fig. 1. Samples of mounting methods (a) heat shrinking, (b) crimping, and (c) clipping (with trimmed A-fins). The pictures show the mounting of either an aluminum sheath or the aluminum fins to steel tubing.

Table 1
Crimp sample parameters.

Parameter ↓ /Sample →	Unit	Carbon Steel crimp with Sheath (CS-S)	Stainless Steel crimp with Sheath (SS-S)	Carbon Steel crimp with Fin (CS-F)
Crimp material		Carbon steel	Stainless steel	Carbon steel
Sheath diameter	mm	27.5	27.5	34.9*
Tube diameter	mm	21.3	21.3	26.9

* The A-fin was used here with a base thickness of 4 mm as detailed in Fig. 2 and Table 2.

As the spring steel clips are costly to produce and at current rates of production cannot be standardized to reduce costs, minimizing the number of clips used per length of tubing is desirable. In addition, a better understanding of the strength of the connection in comparison to other methods can be gained by further testing.

4. Testing methods and experimental setup

In order to analyze the connection between fins and tubes, various factors need to be assessed. On the one hand, the connection needs to be mechanically stable, also after thermal cycling. On another hand, the connection needs to allow for a good thermal contact during storage operation. Several tests were constructed to analyze these factors.

The mechanical stabilities of the three mounting methods were assessed on a small scale after thermal cycling in a salt bath through physical removal of the mounting method.

The stability of the clipping method was analyzed in vertically mounted finned-tubes that were thermally cycled and analyzed for movement of the fins.

The two most promising mounting methods from the mechanical removal tests – clipping and crimping – were tested in a lab-scale storage unit, so that a direct comparison of charging and discharging characteristics as well as analysis of the bond pre- and post-operation was possible.

This testing spectrum allows for a more complete analysis of the various manufacturing factors than an analytical approach does. Each of these methods is described here, with the results and discussion following in sections 5 and 6.

4.1. Description of cycling and mechanical removal tests

One of the tests conducted is designed to assess the thermal cyclical stability of the strength of the different mounting methods. For this, samples were mounted in an apparatus and then pressure was applied to the 'fin' material in a pulling motion until either the maximum load of the pneumatic cylinder was reached or the 'fin' base was
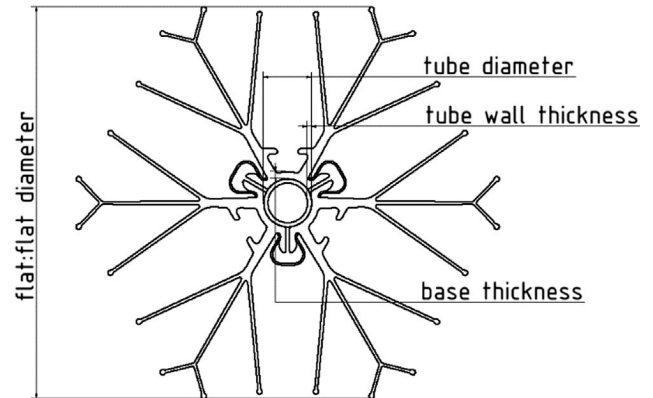
Fig. 2. Drawing of the A-fin assembled with clips to a steel tube showing the fin diameter, the fin base thickness and the tube diameter and wall thickness.

mechanically removed, thereby measuring how much force was needed to remove the fin material. The 'fins' in this test were either a sheath or a reduced fin geometry. Samples were either first thermally cycled in salt and then mounted in the apparatus and reheated to the operating temperature or only heated to the operating temperature and then tested, without prior cycling. These non-cycled samples tests are the reference samples.
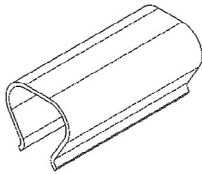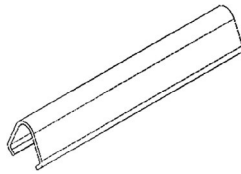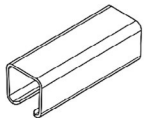
The samples were cycled in alumina crucibles containing sodium nitrate in thermal ovens. The samples of the heat shrinking and crimping methods were mounted using aluminum sheaths, as shown as an example in Fig. 1 (a) and (b) with an Al 6060 aluminum sheath as the 'fin base'. The samples of the clipping mechanism were assembled using fins. In these, the fin arms were removed, leaving the tube piece, clips and fin base as depicted in Fig. 1 (c) for the sample of the A-fin clip. This was done so that the samples fit in the crucibles; as the fin arms were not necessary, this was deemed acceptable.

The cycling was conducted between 250 °C and 350 °C, with a 2 K/min heating or cooling rate and a 2 h holding plateau. For each of the cycled samples, 100 cycles were conducted. Due to the length of the cycling, availability of samples and length of the project, two samples of each type were tested.

Samples are mounted into the pulling device as shown in Fig. 3. More detail is given in Fig. 4 in (a) a schematic and (b) a close-up picture.

A pulling mechanism is put over the sample, so that it can pull, via a pneumatic cylinder, on the aluminum 'fin base' to the right. A rod is slid through the steel tube and affixed with a washer and bolt of the same outer diameter as the tube, and held steady on the left. The sample is mounted in a tubular oven, in order to operate at defined temperatures (350 °C). The pneumatic cylinder pulls on the 'fin base' while distance

Table 2
Fin, tube and clip parameters for the analyzed clip assemblies.

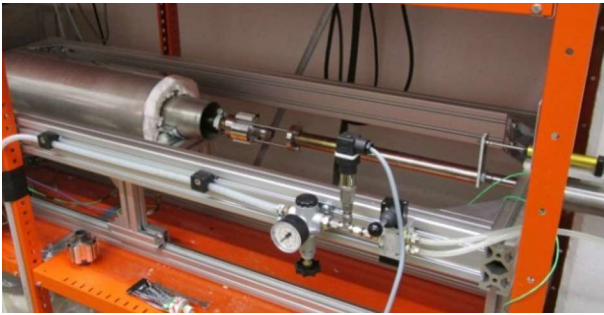| Parameter ↓/Fin →		Unit	A-fin	B-fin	C-fin
Tube	Material		P265GH	16Mo3	16Mo3
	Diameter	mm	26.9	17.2	21.3
	Wall thickness	mm	2.3	2.3	2.3
Fin	Hex-Diameter (flat:flat)	mm	218.58	68.19	149.0
	Base thickness	mm	4.0	2.0	2.5
Clip	Design (at same scale)				
	Length	mm	40	60	30
	No./Circumference		3	2	2

Fig. 3. Mechanical removal testing: Pulling device with tube held on the left while the pneumatic cylinder pulls the sheath the aluminum 'fin base' to the right shown, shown with the tubular oven open.

and load are measured. For initial tests, a smaller pneumatic cylinder with a maximum load of 1700 N was used. This was exchanged for a larger one with a maximal load of 2700 N in later experiments.

4.2. Description of cycling and movement measurement tests

In the gravity tests with vertically mounted finned-tubes, a test was constructed to determine the movement of fins on a tube during thermal cycling while subjected to gravity. To this end, tests were conducted using specimens with clipped-on fins, thermally cycled to assess movement. In this rig, tests are conducted using hot air on the HTF side of the finned-tube. On the PCM side of the finned-tube, air is heated but not circulated. The test infrastructure consists of an air heater mounted to a lower flange and an upper flange from which samples are hung, as shown schematically in Fig. 5. Surrounding the samples are removable heat tracing insulation units, and the entry and exit (top and bottom) of the testing area is closed off from the surroundings using insulation mats, in order to reduce the influence of natural convection.

The testing tube has up to 4 m of EF mounted onto it and is vertically suspended in the rig. Using adapters, various tube diameters and a fin diameter up to 130 mm can be tested. Thermocouples are used in the control of the heat tracing insulation. For added clarity, photos of the C-fin in the test rig are shown in Fig. 6.

The temperatures were cycled to mimic the temperature ranges of various PCMs, with heating and cooling cycle lengths set to 6 h each due to the low thermal conductivity of air. Testing of both the B- and the C-fins has been conducted. The A-fin is too large in outer diameter, so that these cannot currently be tested.

The heights of the fins were measured either using a laser distance measurement or a notched cable at the beginning and end of each cycle at room temperature. This simple comparison of the position allows for the determination of permanent movement, and therefore of the
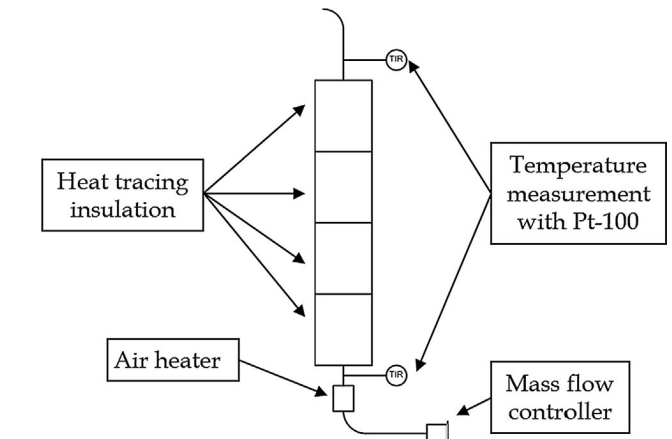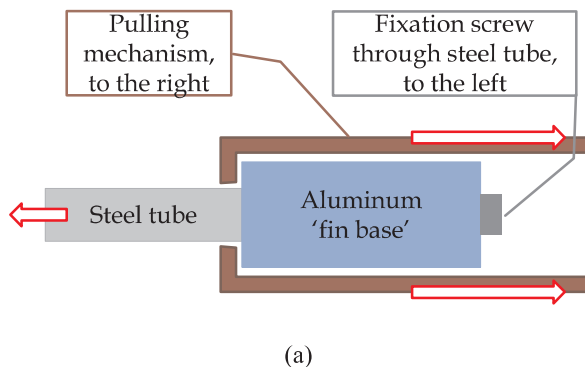

Fig. 5. Movement measurement testing: Schematic of the test rig for analyzing movement of the fins on a tube, showing the tube entering and exiting the heated insulated test section. The air in the tube is heated prior to entering the test section in the air heater at the bottom, and the temperature is measured at the entrance and exit of the test section. Mass flow is controlled prior to the heating of the air flow.

stability of the bond.

4.3. Description of testing under operating conditions

A storage unit was built to verify modeling of the A-fin geometry and to test several design features, as reported in [23–26]. A schematic of the storage unit and a picture of the assembled unit are shown respectively in Fig. 7 (a) and (b). Two mounting methods – crimping and clipping – were tested in this environment. This gives more insight into thermal cycling in salt of longer fin pieces and their mounting methods than can be determined from lab-scale oven tests. Data from thermocouples mounted in the PCM are used to compare similar test parameters for the thermodynamic properties of the fin-tube connection in a PCM environment.

The storage unit is built with an upper header from which the tube register hangs. This is surrounded by an insulated container with 3.3 tons of sodium nitrate as the PCM. The 18 finned tubes with a 0.8 m finned-tube length in this test rig are flanged between the two headers. These flanges make it possible to change tubes in the assembly. Thermal cycling was conducted up to 350 °C, with temperatures measured during cycling and optical analysis of the mounting method conducted before and after testing. A full set of tests were conducted with the clipping mounting method.

For the crimping mounting method, two central tubes were switched to this type of mounting method and comparative tests measured. Switching only two tubes allowed for a comparison between tubes in

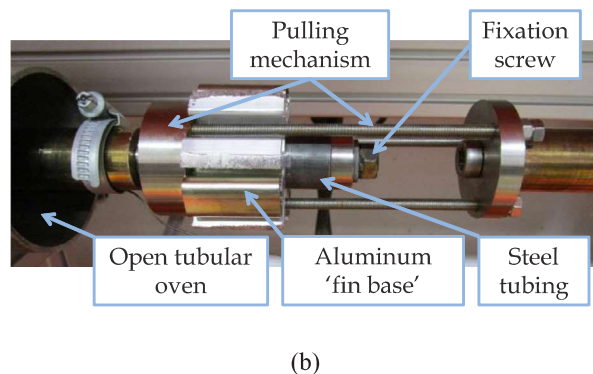(a)   (b)

Fig. 4. Mechanical removal testing: Pulling device with tube held on the left while the pneumatic cylinder pulls the sheath the aluminum 'fin base' to the right shown as (a) schematic and (b) picture.
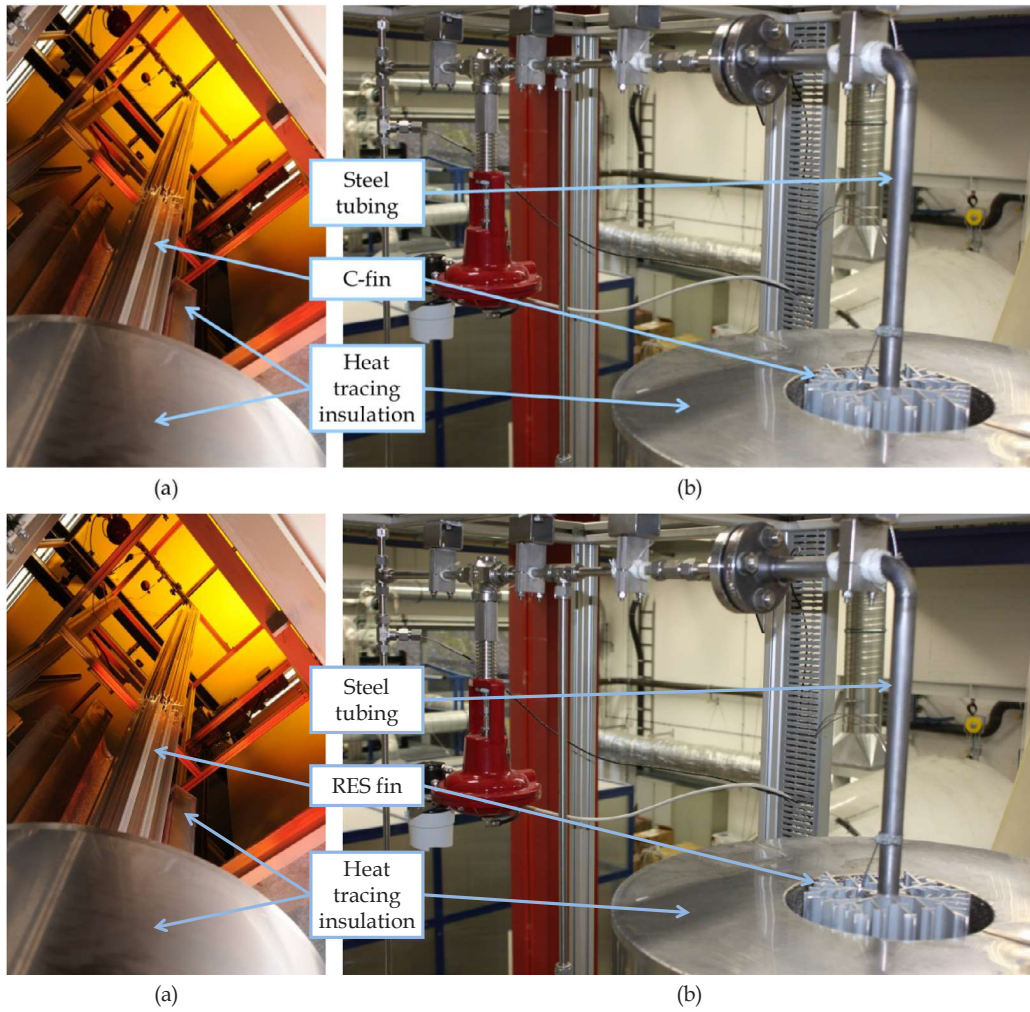
Fig. 6. Movement measurement testing: Pictures of the C-fin mounted in the gravity test rig, showing (a) the heat-trace insulation partially removed and (b) the top of the rig, with the fin at the top of the heat-trace insulation, shown without the insulation as a barrier.

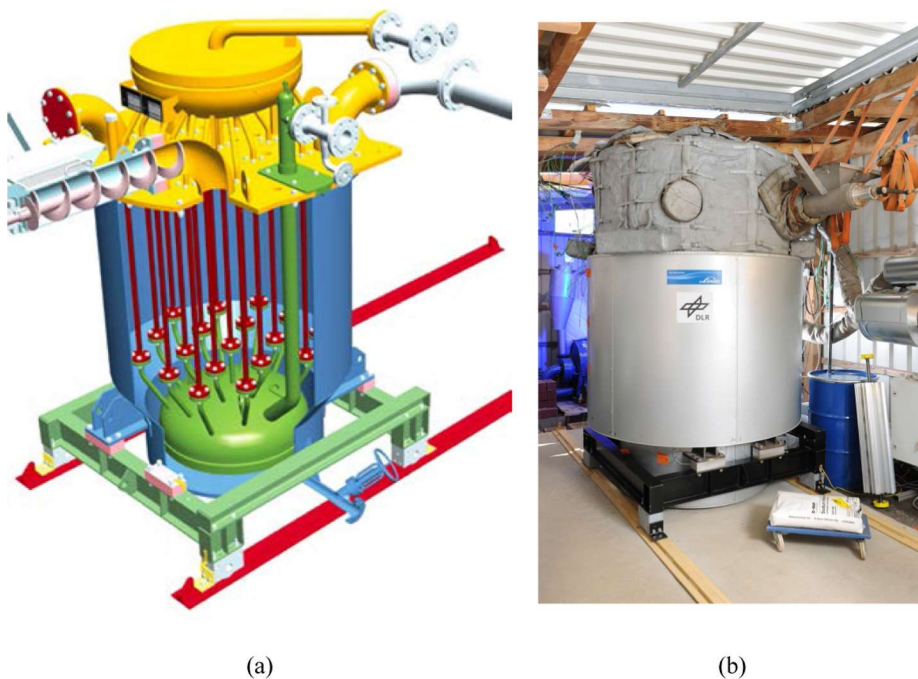**Fig. 7.** Operating condition testing: Laboratory scale storage unit for testing the optimized fin design and comparing the clipped and crimped fin-tube assemblies shown in (a) the design cut-out, without fins on the (red) tubes for clarity and (b) as-built in the testing environment. (For interpretation of the references to colour in this figure legend, the reader is referred to the web version of this article.)
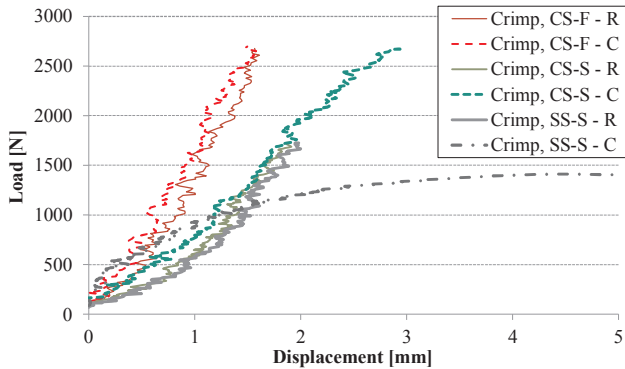
Fig. 8. Mechanical removal testing: Load displacement diagram of reference (R) and cycled (C) samples of the carbon steel (CS) and stainless steel (SS) fin (F) and sheath (S) based samples.

the same test, to ensure that other parameters remained the same.

5. Results

Results from the three testing methods – cycling and mechanical removal tests, cycling and movement measurement tests and testing under operating conditions – are described with the test plans in the following sections.

5.1. Results of cycling and mechanical removal tests

Mechanical removal tests were conducted with all three assembly methods. As the heat shrinking samples disassembled with gravity while removing them from the cycling crucible, all further work with this method was abandoned.

The load displacement diagrams comparing reference (uncycled) and cycled samples of three different crimp samples detailed in Table 1 are shown in Fig. 8. Data from one of the samples is shown. Results from the sample pairs were comparable.

Both crimp samples using a carbon steel crimp (CS-F in red/skinny and CS-S in green/mid-thickness) show no relevant change in the load displacement between a reference (R) and a cycled (C) sample. Due to the similar coefficient of thermal expansion of the carbon steel tube and the carbon steel crimp, the thermal cycling and elevated temperatures do not affect the mounting. In all four sample types, the aluminum sheaths could not be removed from the tubes. Also, a difference in general slope is observed, with the CS-F sample having a steeper slope. This shows that the sample is mounted even more firmly.

The SS-S sample (grey), on the other hand, has a significant loss of strength between the reference (R, solid) and cycled (C, dash) sample. The stainless steel crimp material has a slightly higher coefficient of thermal expansion in comparison to the tube material. This difference results in a loosening of the mounting at elevated temperatures and the removal of the aluminum sheath with a force of approximately 1500 kN. Thus, stainless steel crimps are not suitable in combination with carbon steel tubes.

In the clip samples shown in Fig. 9, the differences between reference (solid) and cycled (dash) samples is clear for all three types. The A-fin (blue) and C-fin (red) mountings are firm as reference samples; after cycling, both of the A-fin and C-fin mounting can be pulled along the tube, though the A-fin mounting requires a higher load. The B-fin (grey, thick) can be dismounted even in the reference state. After sampling, the B-fin (grey, dash) is moved constantly with increasing load.

5.2. Results of cycling and movement measurement tests

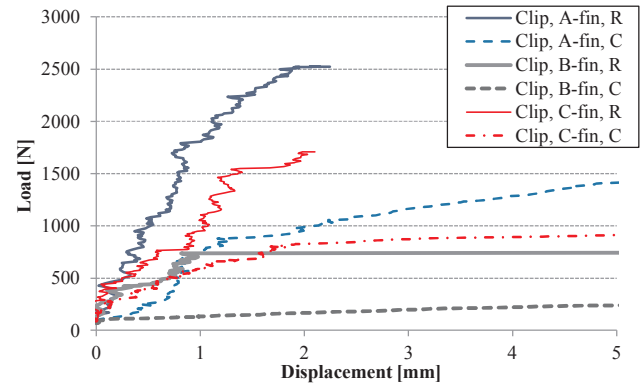Shown in Table 3 is a summary of the tests and results with the C-

Fig. 9. Mechanical removal testing: Load displacement diagram of reference (R) and cycled (C) samples of the clip mountings.

Table 3
Movement measurement testing: Test plan and results for the cycling and gravity tests. Each temperature range was cycled 100 times.

Fin	Fin length(s) [m]	Clips [%]	Lower and upper plateau temperatures [°C]	Movement
C-fin	2 * 2 m	50	100–220	none
			175–275	
			285–325	
	4 * 0.95 m	47	175–275	none
		40	285–325	
		27	Constant at 340	
		9.5	ca. 2 months	
B-fin	2 * 1.8 m	20	100–220	4 mm
			175–275	no further
			285–325	movement
		26	100–220	none
			285–325	none

and B-fins, mounted in the cycling and movement measurement test rig via clipping with different numbers of clips. The temperature was cycled between an upper and a lower temperature.

Two C-fin mountings were tested; one with two segments, each 2 m long, with 50% clips per length and the other with four fin segments, each 0.95 m long and with different numbers of clips. After each temperature range, the unit was cooled to room temperature and movement was checked. Thereafter, the next higher temperature range was cycled. None of the segments showed any enduring movement. All tests were conducted on the same inner tube. Dismantling of the fins from the tubes showed material deposits on the tube and grooves on the fins (see Fig. 10), showing evidence for a thermal weld between the aluminum and the steel during cycling and likely a very good thermal contact.

Two B-fin samples with 20% and 26% clips were tested, which were mounted in two 1.8 m sections per tube. In the 20% tests, with the lowest number of clips per length, there was 4 mm movement of the fins at the lowest cycling temperature range of 100–220 °C. There was no further movement during the higher temperature ranges. With 26% clips, there was no movement in any of the temperature ranges.

5.3. Results from testing under operating conditions

Various cycles were measured with both the clipping and the crimping mounting of the A-fins in the storage unit. First results were reported by Johnson et al. in [24]. The aspect of interest in this paper is the direct comparison of the thermodynamics of the two mounting methods as well as analysis of the fins and tubes after dismantling.

The analysis of a discharging cycle shows a large time difference between clipped and crimped finned-tubes in reaching a reference temperature. This reference temperature is set to 300 °C to make sure
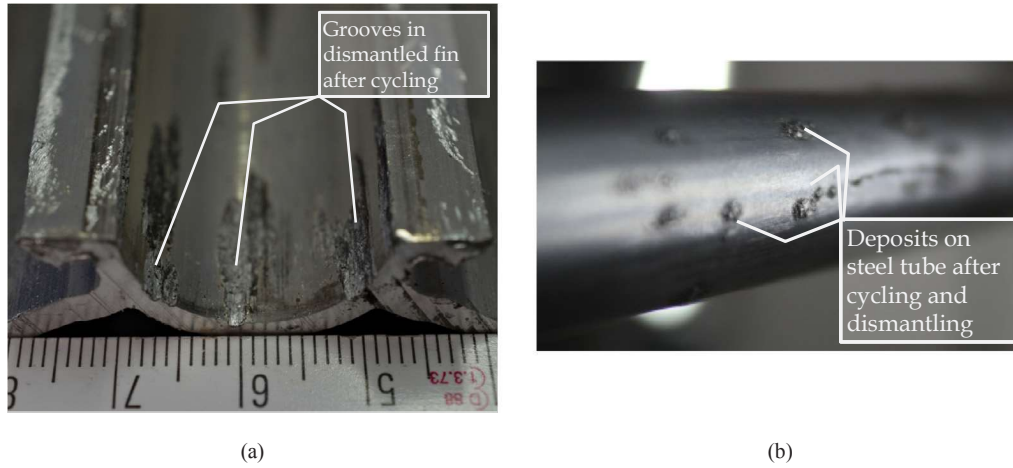
(a)   (b)

Fig. 10. Movement measurement testing: Material exchange and marking of fins after thermal cycling and dismantling of the fin-tube assembly in fins mounted with clipping to tube with (a) grooves in the fin on the mounting surface between fin and tube and (b) deposits on the steel tube.

Fig. 11. Operating condition testing: PCM temperature over time for two measurement positions during discharging with HTF temperature 20 K below PCM melting temperature for both clipped and crimped A-fin geometries.
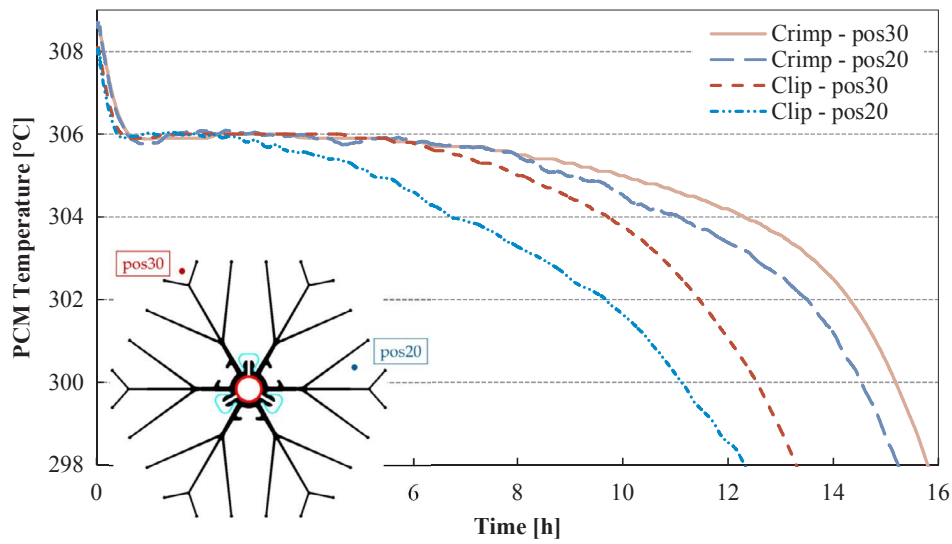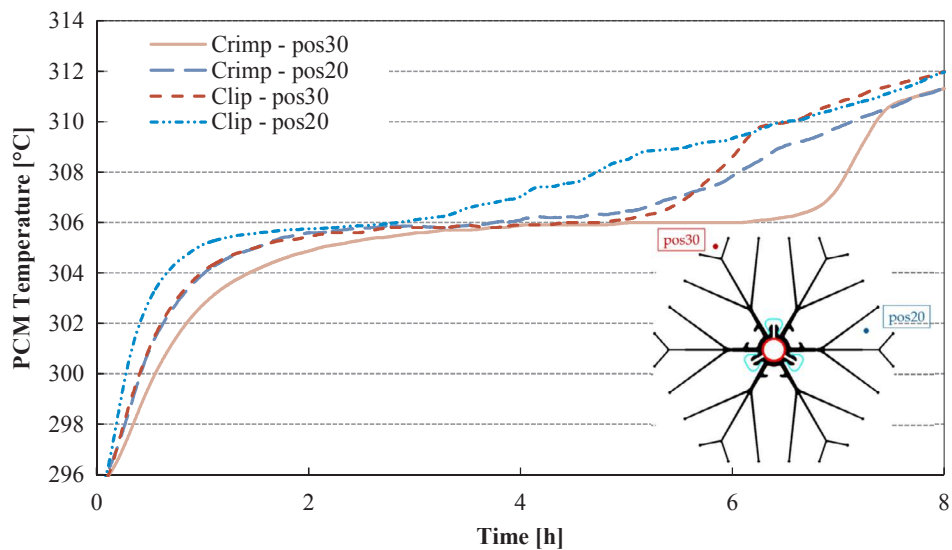

Fig. 12. Operating condition testing: PCM temperature over time for two measurement positions during charging with HTF temperature 20 K above PCM melting temperature for both clipped and crimped A-fin geometries.

that all PCM is solidified. Fig. 11 presents the results of a cycle with an HTF temperature that is 20 K below the melting temperature (306 °C) for two thermocouple measurement positions (pos20 and pos30) in the fin geometry of the central tube's middle measurement level. The measurements at other positions are discussed in [24]; these positions were chosen for analysis for their representative positions. The blue lines refer to pos20 for both the clipped and crimped mounting and the red lines refer to pos30 of the same. The crimping method results in a several hour slower discharge with +27% and +21% for the two positions under the same conditions. This shows that the heat transfer is much better in the clipped mountings than in the crimped ones.

A similar behavior is observed when analyzing a charging cycle with an HTF temperature that is 20 K above the PCM's melting temperature. The reference temperature for measuring the time difference is set to 306.3 °C for two reasons. First, in contrast to the solidification process, a clear end of the phase change process is visible. Secondly, the natural convection balances the temperature distribution with the PCM, meaning that the temperature increase in positions that melted early is slowed down. Once all of the PCM is melted, the temperature increases uniformly in all positions. This effect is not observed in the solidification process because of the heat transfer limitation due to heat conduction only. This limitation during solidification has been shown in [24] and can be observed by comparing the much faster melting time in Fig. 12 to the slower solidification time shown in Fig. 11 for comparable test conditions.

Fig. 12 also compares the clipping and crimping mounting method using the A-fin geometry, based on the temperature for the pos20 and pos30 in the central tube's medium measurement level. Again, this tube is chosen for its representative results. The figure shows a significantly slower melting time and, thus heat transfer for the crimping mounting method differing by +41% for pos20 and +30% for pos30.

After the experiments were concluded, the tubes were dismantled. In the clipped fins and tubes, there was a constant layer of rust along the entire fin length, as shown in Fig. 13(a). This shows that there were large surface areas with contact between the fins and tubes, confirming the results of the cycling and movement measurement tests discussed above.

Dismantling of the crimping showed no rust on the fins (Fig. 13(b)). In addition, a gap had developed between the tubes and the fins, shown by the fin deformation in Fig. 13(c). The fins were mounted with a fixed bearing crimping at the top and a sliding bearing crimping at the bottom, to allow for thermal expansion. A radial expansion in the middle of the fins was expected, as the fins were held radially only at the top and bottom. However, the size of the gap, also at the bottom of the tube, suggests that the sliding bearing did not slide as much as would have been necessary for an acceptable level of thermal contact. With a gap between the fin and the tube, there is no good thermal contact. This explains the much slower cycle times seen in Figs. 11 and 12.
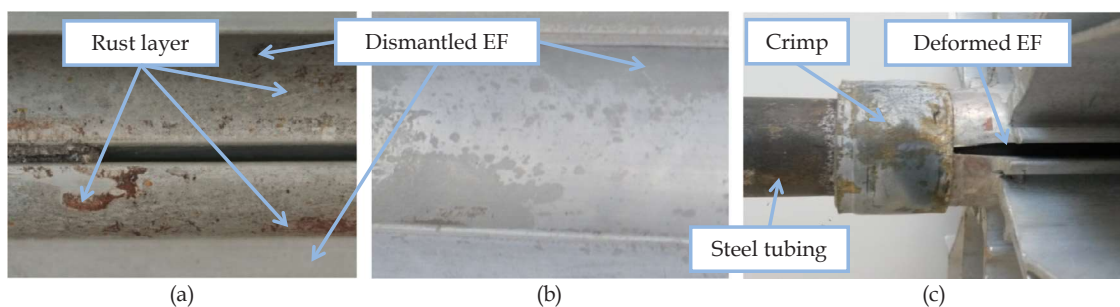
6. Discussion

The mechanical removal of the mounting method only gives insight into one bond, and not the strength created by the friction of an entire fin length pressed to an entire tube length. Therefore, the results for the clipping method in the mechanical removal tests are conservative. In addition, testing of a larger number of samples would strengthen the results shown here.

The movement measurement tests were conducted with air as both the HTF and the surrounding 'storage material'. In a storage unit, there is PCM salt around the tubes and aluminum fins. Salt has a negative change in volume from the liquid to the solid state, see [17], so that any salt that creeps between the fins and tubes does not expand during solidification as water/ice does, but shrink. Therefore, a ratcheting of the space between fin and tube would not occur. The results show that a possible issue of concern – the softness of aluminum at higher temperatures – is actually of little concern. Even the B-finned-tube with only 20% and the C-fin with 9.5% clips per tube showed no movement at higher temperatures. This is likely due to the weld-type bond formed between the aluminum and steel at higher temperatures with the movement of the materials in thermal expansion.

Testing under operating conditions showed that the crimping method has significantly slower discharge times than the clipping method. This time difference is caused by a gap between the HTF tube and the fins, limiting the heat transfer at this interface. Both charge and discharge cycles show similar time differences, meaning that the main heat transfer limitation is caused by this gap, but not by the dominant heat transfer between PCM and fin, i.e. heat conduction during discharge and natural convection during charging. However, for a detailed understanding of the creation of the gap and the quantitative heat transfer performance, further research with a different experimental setup is necessary.

Apart from the mentioned assembly methods, first trials were conducted by soldering the fins to the steel tubes. The trials at ambient temperatures showed promising results with regard to the bond strength, but further development and testing concerning the assembly method and thermal cycling is required.

7. Conclusions

Although these tests were conducted with a variety of tubes and fins as described above, the combination of all of these tests gives good insight into the methods of creating a durable mounting method in finned-tube assemblies in high temperature latent heat storages. Only the clipping method showed promising results with regard to the bond strength and the heat transfer performance. The crimping method offered the highest bond strength, but could not achieve a similar heat transfer performance as achieved for the clipped tubes. Finally, the heat shrinking method proved not to be feasible due to the missing bond strength at high temperatures.

However, to better understand why the gap for the crimping method

Fig. 13. Operating conditions testing: Dismantled components after testing under operating conditions. Inner side of a fin from a (a) clipped assembly and (b) crimped assembly. (c) Crimped assembly showing gap between fins and tube.

occurred, a more detailed analysis of a single finned-tube and the fin-tube connection is recommended. First gravity cycling tests for the preferred clipping mounting method show that even with a low number of clips per tube, the fin can be held through thermal cycling. Another possibility is to combine the crimping and clipping methods for ensuring both a high bond strength as well as sufficient thermal contact. These results can be used for reducing costs and optimizing design of high temperature latent heat storages.

References

[1] S. Kuravi, J. Trahan, D.Y. Goswami, M.M. Rahman, E.K. Stefanakos, Thermal energy storage technologies and systems for concentrating solar power plants, Prog. Energy Combust. Sci. 39 (2013) 285–319, https://doi.org/10.1016/j.pecs.2013.02.001.

[2] M. Seitz, S. Hübner, M. Johnson, Detailed partial load investigation of a thermal energy storage concept for solar thermal power plants with direct steam generation, AIP Conf. Proc. 1734 (2016) 050042, , https://doi.org/10.1063/1.4949140.

[3] B. Cárdenas, N. León, High temperature latent heat thermal energy storage: Phase change materials, design considerations and performance enhancement techniques, Renew. Sustain. Energy Rev. 27 (2013) 724–737, https://doi.org/10.1016/j.rser.2013.07.028.

[4] M. Kabbara, D. Groulx, A. Joseph, Experimental investigations of a latent heat energy storage unit using finned tubes, Appl. Therm. Eng. 101 (2016) 601–611, https://doi.org/10.1016/j.applthermaleng.2015.12.080.

[5] M.D. Muhammad, O. Badr, Performance of a finned, latent-heat storage system for high temperature applications, Appl. Therm. Eng. 116 (2017) 799–810, https://doi.org/10.1016/j.applthermaleng. 2017.02.006.

[6] A. Kumar, S.K. Saha, Energy and exergy analyses of medium temperature latent heat thermal storage with high porosity metal matrix, Appl. Therm. Eng.109, Part B (2016) 911–923, https://doi.org/10.1016/j.applthermaleng. 2016.04.161.

[7] M. Johnson, J. Vogel, M. Hempel, A. Dengel, M. Seitz, B. Hachmann, High Temperature latent heat thermal energy storage integration in a co-gen plant, Energy Procedia 73 (2015) 281–288, https://doi.org/10.1016/j.egypro.2015.07.689.

[8] L.C. Chow, J.K. Zhong, Thermal conductivity enhancement for phase change storage media, Int. Commun. Heat Mass Transfer 23 (1996) 91–100, https://doi.org/10.1016/0735-1933(95)00087-9.

[9] Z.G. Wu, C.Y. Zhao, Experimental investigation of porous materials in high temperature thermal energy storage systems, Sol. Energy 85–7 (2011) 1371–1380, https://doi.org/10.1016/j.solener.2011.03.021.

[10] W.-D. Steinmann, D. Laing, R. Tamme, Latent heat storage systems for solar thermal power plants and process heat applications, J. Solar Energy Eng., Trans. ASME 132 (2010) 210031–210035, https://doi.org/10.1115/1.4001405.

[11] V. Zipf, A. Neuhäuser, D. Willert, P. Nitz, S. Gschwander, W. Platzer, High temperature latent heat storage with a screw heat exchanger: design of prototype, Appl. Energy 109 (2013) 462–469, https://doi.org/10.1016/j.apenergy.2012.11.044.

[12] H. Pointner, W.-D. Steinmann, M. Eck, Introduction of the PCM flux concept for latent heat storage, Energy Procedia 57 (2014) 643–652, https://doi.org/10.1016/j.egypro.2014.10.219.

[13] P. Garcia, M. Olcese, S. Rougé, Experimental and numerical investigation of a pilot scale latent heat thermal energy storage for CSP power plant, Energy Procedia 69 (2015) 842–849, https://doi.org/10.1016/j.egypro.2015.03.102.

[14] P. Garcia, S. Rougé, P. Nivelon, Second test campaign of a pilot scale latent heat

thermal energy storage – durability and operational strategies, AIP Conf. Proc. 1734 (2016) 050016, https://doi.org/10.1063/1.4949114.

[15] H. Walter, A. Beck, M. Hameter, Transient analysis of an improved finned tube heat exchanger for thermal energy storage system, in: ASME 2015 9th International Conference on Energy Sustainability, ES 2015, Collocated with the ASME 2015 Power Conference, the ASME 2015 13th International Conference on Fuel Cell Science, Engineering and Technology, and the ASME 2015 Nuclear Forum, 2015. doi: 10.1115/ES2015-49144.

[16] D. Laing, T. Bauer, N. Breidenbach, B. Hachmann, M. Johnson, Development of high temperature phase-change-material storages, Appl. Energy 109 (2013) 497–504, https://doi.org/10.1016/j.apenergy.2012.11.063.

[17] T. Bauer, D. Laing, R. Tamme, Characterization of sodium nitrate as phase change material, Int. J. Thermophys. 33 (2012) 91–104, https://doi.org/10.1007/s10765-011-1113-9.

[18] W.-D. Steinmann, D. Laing, R. Tamme, Development of PCM storage for process heat and power generation, J. Solar Energy Eng., Trans. ASME 131 (2009) 410091–410094, https://doi.org/10.1115/1.3197834.

[19] D. Laing, T. Bauer, D. Lehmann, C. Bahl, Development of a thermal energy storage system for parabolic trough power plants with direct steam generation, J. Solar Energy Eng., Trans. ASME 132 (2010) 210111–210118, https://doi.org/10.1115/1.4001472.

[20] A. Pizzolato, A. Sharma, K. Maute, A. Sciacovelli, V. Verda, Topology optimization for heat transfer enhancement in latent heat thermal energy storage, Int. J. Heat Mass Transf. 113 (2017) 875–888, https://doi.org/10.1016/j.ijheatmasstransfer.2017.05.098.

[21] K.-H. Brensing, B. Sommer, Steel Tube and Pipe Manufacturing Processes, (n.d.). http://www.smrw.de/files/steel_tube_and_pipe.pdf.

[22] Aluminium-Zentrale, Aluminium-Taschenbuch, Aluminium-Verlag: Düsseldorf, 14. Auflage, 1983. ISBN-13: 9783870171698.

[23] S. Hübner, M. Eck, C. Stiller, M. Seitz, Techno-economic heat transfer optimization of large scale latent heat energy storage systems in solar thermal power plants, Appl. Therm. Eng. 98 (2016) 483–491, https://doi.org/10.1016/j.applthermaleng.2015.11.026.

[24] M. Johnson, S. Hübner, C. Reichmann, M. Schönberger, M. Fiß, Experimental analysis of the performance of optimized fin structures in a latent thermal energy storage test rig, AIP Conf. Proc. 1850 (2017) 080013, https://doi.org/10.1063/1.4984434.

[25] C. Reichmann, Untersuchungen zum Wärmeübergang in Hochtemperatur-Latentwärmespeichern, Universität Stuttgart (2016).

[26] M. Johnson, S. Hübner, DSG-Store Projektabschlussbericht, DLR Linde AG (2016), https://doi.org/10.2314/GBV:871999897.

[27] M. Johnson, J. Vogel, M. Hempel, B. Hachmann, A. Dengel, Design of high temperature thermal energy storage for high power levels, Sustain. Cities Soc. 35 (2017) 758–763, https://doi.org/10.1016/j.scs.2017.09.007.

[28] Energy Transfer, n.d. http://www.finnedtube.com/05.04.2018.

[29] Wieland-Werke, n.d. http://www.wieland-thermalsolutions.com/internet/en/products/finned_tubes/hochberippte_rohre/Hochberippte_Rohre.jsp, 05.04.2018.

[30] Schmöle, n.d., http://www.schmoele.de 05.04.2018.

[31] A. Sciacovelli, V. Verda, Second-law design of a latent heat thermal energy storage with branched fins, Int. J. Numer. Meth. Heat & Fluid Flow 26 (2) (2016) 489–503.

[32] A. Pizzolato, A. Sharma, K. Maute, A. Sciacovelli, V. Verda, Design of effective fins for fast PCM melting and solidification in shell-an-tube latent heat thermal energy storage through topology optimization, Appl. Energy 208 (2017) 201–227, https://doi.org/10.1016/j.apenergy.2017.10.050.

[33] S. Ziaei, S. Lorente, A. Bejan, Morphing tree structures for latent thermal energy storage, J. Appl. Phys. 117 (2015) 22, https://doi.org/10.1063/1.4921442.

[34] G. Urschitz, H. Walter, J. Brier, Experimental investigation on bimetallic tube compositions for the use in latent heat thermal energy storage units, Energy Convers. Manage. 125 (2016) 368–378, https://doi.org/10.1108/HFF-01-2015-0040.

[35] H. Posselt, M. Schöneberger, S. Hübner, Heat transfer tube, heat transfer reservoir and method for producing a heat transfer tube, WO/2017/016656, 02.02.2017.

[36] B. Hachmann, T. Bauer, Heat Transfer Tube – Wärmeübertragungsrohr, WO2011/069693-A1, n.d.

2.4. Paper III: Thermal storage design

This article, entitled "Design of High Temperature Thermal Energy Storage for High Power Levels," was first presented at *Greenstock* in Beijing, China, May 2015, and later published in *Sustainable Cities and Society*, vol. 35, pp. 758-763, copyright Elsevier, 2017 and was co-authored by Julian Vogel, Matthias Hempel, Bernd Hachmann and Andreas Dengel. This author is the first author.

The storage system was designed and analyzed with the development of an iterative multi-step method allowing for upscaling in both power and capacity as well as design for specific system requirements. The method spans from the design of the fin, based on both empirical and geometrical information, to the heat transfer analysis of a storage system. The analysis is comprised of several steps: a heat transfer analysis of the cross-section of one tube without modeling the heat transfer fluid, a transfer from the cross-section to a simplified one-dimensional radial model and a two-dimensional axial and radial analysis coupling the axial flow of the heat transfer fluid and the radial heat transfer into the storage. The developed analysis method and the resulting storage system are presented and the comparison of different fin designs shows the suitability of each fin for different applications. The upscaling in thermal power leads to the development of a very dense fin structure and tight tube-spacing. The upscaling in capacity leads to the development of a design model with capabilities for analysis of thermal losses and possible non-ideal flow through the headers. With the development of a design method from system parameters to fin design, tube length and tube number, storage units and systems can be thermally designed.

The author is responsible for the conceptualization, data curation, formal analysis, funding acquisition, the overall methodology, project administration, supervision, as well as the writing of the original draft of the paper. Julian Vogel primarily developed the specific methodology for two-dimensional numerical analysis of temperature and phase change of a cross-section, including formal analysis, visualization, writing of parts of the methods and review and editing of the paper. Matthias Hempel primarily developed the methodology for reduction to a one-dimensional simplified model, including formal analysis, some of the visualization and review and editing of the paper. Bernd Hachmann assisted in the design of the fin analyzed in the formal analysis. Andreas Dengel provided system data resources for the development of the storage design.
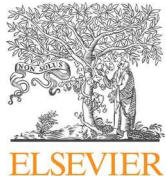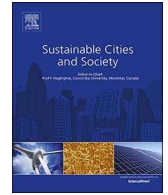
Design of high temperature thermal energy storage for high power levels ☆

Maike Johnson[a],[*], Julian Vogel[a], Matthias Hempel[a],[1], Bernd Hachmann[b], Andreas Dengel[c]

[a] German Aerospace Center(DLR), Pfaffenwaldring 38-40, 70569 Stuttgart, Germany
[b] F.W. Brökelmann GmbH & Co. KG, Oesterweg 14, 59469 Ense-Höingen, Germany
[c] Steag New Energies, St. Johannerstraße 101-105, 66115 Saarbrücken, Germany

ABSTRACT

A latent heat thermal energy storage unit has been modeled, simulated and designed for integration into a cogeneration plant that supplies steam to industrial customers in Saarland, Germany. The design consists of a vertical bundle of extended finned tubes surrounded by phase change material in the shell. The heat transfer fluid water/steam flows through the tubes between the upper and lower headers. A new fin design was developed to achieve the required high power levels.

The storage system was designed and analyzed with the development of an iterative multi-step method. The method spans from the design of the fin, based on both empirical and geometrical information, to the heat transfer analysis of a storage system. The analysis is comprised of several steps: a heat transfer analysis of the cross-section of one tube without modeling the heat transfer fluid, a transfer from the cross-section to a simplified one-dimensional radial model and a two-dimensional axial and radial analysis coupling the axial flow of the heat transfer fluid and the radial heat transfer into the storage. The developed analysis method and the resulting storage system are presented and the comparison of different fin designs shows the suitability of each fin for different applications.

1. Introduction

A thermal energy storage unit is to be integrated into a cogeneration plant. This storage will act as an intermediate back-up to a gas turbine coupled with a heat recovery steam generator (HRSG), so it is situated in parallel to the HRSG, between the feedwater pump and the steam main. This layout is shown in Fig. 1. This plant produces steam for several customers, including one with very specific and constant steam quality requirements.

Currently, a fossil-fuel fired standby boiler is maintained at warm load and in the case of a turbine trip, is heated from warm to full load in two minutes. The storage unit will be integrated so that it is kept on standby and the backup boiler will be reduced to cold load, which requires significantly less fossil fuel. From cold load, the backup boiler needs 15 min to reach full load. During this time, the storage unit will produce the required 6 MW of superheated steam at 26 bar and a minimum of 300 °C for the industrial customer. This combination of parameters leads to a minimum required capacity of 1.5 MW h. The standby storage unit is being developed as a latent heat energy storage unit. Using the latent heat of fusion of the storage material side with a

solidification temperature near the required steam temperature, the volume of the entire storage unit is reduced in comparison to a sensible heat storage unit. Latent heat energy storage allows for a leveling of the discharge temperature due to isothermal phase change. The planned integration is discussed in more detail by Johnson et al. (2015).

2. Methodology

Preliminary design considerations and a combination of heat transfer simulation methods are used for the development of a latent heat thermal energy storage unit for a specific application, and moreover one that produces superheated steam.

2.1. Preliminary design

The system into which the storage unit is to be integrated determines the required parameters: charging and discharging temperature, pressure and heat transfer fluid (HTF), discharging power and capacity. As the HTF in this system is water/steam, a latent heat thermal energy storage using the heat of fusion for heat storage was
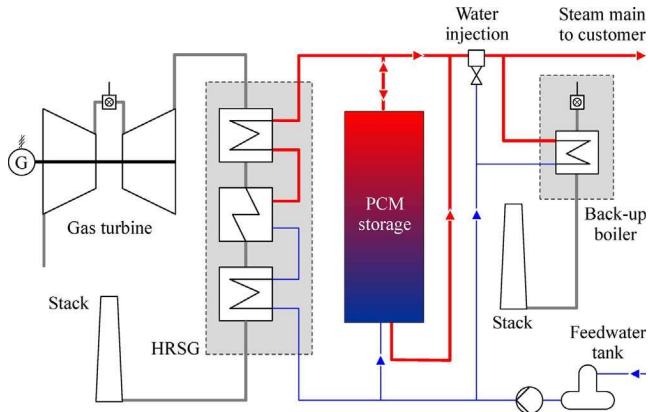
Fig. 1. Layout of the cogeneration plant showing the latent heat thermal energy storage integrated in parallel to the HRSG and the back-up boiler.

developed. Both the HTF and the phase change material (PCM) maintain a constant temperature during phase change, which allows for small temperature differences between the two media during both charging and discharging (Seitz, Cetin, & Eck, 2014). The inherent properties of the storage material determine the phase change temperature and heat of fusion, so that a storage material must be selected that is appropriate for the system requirements, specifically for the pressure and temperature of the HTF. Based on the system parameters for charging and discharging the storage unit, sodium nitrate (NaNO₃) with a melting temperature of 306 °C and a latent heat of 178 J/g was chosen as the storage material.

Ideally, the storage material has a high thermal conductivity in order to charge and discharge quickly. However, most applicable materials have low thermal conductivities (Kenisarin, 2010). To overcome low thermal conductivity, various designs and storage concepts have been researched and tested (Mehling & Cabeza, 2008). In this case, a vertically finned tube concept using extruded aluminum fins clipped onto steel tubes was chosen. The developed storage system design is an adaptation of a shell and tube heat exchanger, with extended finned tubes mounted between two headers and the PCM storage medium on the shell side of the tube bundle. The HTF evaporates in the tube bundle. Various storage units at DLR have been tested with extended fins (Steinmann, Laing, & Tamme, 2009), including an evaporator/condenser storage (Laing et al., 2012).

As the storage unit required by the system in this project requires only 15 min of discharge time, the ratio of power level to capacity is very high. In the latent heat TES unit built and tested within the ITES project in Carboneras, Spain, a capacity of ca. 700 kW h, a peak power level of ca. 700 kW (Laing et al., 2012) and steady-state of 200 kW were measured (Laing, Bauer, Breidenbach, Hachmann, & Johnson, 2013). Due to the higher ratio of power to capacity required in this application, both a smaller tube spacing and a denser fin structure are required. The tube spacing has been set at a triangular formation to optimize the space between tubes, which results in a regular hexagonal spacing of the tubes.

With this spacing, an empirically designed axial fin is drafted. Due to the method of aluminum extrusion, the initial design combines manufacturing feasibility, assembly techniques and heat transfer requirements. The extrusion feasibility must be considered: the ratio of length-to-width of the areas between the branches of aluminum has to be small in order to avoid a failure in the tooling for the extrusion. A fixation nub for the clips and room for assembly of the clips over the two fin halves have to be incorporated as well.

The heat transfer aspects of the design allow for heat to be transferred between the HTF and the PCM. For high power levels, the distance or resistance from the storage material to the HTF needs to be minimized, as researched by Sciacovelli and Verda (2016), Hübner,

Eck, Stiller, and Seitz (2016), and Ziaei, Lorente, and Bejan (2015). Research from Sciacovelli & Verda approached the problem with CFD calculations including calculations of entropy generation in an iterative design process. Hübner et al. also used an iterative design approach with two-dimensional calculations, analyzing the designs for discharging parameter comparisons and including economic considerations in the comparisons. Ziaei et al. uses a constructal analytical approach for the calculations of the charging characteristics, analyzing the effects of branching on the melting characteristics. Reduction of this resistance can be achieved with evenly distributed highly conductive aluminum introduced into the storage material. The simplest such design is a star form, with 'rays' going out from a central tube. This results in a large proportion of the aluminum near the central tube, with much less material further from the tube. To have a better heat transfer between the outer areas of storage material and the central tube, a branched design was developed, so that in the outer areas of the fin the surface area is further increased by branches in the fin.

2.2. Numerical heat transfer model

For the numerical simulation of the heat transfer, a subsystem of the tube register, consisting of a single tube with mounted fins and surrounding PCM, is simulated; see Fig. 2(a). The HTF flows through the tube and evaporates or condenses while transferring heat to or from the PCM. Because of the complex geometry with different fluid and solid zones as well as a long tube length, the system is simplified to reduce the simulation effort. Three steps lead to the final simulation result: a heat transfer analysis of the cross-section of one tube without modeling the heat transfer fluid, a transfer from the cross-section to a simplified one-dimensional radial model and a two-dimensional axial and radial analysis coupling the axial flow of the heat transfer fluid and the radial heat transfer into the storage.

The material properties used in these models for this application for the tube, the fin and the PCM at its melting temperature are given in Table 1. The properties of the PCM are mean values of the solid and liquid state near the melting temperature. The mean material properties lead to a maximum deviation of 2.7% in the thermal diffusivity, which is acceptable for this study and simplifies the modeling approach significantly.

The first step of the analysis is a heat transfer analysis of a detailed two-dimensional cross-section with constant boundary conditions, which is conducted using a model implemented in ANSYS® FLUENT®. The fin design shown here has two symmetry lines that allow for simplification to a quarter section. For this first step, reference conditions are used. This includes a constant temperature boundary condition on the inside tube wall that results in a fixed temperature difference between the phase change temperature and the discharging temperature. For evaluation, the heat transfer rate and the state of charge (SoC) are recorded over time. These are regarded as characteristic curves for the cross-section. The simulation mesh, simulation state of temperature and the resulting characteristic curves are shown in Fig. 2(b), respectively from top to bottom. These results show qualitatively how the distribution of the aluminum across the cross-section influences the heat transfer. A uniform heat distribution over the area is desirable, so that no pockets of phase change material are left molten while the rest of the area is discharged.

In the second step, simulation results from the cross-section are used to derive a simplified model in Dymola® that replaces the fin and PCM with a single material having effective material properties. The radial discretization, the temperature results over time and the resulting heat flow rate in comparison with the detailed model are shown in Fig. 2(c), respectively from top to bottom. For this model, the domain is also simplified as being axisymmetric, which results in a circular cross-section. The diameter of the cross section varies depending on the hexagonal fin dimensions, such that the area of the circle is equal to the area of the hexagon; for this simulation, the diameter of the circular
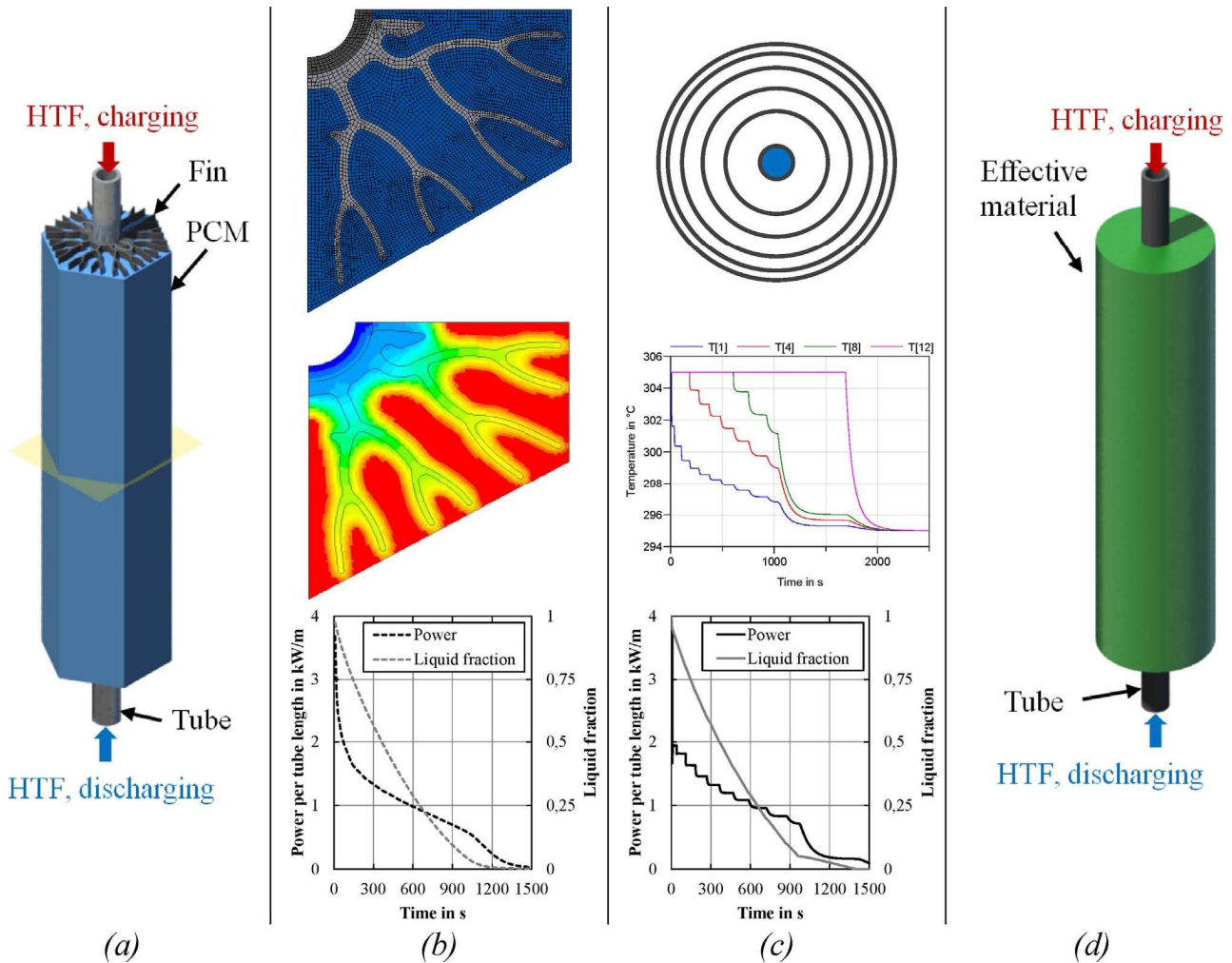
Fig. 2. Simulation methodology for a storage system shown in various steps. (a) A single tube assembly, shown here in a shortened form, is created, from which (b) a cross-section is analyzed for heat transfer properties. (c) A transfer of results simplifies the design to a simplified radial model, which is followed by (d) a heat transfer analysis of a tube assembly with coupled axial HTF-flow and a radial conduction model.

cross-section is 73.6 mm. The use of polar coordinates and symmetry lead to a one-dimensional discretization into annular rings. The density, the specific heat capacity and the latent heat of the effective material are averaged as in the work of Bauer (2011). However, the heat conductivity calculated this way is too high and results in a faster phase change than with the detailed cross-sectional model. Hence, it is adjusted to better fit the detailed fin model. The thermal conductivity in each ring only partially correlates to the fin fraction found in this ring, because the surface area for heat transfer also influences the rate of heat transfer. The conductivity is therefore not calculated from the fin fraction, but is calculated such that the solidification rate in the simplified model corresponds to that in the detailed model. The resulting material properties of the effective material, given as a range from 0.12 to 169 W/mK for the thermal conductivity, are given in Table 1. For the constant reference boundary conditions, the resulting heat flow rate of the simplified one-dimensional (1D) model is shown in comparison to

that of the detailed cross-sectional two-dimensional (2D) model in Fig. 3. These curves show that the models are in good agreement after an initial numerical roughness. This roughness is due to the discretization in the one-dimensional model and has negligible effects on the system simulations.

In the third step, also in Dymola®, the entire storage is simulated by coupling the simplified radial effective material model with a model for axial flow of the HTF in the tubes Fig. 2(d). This model is adapted from the model by Stückle, Laing, and Müller-Steinhagen (2014). This leads to an axisymmetric 2D discretization with cylindrical coordinates for the three-dimensional domain. The number of tubes can be adapted in this step until a sufficient capacity or discharging time is achieved.

3. Results

The storage unit for this application has been designed to produce

Table 1
Thermodynamic properties of tube, fin, mean values of PCM between solid and liquid state and effective material of PCM and fin.

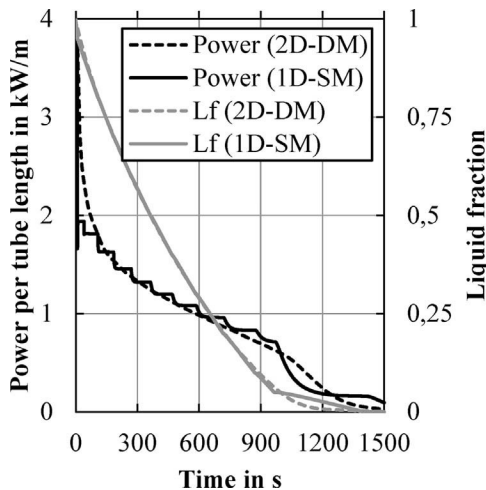| Property [Unit] ↓/Material →		Steel tube(1.5415)	Aluminum fin(EN AW 6060)	NaNO₃ PCM (Bauer, Laing, & Tamme, 2012)	Effective material
Density	[kg/m³]	7850	2700	2010.5	2114.5
Spec. heat capacity	[J/(kg K)]	554	1020	1655	1532.8
Heat conductivity	[W/(m K)]	45	210	0.55	0.12…169
Latent heat	[kJ/kg]	–	–	178	143.73

Fig. 3. Heat flow rate over time for constant reference boundary conditions in detailed 2D cross sectional model (2D-DM) and simplified 1D model (1D-SM) for power and liquid fraction (Lf).

superheated steam for an operating cogeneration plant. The system requires a minimum of 15 min for the back-up boiler to be powered from cold to full load. The following results are split into a section on the thermal performance analysis of the fin design and the storage simulation and performance.

3.1. Thermal performance analysis of the fin design

Various extended finned tube designs were created and analyzed for differing applications. Three designs discussed here are shown in Fig. 4, with the critical parameters listed in Table 2.

The radial fin design in Fig. 4(a) has a tube spacing of 100 mm and was integrated in the storage documented in (Laing et al., 2013). Also documented in this journal article are experiments using the axial fin design with a tube spacing of 160 mm shown in Fig. 4(b), which was designed for longer charging and discharging times. In comparison, the new fin design shown in Fig. 4(c) shows a much denser aluminum structure and smaller tube spacing. This smaller tube spacing was chosen due to the high power-to-capacity ratio required in the application. According to discussions with manufacturers, the smallest tube spacing that can be welded efficiently is 70 mm.

For a comparison of the three designs, simulations were conducted at reference conditions, shown in Fig. 5. The simulated cycle starts at the melting temperature and discharges to 10 K below the melting temperature of the simulated storage material. Shown in Fig. 5(a) is a comparison of the power per meter tube for one tube during discharging over the energy transferred during the discharging process; in Fig. 5(b) are results from the same simulations, showing the power per capacity of a storage section over the state-of-charge (SoC). Due to the differing tube spacings and the differing amounts of aluminum and storage material per extended fin design assembly, these ratio comparisons are necessary. The results comparing the power per tube length in Fig. 5(a) and the energy per tube length in Table 2 show that there is an almost linear relationship (with an R^2 value of 0.9969 for the trendline between these points) between the energy transferred during

Table 2
Geometric properties and capacities of the fin designs Radial-100, Axial-160 and Axial-70. Capacity calculations made with a 10 K temperature difference in $NaNO_3$.

Property [Unit] ↓/Fin design →		(a)Radial-100	(b)Axial-160	(c)Axial-70
Tube spacing	[mm]	100	160	70
Fin fraction	[%]	7.9	14.1	17.0
PCM fraction	[%]	87.7	84.3	77.6
Energy per tube length	[kW h/m]	0.83	2.03	0.36
Energy per storage volume	[kW h/m³]	95.3	91.6	84.3
Fin mass per capacity	[kg/kW h]	2.29	4.14	5.32

discharge for a single tube and the tube spacing, regardless of the fin fraction, which, as shown in Table 2, ranges from 7.9% to 17.0%. Energy per unit of storage volume logically decreases with increased fin fraction. For an overall maximized storage capacity, the optimum tube spacing for further storage unit parameters such as mass flow of the HTF must be paired with a minimized fin fraction, which is shown overall in the PCM fraction given in Table 2.

The high power level attained with the new fin design is shown in Fig. 5(b) with the comparison of the power per unit capacity over the state of charge (SoC) of the storage section. The significantly higher power shown by the red solid line is designed to yield the required 6 MW of superheated steam. As the steam temperature is controlled by water injection to meet the temperature requirements, the slope of the red curve during discharging is not critical to this application. The Axial-160 fin design, on the other hand, shows a much lower but more constant power per capacity level throughout discharging.

The Axial-70 fin design is shown in various degrees of discharging in Fig. 6 and has an even distribution of aluminum throughout the cross-section and allows for a high power rate during the latent discharging of the storage unit.

3.2. Storage simulation and performance

With the novel fin design, a storage unit is designed and its performance is analyzed with the multi-step simulation model described above. For this application, an inlet feedwater temperature of 103 °C is used for discharging the storage. During the required discharging duration of at least 15 min, the outlet steam temperature must not fall below 300 °C. The storage was designed with an additional discharging time of at least 10 min, in total 25 min, increasing plant flexibility and introducing a design safety margin. This discharge time correlates to a storage unit made up of 852 finned tubes, each with a fin length of 5.6 m. The simulation results of discharging the storage are shown in Fig. 7, where the constant feedwater inlet temperature and the steam outlet temperature are given. The outlet steam temperature reaches the required limit of 300 °C after 28 min, which satisfies the required discharge time and safety margins.

Also shown are the simulated temperatures averaged across the cross-section of the storage material at the top, middle and bottom of the storage material. These temperature distributions show a large difference in temperatures across the storage at the end of discharging. Considering the operation in once-through mode, the high fin density and the large temperature difference between the charged storage unit
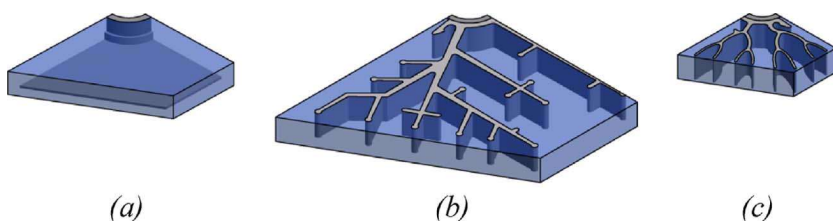

(a)   *(b)*   *(c)*

Fig. 4. Three different fin designs and tube spacings: (a) Radial-100, (b) Axial-160 and (c) Axial-70.
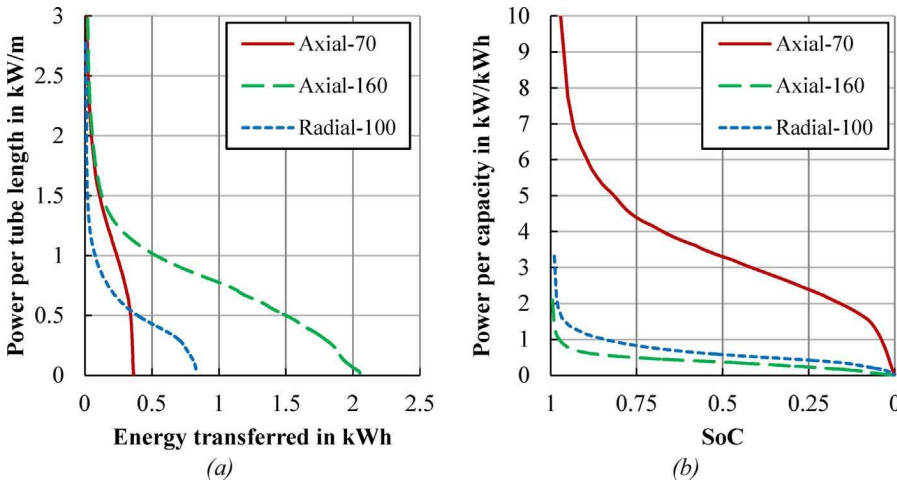
Fig. 5. Three fin design results for (a) power per tube length over energy released and (b) power per capacity over state-of-charge (SoC).

and the inlet feedwater, these temperature distributions are to be expected.

4. Discussion

The layout of high temperature latent heat thermal energy storage units needs to be designed for specific system requirements and take into account factors such as feasibility, transient effects, environmental effects and economics. These various factors lead to a challenging design. This paper presents a method for designing latent heat thermal energy storage units for specific application requirements. Specifically, a storage design for a high power and temperature application is detailed for the integration in an operating cogeneration plant. The method shown here can iteratively be used to design a storage unit for system requirements such as power, capacity and temperature. Thermal losses to the environment are not taken into consideration in the current model. For the short discharge duration, these have little effect. However, as the storage is a standby storage, the environmental effects between charging and discharging the storage can be significant for determining the intermediate re-charge cycle and optimal insulation. Additional calculations are required for the HTF calculations, such as pressure loss and flow distribution, as well as for economic optimizations.

A comparison of the fin fraction and tube spacing between three

designs are shown, demonstrating the relationship between material use or surface area and thermal power. The Axial-70 fin design has been produced and is being integrated into a large latent heat thermal energy storage unit being built within the framework of this project. Model validation and analysis will be conducted as a part of the commissioning and testing work.

5. Conclusions

A simulation methodology is presented for the design of high temperature latent heat thermal energy storage units using a multi-step process. The analysis process begins with a preliminary fin design based on system requirements combined with both storage unit and fin extrusion experience. This design is simulated in a two-dimensional ANSYS® FLUENT® model to determine heat transfer and phase change characteristics. This model is then simplified to a one-dimensional Dymola® representation, in which the fin geometry and PCM are converted to effective materials in annular rings about the central tube. As a following step, the ring model is coupled with an HTF model and concatenated axially in order to calculate a single tube, also in Dymola®. A storage system using a multiple of the tubes and corresponding initial and system parameters is calculated. With this method, the design and performance analysis of a high temperature latent heat thermal energy storage at a relevant industrial scale has been presented for the first
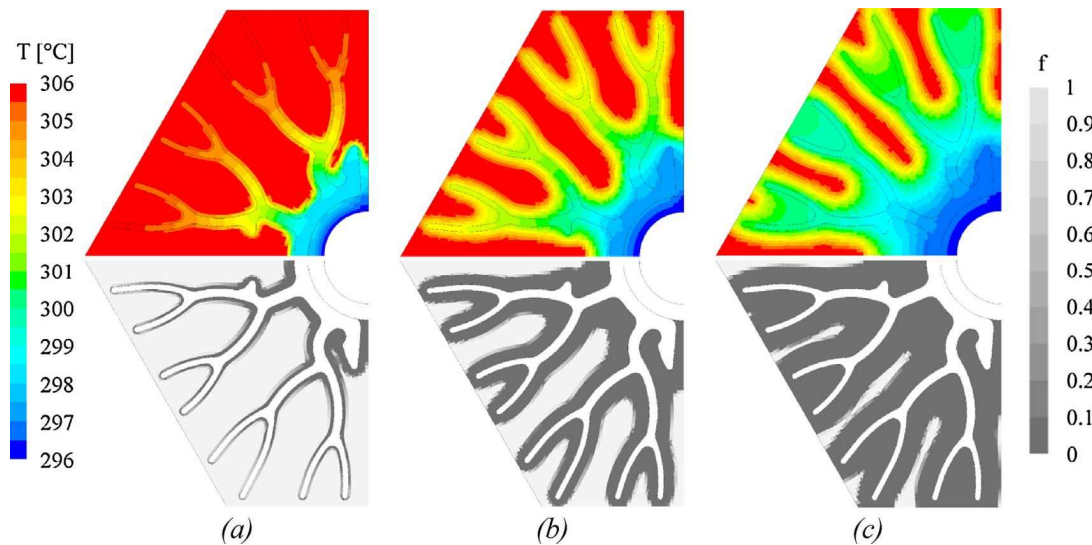

Fig. 6. Temperature T and liquid phase fraction f from the detailed cross-sectional model at three different stages of solidification: (a) 82.1% SoC after 100 s, (b) 40.8% SoC after 500 s and (c) 13.9% SoC after 900 s.
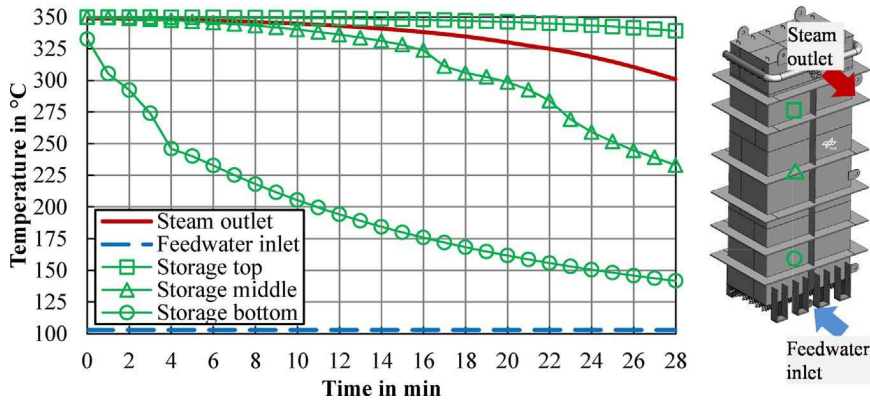
Fig. 7. Simulation results during discharging of the inlet and outlet temperatures of the HTF and the temperature distribution over the height of the storage unit, with the schematic at the right showing the approximate positions in relation to the storage unit.

time.

Using this method, the design of the storage unit and storage unit integration and controls has been successfully concluded, resulting in a storage unit with 852 finned tubes, each with a 5.6 m fin length. The required discharge time of at least 15 min will be fulfilled, with a safety margin of more than 10 min. The storage unit is currently in build, so that commissioning and testing can be conducted to validate this simulation method.

References

Bauer, T. (2011). Approximate analytical solutions for the solidification of PCMs in fin geometries using effective thermophysical properties. *International Journal of Heat and Mass Transfer, 54*, 4923–4930. http://dx.doi.org/10.1016/j.ijheatmasstransfer.2011.07.004.

Bauer, T., Laing, D., & Tamme, R. (2012). Characterization of sodium nitrate as phase change material. *International Journal of Thermophysics, 33*, 91–104. http://dx.doi.org/10.1007/s10765-011-1113-9.

Hübner, S., Eck, M., Stiller, C., & Seitz, M. (2016). Techno-economic heat transfer optimization of large scale latent heat energy storage systems in solar thermal power plants. *Applied Thermal Engineering, 98*, 483–491. http://dx.doi.org/10.1016/j.applthermaleng.2015.11.026.

Johnson, M., Vogel, J., Hempel, M., Dengel, A., Seitz, M., & Hachmann, B. (2015). High temperature latent heat thermal energy storage integration in a co-gen plant. *Energy Procedia, 73*, 281–288. http://dx.doi.org/10.1016/j.egypro.2015.07.689.

Kenisarin, M. M. (2010). High-temperature phase change materials for thermal energy storage. *Renewable and Sustainable Energy Reviews, 14*, 955–970. http://dx.doi.org/10.1016/j.rser.2009.11.011.

Laing, D., Eck, M., Hempel, M., Johnson, M., Steinmann, M., Meyer-Gruenfeld, M., et al. (2012). *High temperature PCM storage for DSG solar thermal power plants tested in various operating modes of water/steam flow. Sol. PACES Conf.*.

Laing, D., Bauer, T., Breidenbach, N., Hachmann, B., & Johnson, M. (2013). Development of high temperature phase-change-material storages. *Applied Energy, 109*, 497–504. http://dx.doi.org/10.1016/j.apenergy.2012.11.063.

Mehling, H., & Cabeza, L. F. (2008). *Heat and cold storage with PCM.* Berlin Heidelberg: Springerhttp://dx.doi.org/10.1007/978-3-540-68557-9.

Sciacovelli, A., & Verda, V. (2016). Second-law design of a latent heat thermal energy storage with branched fins. *International Journal of Heat and Fluid Flow, 26*, 489–503. http://dx.doi.org/10.1108/HFF-01-2015-0040.

Seitz, M., Cetin, P., & Eck, M. (2014). Thermal storage concept for solar thermal power plants with direct steam generation. *Energy Procedia, 49*, 993–1002. http://dx.doi.org/10.1016/j.egypro.2014.03.107.

Stückle, A., Laing, D., & Müller-Steinhagen, H. (2014). Numerical simulation and experimental analysis of a modular storage system for direct steam generation. *Heat Transfer Engineering, 35*, 812–821. http://dx.doi.org/10.1080/01457632.2013.828556.

Steinmann, W.-D., Laing, D., & Tamme, R. (2009). Development of PCM storage for process heat and power generation. *Journal of Solar Energy Engineering, 131*, 041009. http://dx.doi.org/10.1115/1.3197834.

Ziaei, S., Lorente, S., & Bejan, A. (2015). Morphing tree structures for latent thermal energy storage. *Journal of Applied Physics, 224901*, 1–5. http://dx.doi.org/10.1063/1.4921442.

2.5.   Paper IV: Physical storage integration

This article, entitled "Design and Integration of High Temperature Latent Heat Thermal Energy Storage for High Power Levels," was first presented at *ASME IMECE* in Pittsburgh, USA, November 2018 and later published in the *Proceedings of the ASME IMECE*, IMECE2018-86281, copyright ASME, 2018. It was co-authored by Bernd Hachmann, Andreas Dengel, Michael Fiß, Matthias Hempel and Dan Bauer and this author is the first author.

This paper discusses the detailed design of the storage and system, including the simulations of the system integration. The discussion of the engineering design of the headers and the method for finned-tube attachment show the details required in upscaling capacity. This upscaling in an operating plant also led to the development of a retention-type foundation. The full system integration allowing for both charging and discharging a real system is discussed, showing the integration as a whole as necessary for meeting system demands.

The author is responsible for the conceptualization, data curation, funding acquisition, investigation, methodology, project administration, supervision, visualization, and writing of the original draft of this article. The assembly methodology for the finned tubes was developed by Bernd Hachmann. The header design was developed by the author, Michael Fiß and the company contracted to build the storage unit. Andreas Dengel oversaw and coordinated the system design in collaboration with the author. Matthias Hempel conducted the simulations according to parameters given by the author. Dan Bauer provided resources, supervision and review of the article.

IMECE2018-86281

DESIGN AND INTEGRATION OF HIGH TEMPERATURE LATENT HEAT THERMAL ENERGY STORAGE FOR HIGH POWER LEVELS

Maike Johnson
German Aerospace Center
Stuttgart, Germany

Bernd Hachmann
F.W. Brökelmann GmbH & Co. KG
Ense-Höingen, Germany

Andreas J. Dengel
Steag New Energies GmbH
Saarbrücken, Germany

Michael Fiß
German Aerospace Center
Stuttgart, Germany

Matthias Hempel
German Aerospace Center
Stuttgart, Germany

Dan Bauer
German Aerospace Center
Stuttgart, Germany

ABSTRACT

A latent heat thermal energy storage unit is being integrated into a heat- and power cogeneration plant in Saarland, Germany. This storage unit system will act as an intermediate backup to a heat recovery steam generator and gas turbine and is therefore situated in parallel to this unit, also between the feedwater pumps and the steam main. The steam required is superheated, with a nominal thermal power of 6 MW. The storage unit needs to provide steam for at least 15 minutes, resulting in a minimum capacity of 1.5 MWh. Integration of this storage unit will increase efficiency and decrease fossil fuel use by reducing the use of a conventional backup boiler, while maintaining the steam supply to the customer.

The detailed design and a partial build of the storage unit has to-date been successfully concluded, as well as system design and build. Hot and cold commissioning of the storage unit, including filling of the storage unit, will commence following the completion of the storage unit. With the integration of this storage unit, fossil fuel use will be reduced in this power plant. Additionally, the production of superheated steam at a high power level in a latent heat storage unit and a comparison with simulation tools will be possible. This project includes the design, build, commissioning and testing of the storage unit. The paper discusses the detailed design of the storage and system, including the simulations of the system integration.

1   INTRODUCTION

The storage unit system, comprising of a latent heat thermal energy storage unit, piping, valves, a foundation, control systems and thermal insulation is being integrated into a heat- and power cogeneration plant in Saarland, Germany. This system will act as an intermediate backup to a heat recovery steam generator (HRSG) and gas turbine and is therefore situated in parallel to this unit and the existing backup boilers, as shown in Figure 1. The steam required is evaporated and superheated from feedwater, and has a nominal thermal power of 6 MW. The storage unit is required to provide steam for at least 15 minutes at a minimum flow rate of 8 t/h. These parameters result in a minimum storage capacity of 1.5 MWh.

In the current system, a conventional backup boiler is kept at a minimal load, so that it can assume full steam production within two minutes if the gas turbine trips. It produces the necessary steam until the gas turbine and HRSG are back in operation.

With the integration of the thermal energy storage unit, the conventional backup boiler is held at a warm load, from which it needs 15 minutes to reach full operational load and production. Depending on how often the storage unit is needed as well as the demand for steam from the other steam customers, the load reduction of the backup boiler could amount to energy savings of approximately 5000 MWh/a.

For this ramp-up time, the storage unit will provide the minimum steam load. Thereafter, the conventional backup boiler produces steam until the cause for the gas turbine tripping has been alleviated.

1

Once the gas turbine and HRSG are operating again, the storage unit is charged using steam from this HRSG. Using a bypass and a control valve, the steam exiting the storage system during charging also meets the requirements of the industrial customer.

The storage unit uses extended finned tubes in a tube-and-shell latent heat storage concept with sodium nitrate as the phase change material (PCM), storing the energy both in a combination of sensible and latent heat. The detailed simulations and thermodynamic design are described in (1) and the integration of the storage unit into the system in (2).
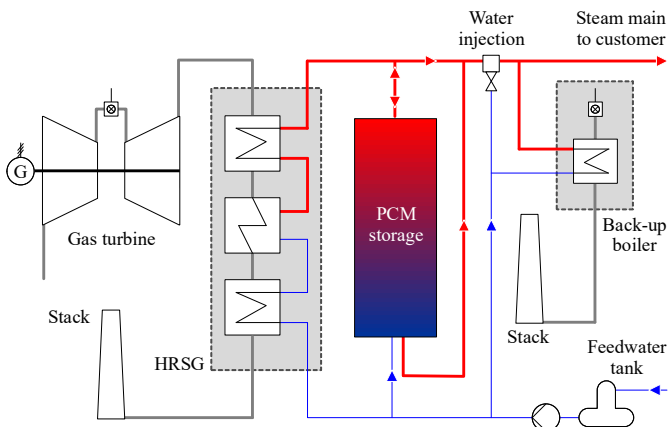
Figure 1: Layout of the cogeneration plant showing the latent heat thermal energy storage integrated in parallel to the HRSG and the backup boiler (2).

Following the basic design of the storage unit and the system, the detailed design of the storage unit system was conducted. The storage unit and system need to accommodate both the charging and discharging of the unit, including switching of operation modes, while consistently providing high quality steam to the industrial customer. Various operating conditions were simulated and the design of the system and the storage planned to meet these requirements, as well as the permitting requirements for operation in a power plant.

2   STORAGE SYSTEM DESIGN AND BUILD

The storage unit design includes 852 extended finned tubes and approx. 32 tons of sodium nitrate ($NaNO_3$) as the storage material mass, with a minimized volume of the headers for fast mode switching between standby and discharging. The build of the storage is, at the time of writing, almost fully completed, with just the mounting pins for the thermal insulation to be clarified and welded. After this, the pressure testing and delivery can occur.

Experiences with the fin assembly, the tight tube spacing, and the dense fin structure can be reported. The system for the integration has been designed and the foundation for the storage built.

2.1   ASSEMBLY METHOD FOR FINNED TUBES

The finned tube design is comprised of a central tube onto which two axial fin segments are clipped using spring steel

clips, as shown in Figure 2. The heat transfer material water/steam flows through central tube, which therefore has to withstand pressures up to 26 bar at up to 350 °C. This tube is therefore made of steel. The fin segments transfer heat from the heat transfer fluid and the steel tube to the surrounding storage material. As such, these fins need to have a high thermal conductivity, but do not need to withstand mechanical pressures. The material used in these fins is aluminum.
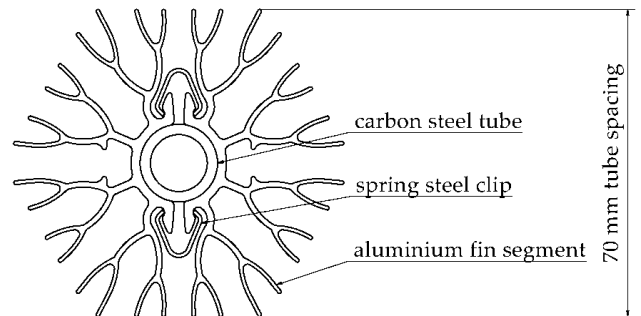
Figure 2: Drawing of fin design showing central steel tube, two fin segments and assembly clips.

The fins are clipped onto the tube with clips that allow for independent thermal expansion of the steel tube and aluminum fins, while ensuring a continuously good thermal contact between the two materials. Spring steel allows for this flexible expansion while maintaining strength at the operating temperatures.

As the specified high power level of 6 MW requires a dense fin structure and small tube spacing, and the storage unit design requires 852 finned tubes to supply the 1.5 MWh capacity, each with a fin length of 5.6 m, a semi-automatic assembly method for the mounting of the fins onto the tubes was developed.

Figure 3 shows the assembly mechanism. During assembly, first, two fin segments are slid onto the assembly mechanism and clips slid at the designed spacing along the assembly. The assembly mechanism then pneumatically pulls the two fin segments apart, which are now joined by the clips. This allows for the central tube to be slid between the aluminum fins. The assembly mechanism is then relaxed, and the mounted finned-tube assembly can be removed. The assembly method was proven as feasible and accurate, and further automation would be possible for an economical production of higher quantities of finned tubes.

Figure 3: Finned-tube assembly mechanism with a fined tube in the mechanism.

The fin segments are shown in Figure 4(a) and the mounted finned tube in (b). Each fin segment is 5.6 m long and the tubes are 6 m, allowing for welding into the headers.
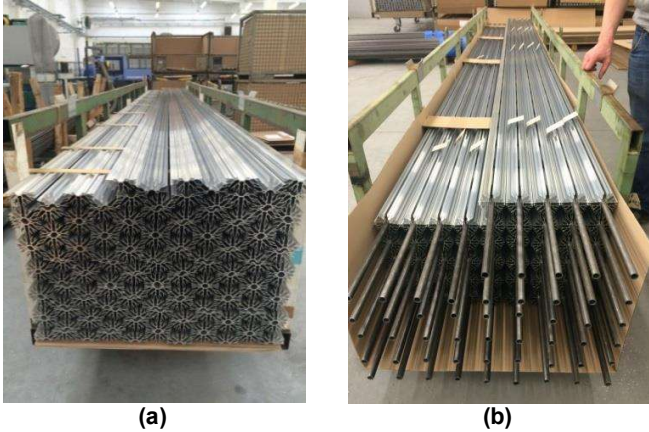

(a)   **(b)**
Figure 4: Finned-tube assembly showing (a) the prepared fin segments and (b) mounted finned tubes.

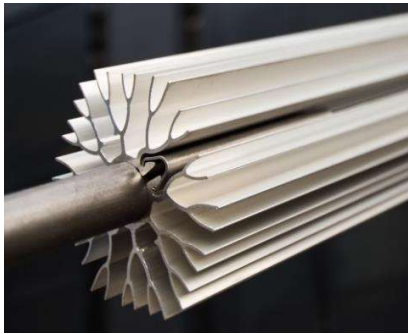Figure 5 shows a close-up of a mounted fin, tube and clip assembly.

Figure 5: Assembled finned-tube.

2.2 HEADER DESIGN

The storage unit is designed to be discharged using feedwater that evaporates. It is charged using superheated steam that for most of the charging time remains in the steam phase. Therefore, the upper header is designed for steam and the lower header for either water or steam.

The lower header has to have a very low internal volume to allow for the required fast switch time of two minutes. During these two minutes, feedwater flows into this volume and pushes steam up through the storage unit, while heating and evaporating and thereby expanding.

In order to meet these requirements, the lower header is designed as shown in Figure 6(a) with tapered tubes welded to each of the tubes coming out of the tube plate at the bottom end of the storage. The tapering is for volume reduction. These tapered tubes flow into a semi-header, which is optimized for weldability and internal volume. The single, main header below this is located in the middle of the storage unit. It is slanted, so that any condensate that forms during the beginning of charging and in standby operation flows out of the unit.
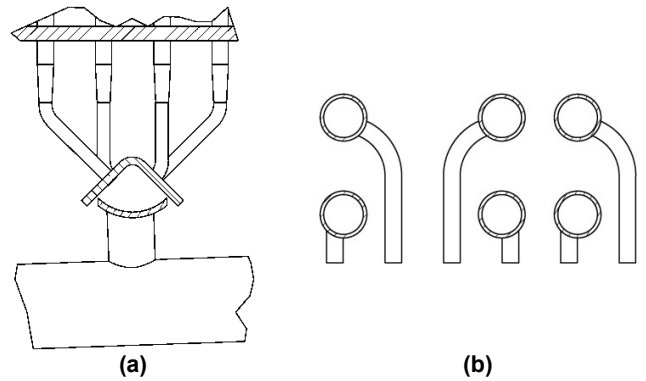

(a)   **(b)**
Figure 6: Detail of the (a) lower header design, showing the narrowing of the individual tubes below the tube plate to minimize the volume in the header. Four rows of tubes connect downwards to one semi-header. This connects to a slanted main header. (b) The upper header design shows the tubes from the tube bundle attaching to stacked semi-header rows.

The upper header, as shown in Figure 6(b), is less critical from a thermo-mechanical or operational standpoint, as it is only used for steam and does not experience the temperature gradients that the lower header does. It does need to be designed so that the storage unit can be filled with storage material. To this extent, the semi-header rows are aligned above one another allowing for slits between which the storage material can be filled into the unit.

2.3 STORAGE UNIT BUILD

The storage unit is being built by Seab GmbH and has been built row for row in a horizontal position, with a side and the tube plate welded as a base (Figure 7). Each row of finned tubes was aligned and welded to an upper header row as shown in Figure 8(a), and this assembly then inserted into the tube plate and welded there. Figure 8(b) shows a detail of the assembled finned-tubes and Figure 9 the completed lower header. The green coils of thermocouples visible in some pictures are for analysis of the design as well as operational parameter determination.

Storage unit build will be followed by pressure testing, transport, filling and commissioning of the system, currently planned for autumn 2018.

Figure 7: Storage unit build showing first rows welded into the tube plate assembly and lying on the side wall.

| (a) | (b) |

Figure 8: Storage unit build showing (a) prepared tube rows with upper headers and (b) detail of the assembled finned tubes.

Figure 9: Storage unit build showing complete assembly of the lower header construction.

2.4 SYSTEM DESIGN

The system components, controls and foundations for the integration of the storage unit into the operating cogeneration plant have been designed and partially built.

As shown in Figure 1, the storage will be integrated in parallel to the HRSG and the current standby and backup boiler. The storage unit will be integrated along the back wall of the plant in Saarland, Germany, as shown in the photomontage in Figure 10.
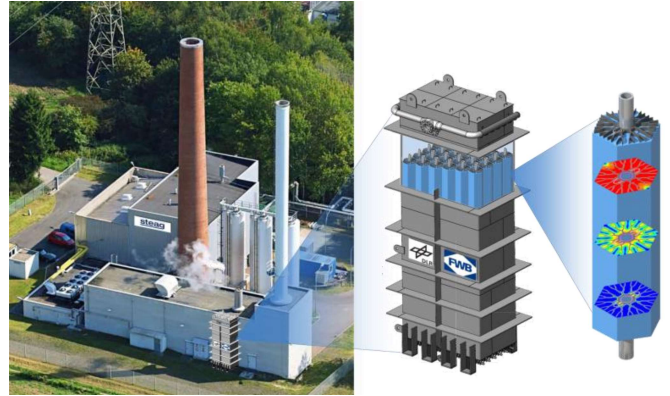

Figure 10: Photomontage of the storage unit erected along the wall of the cogeneration plant in Saarland, Germany.

The foundation needs to carry the weight of the storage unit filled with sodium nitrate (in total ca. 56 t) as well as the insulation and any extra loads such as people during filling of the storage, water weight of heat transfer fluid in the storage unit and piping and snow, as this unit is being erected outside of any buildings. In addition, the foundation needs to be designed to contain the sodium nitrate if there were to be a leak in the unit, and be designed for the pipework of the integration, including feedwater coming into the bottom of the storage unit during discharging and condensate and/or steam coming out of the bottom of the storage unit during charging. The build and plan of this foundation are shown in Figure 11 and Figure 12, respectively.
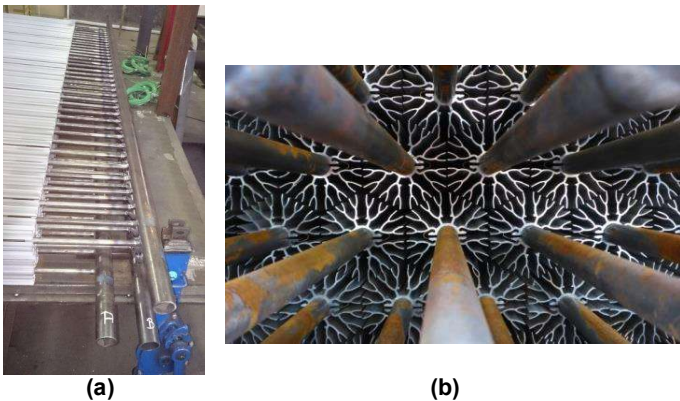

Figure 11: Foundation for the storage unit prepared for storage erection.

In order to meet these requirements, the foundation is built as a containment well (or pit), into which the molten salt, at temperatures between 306 °C and 350 °C, can flow and be contained if there is a leak. The concrete and rebar have to withstand these temperatures while maintaining static stability. The foundation also allows for the removal of condensate from the system, which is brought around the building to the site at which it can flow into the condensate pool from the plant.
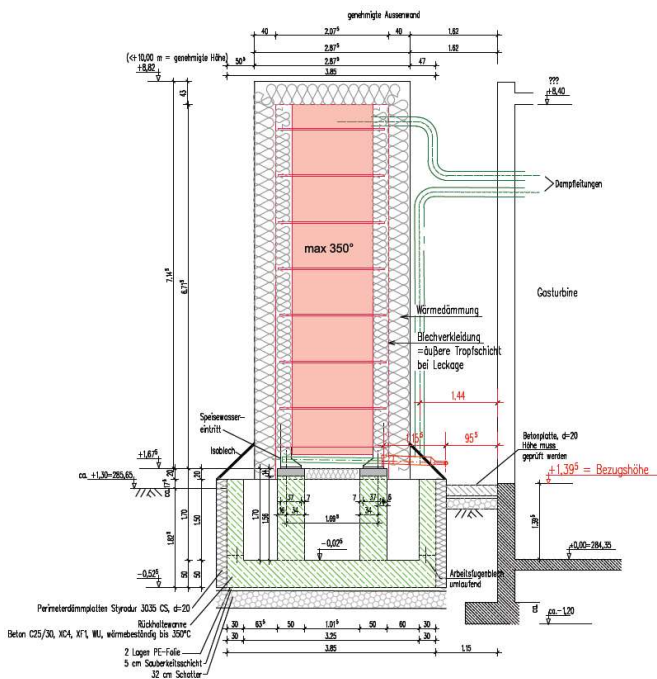
Figure 12: Foundation for the storage unit as a plan.

3 SIMULATION RESULTS

System simulations of discharging and charging, with a bypass operation for charging of the storage unit, have been conducted using the model described in (1). The discharging system requirements are 15 minutes of steam at a minimum of 300 °C and a pressure of at least 21 bar. Steam at temperatures above 300 °C will be temperature controlled down to this temperature using water injection.
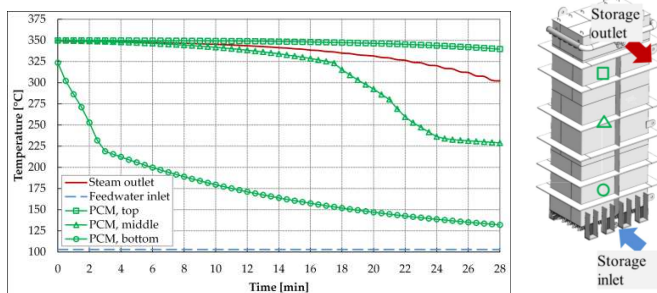

Figure 13 shows the simulation results from the design of the storage unit. Shown here are the input flow in blue at a constant 103 °C, and a slowly sinking outlet line in red, beginning at 350 °C and ending at 300 °C, at which point the storage unit is considered discharged in this application. This occurs after about 28 minutes, showing that the storage unit has been oversized for increased supply security as well as plant flexibility.

Discharging with these cut-off criteria results in only a portion of the storage material being solidified, as can be interpreted from the green temperature plots in
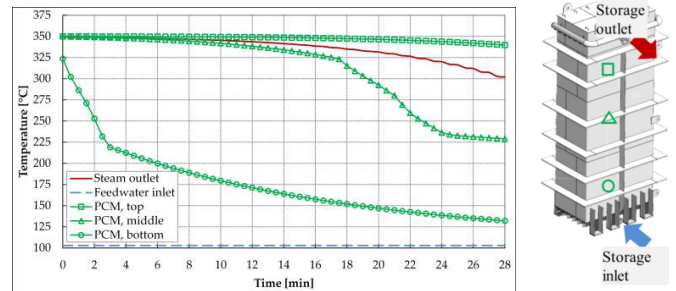

Figure 13. The green lines depict the averaged temperatures of the PCM at cross-sections of the storage at the top, middle and bottom of the unit. The phase change temperature of the PCM is 306 °C, which means that the PCM at the bottom of the storage unit undergoes a phase change very quickly, after less than two minutes of discharging. The PCM in the middle of the storage unit undergoes phase change after approximately 19 minutes and the top of the storage unit is still liquid at the cut-off point at 28 minutes. According to the simulations, approximately 27 % of the PCM remains liquid throughout normal operating conditions.
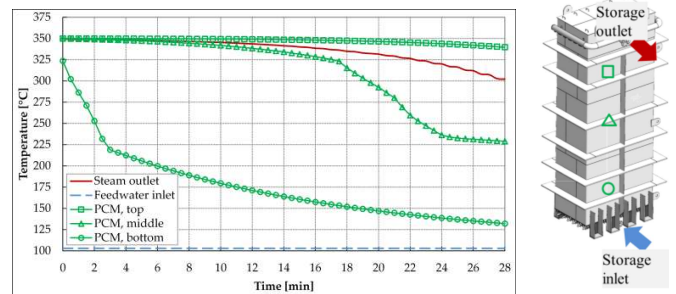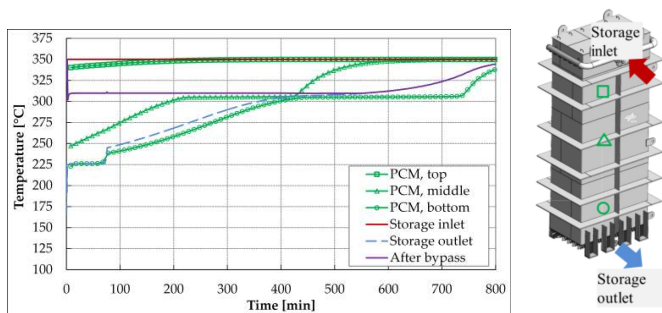

Figure 13: Discharging temperatures of the averaged values in the PCM at the top, middle and bottom as well as the storage outlet and inlet temperatures. The schematic on the right shows approximate calculation locations. (1)

Charging of this storage system requires that the storage system outlet be of a steam quality that the industrial customer can use for as much time as possible. This results in a sensible charging of the storage unit for a large percent of the charging time, and a much longer storage charging time in comparison to the discharging – ca. 800 minutes compared to 28 minutes. As the power plant and customer can use this steam during charging, this long charging time is acceptable.

The temperatures of the averaged values in the PCM at the top, middle and bottom as well as the storage outlet and inlet temperatures are shown in Figure 14. The storage is charged from the top, so that inlet and outlet of the storage switch with the change in operating modes. A new line (purple) is introduced in this figure – the temperature after the bypass and after the storage unit (see Figure 1). This is the mixing temperature of the storage outlet and bypass steam that is sent to the industrial customer, prior to any temperature adjustment by water injection. This temperature adjustment would be necessary after about 600 minutes of charging.

5

Figure 14: Charging temperatures of the averaged values in the PCM at the top, middle and bottom as well as the storage outlet and inlet temperatures and the temperature after mixing the storage outlet steam with the bypass steam after the bypass. The schematic on the right shows approximate calculation locations.
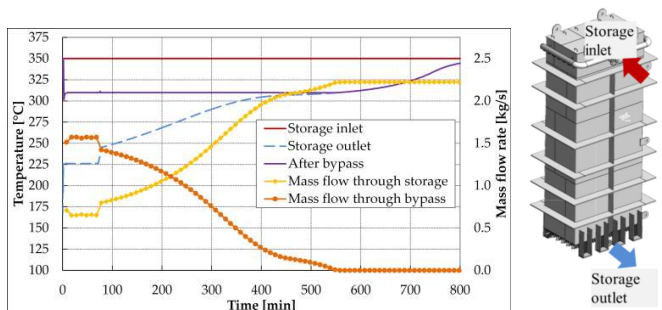
Figure 15: Charging temperatures of the storage inlet and outlet, and mixed bypass temperatures as well as the mass flow rates through and bypassing the storage unit. The schematic on the right shows approximate calculation locations.

In order to attain these mixing temperatures that are above 300 °C for most of the charging time, a regulation of the mass flow going through the storage unit and the bypass is necessary. Figure 15 shows the initially high mass flow rate through the bypass (orange dots) steadily decreasing after about one hour, when the temperature at the storage outlet reaches the evaporation temperature at operating pressure – ca. 226 °C. Only for the last 250 minutes of charging does the entire mass flow rate of 2.2 kg/s flow through the storage unit.

4   CONCLUSIONS AND OUTLOOK

The detailed design and a partial build of the storage unit has to-date been successfully concluded, as well as system design and build. Hot and cold commissioning of the storage unit, including filling of the storage unit, will commence following the completion of the storage unit. The control of the mass flow rates through the bypass and the validation of both this model and the fin model will take place with testing at different flow rates and valve opening rates.

With the integration of this storage unit, fossil fuel use will be reduced in this power plant. Depending on how often the storage unit is needed as well as the demand for steam from the other steam customers, the energy saving could be approximately 5000 MWh/a.

The production of superheated steam at a high power level in a latent heat storage unit and a comparison with simulation tools will be possible. This project includes the design, build, commissioning and testing of the storage unit.

REFERENCES

[1] Johnson, M., Vogel, J., Hempel, M., Hachmann, B., Dengel, A. (2017). Design of High Temperature Thermal Energy Storage for High Power Levels, *Sustainable Cities and Society*, 35, 758-763, doi: 10.1016/j.scs.2017.09.007.

[2] Johnson, M., Vogel, J., Hempel, M., Dengel, A., Seitz, M., Hachmann, B. (2015). High Temperature Latent Heat Thermal Energy Storage Integration in a Co-gen Plant, *Energy Procedia*, 73, 281-288. doi:10.1016/j.egypro.2015.07.689.

2.6. Paper V: Process integration

This article, entitled "High temperature latent heat thermal energy storage integration in a co-gen plant," was first presented at the *9ᵗʰ International Renewable Energy Storage Conference (IRES 2015)* in Düsseldorf, Germany, March 2015 and later published in *Energy Procedia*, vol. 73 (June), pp. 281-288, 2015. It was co-authored by Julian Vogel, Matthias Hempel, Andreas Dengel, Markus Seitz and Bernd Hachmann and this author is the first author.

The design of the fins, storage unit design and planned integration in the cogeneration plant are presented. This paper shows an overview of the development of the storage unit and system, detailing the overall process.

The author is responsible for the conceptualization, data curation, funding acquisition, investigation, methodology, project administration, supervision, visualization, and writing of the original draft of this article. Julian Vogel and Matthias Hempel are both responsible for the formal analysis, investigation and review of the article, and Julian Vogel is also responsible for visualization of the results and writing of the numerical methods section. Andreas Dengel is responsible for the resources for the system integration and investigation. Markus Seitz is responsible for the conceptualization and investigation. Bernd Hachmann assisted in the design of the fin analyzed in the formal analysis.

9th International Renewable Energy Storage Conference, IRES 2015

High temperature latent heat thermal energy storage integration in a co-gen plant

M. Johnson[a]*, J. Vogel[a], M. Hempel[a], A. Dengel[b], M. Seitz[a], B. Hachmann[c]

[a]German Aerospace Center (DLR), Pfaffenwaldring 38-40, 70569 Stuttgart
[b]Steag New Energies, St. Johannerstraße 101-105, 66115 Saarbrücken
[c]F.W. Brökelmann GmbH & Co. KG, Oesterweg 14, 59469 Ense-Höingen

Abstract

Within the framework of the project TESIN funded by the German Ministry of Economic Affairs and Energy, a high temperature latent heat thermal energy storage unit is being developed and will be designed, built, commissioned and tested in an operating cogeneration plant in Saarland, Germany. This plant provides superheated steam to industrial process customers from a gas turbine with a heat recovery steam generator. Currently, a secondary boiler is operated at minimal load, from which it can be heated to full load in 2 minutes. With the integration of the thermal energy storage into the plant, the secondary boiler will be reduced from minimal to warm load operation. In case of a failure of the gas turbine, the storage will produce steam for 15 min. while the secondary boiler is heated from a warm to a hot operating load. This standby load reduction in the secondary boiler will reduce the use of fossil fuels.

The steam demand from the thermal storage is for 8 t/h at around 25 bar and a minimum temperature of 300 °C. This results in a high power level of about 6 MW_{th} and a necessary storage capacity of 1.5 MWh. At this pressure level, the steam is superheated about at least 75 K. The combination of the superheating and the required power level has led to a smaller tube distance than in previous storage units as well as a new axial fin design. The basic storage as well as the fin design combined with nitrate salts as the storage material have been analyzed with simulation tools. Detailed design planning, permitting and build of the system are the coming steps in this part of the project. The design of these fins, storage unit design and planned integration in the cogeneration plant are presented here.

Keywords: Latent heat storage; standby; superheated steam

---

 * Corresponding author. Tel.: +49-711-6862-344; fax: +49-711-6862-747.
 E-mail address: maike.johnson@dlr.de

1. Introduction

The cogeneration plant in Saarland consists of a gas turbine with a heat recovery steam generator (HRSG) and two back-up boilers. The gas turbine burns mine gas from the mine gas network existing in Saarland. Due to the nature of mine gas, the methane content in the supply sometimes varies. This – and technical issues always possible in a heat generator – can result in the gas turbine tripping and the supply of steam to the customer sinking in quality. The customer requires a very constant steam quality for the production processes. To ensure this delivery, Steag New Energies has a back-up boiler running on minimal load. At minimal load, there is a constant firing of fossil fuels. The steam created by this firing is disposed of. In the case of the turbine tripping, this back-up boiler can be transitioned to full load within two minutes, during which time the HRSG produces residual steam. With the integration of a thermal energy storage unit, the back-up boilers can be reduced to a warm load. At warm load, in comparison to minimal load, much less fossil fuel has to be burned in order to keep the pressure vessels at a high temperature. From warm load, it takes 15 minutes to transition to full load. During this time span, the thermal energy storage will supply the necessary steam to the steam main. This standby load reduction in the secondary boiler will reduce the use of fossil fuels.

2. Methodology

2.1. Planned integration into the cogeneration plant

The steam demand for the customer is for 8 t/h at about 25 bar and a minimum temperature of 300 °C. The steam is produced in the HRSG using feedwater with an inlet temperature of 103 °C. In order for a thermal storage unit to allow the standby boiler to be run at warm load, it has to produce steam from this feedwater at the power level of 6 MW for a minimum of 15 minutes. The minimally required storage energy capacity is thereby 1.5 MWh.

Since evaporation is required for discharging, a latent heat thermal energy storage unit has been developed for integration. In a latent heat thermal energy storage unit, the storage material undergoes a phase change from liquid to solid and back again for discharging and charging, respectively. During phase change, the material supplies or stores the latent energy. Each material has its inherent material properties and therefore a set phase change temperature. The higher the specific capacity of the material, the more sensible energy it can store as well. Ideally, the material has a high thermal conductivity, in order to charge and discharge quickly. However, this is often not the case [1]. Due to this low thermal conductivity, various designs and storage concepts have been researched and tested [2]. A method tested in various storage units at DLR is the use of extended fins to increase the overall surface area of the tubes [3]. Extended fins allow for heat to be transferred from the phase change material (PCM) that is far from the tube, while allowing the heat transfer medium to be pressurized in a steel tube. Essentially, the design of extended fin storages is similar to tube-and-shell heat exchangers, so that a foundation of design knowledge for headers and flow can be relied upon. The axially oriented fins analyzed and planned for this storage unit offer potential cost reductions in the assembly and also have thermodynamic benefits. The nitrate salts used as PCMs in the temperature range between 140 °C and 350 °C undergo a volume change during phase change [1]. As PCM will melt along the axial fins during charging, this liquid PCM provides its own channel for movement to the top of the storage area and the volume change in the PCM is no longer critical.

As shown in the integration schematic in Fig. 1, the storage will be charged with steam from the HRSG and discharged with feedwater.During discharging, feedwater(blue line from the feedwater tank at the bottom right) flows into the bottom of the storage, evaporates to steam and is superheated as it rises through the tubes in the storage, leaving the storage as superheated steam. Heat is transferred from the storage material to the water/steam, thereby leading to a solidification of the storage material.
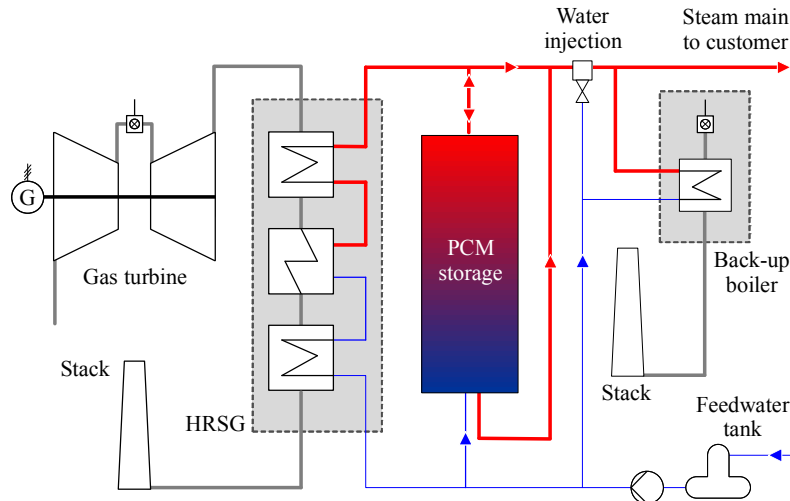
Fig. 1.Schematic of the planned integration of the latent heat thermal energy storage unit in the cogeneration plant.

The storage unit will be charged using steam from the HRSG. When leaving the steam generator (boxed in grey at the left), prior to a water injection that conditions the steam going to the customer to 300 °C, the steam has a temperature of 350 °C and a pressure of 25 bar. The condensation temperature at this pressure level is about 224 °C. To use the flow leaving the storage unit during charging, the storage unit and process engineering have been designed so that steam exits the storage. This steam can be delivered to the industrial consumer as long as the minimal temperature 300 °C is held. Part of the steam will bypass the storage unit during charging, and part will charge the storage unit. During charging, the amount bypassing the storage unit will be reduced based on the temperature after mixing both flows. With this incorporation in the system, the latent heat thermal energy storage unit will discharge latent heat, but be charged using sensible heat.

The storage material has to be properly selected to fit the operating conditions of the process. At a pressure of 25 bar, the evaporation temperature of water is about 224°C. Hence, the steam is superheated about 76 K. The storage material sodium nitrate ($NaNO_3$) satisfies the steam requirement for both charging and discharging with a melting temperature of 306 °C. It also has a relatively large latent heat of 178 J/g [4].

2.2. Principal storage design considerations

The combination of the superheating and the required power level has led to a smaller tube distance than in previous storage units as well as a new axial fin design with a higher fin fraction and better fin distribution throughout the storage material. A PCM storage built and tested in Carboneras, Spain had a capacity of ca. 700 kWh, a peak power level of ca. 700 kW[5] and steady-state of 200 kW [4]. This storage unit had a tube spacing of 100 mm and a radial fin spacing of 10 mm. A lab scale storage module tested with axial fins in a test rig in Stuttgart with a fin length of 1 m and 7 tubes has a capacity of 15 kWh [6]. These tubes were spaced 160 mm apart.

In order to provide 6 MW of power for the required 15 minutes, both the tube spacing had to be reduced as well as the fin geometry revised. After consulting manufacturers, a tube spacing of 70 mm in a triangular alignment was chosen as a minimum distance for which efficient welding is possible. Due to this tight tube spacing, a smaller tube diameter was chosen. This allows for a higher storage capacity within the same nominal storage volume as well as increases flow velocity in the tubes and therefore leads to a better heat transfer. A comparison of the geometries of the fins in the storage tested in Caroneras[3], the lab scale storage [6] and the geometry designed for this storage unit are shown in Table 1.

Various iterations of the fin design were simulated and analyzed. The design process is a combination of designing a fin that has a minimum amount of aluminum that is distributed evenly within the hexagonal space between the triangularly aligned tubes and assessing if this design can be fabricated. The requirements that lead to a design being extrudable are a combination of the width and length of the fins as well as the width and length of the negative areas

between the fins. Enclosed areas in the fin cannot be extruded over long extrusion lengths. The efficiency of a design can be tweaked by adjusting the speed at which a fin is extruded, so that experience and not only mathematical optimums have to be relied upon in optimizing a fin design. This process was therefore iterative, with F.W. Brökelmann creating fin designs that can be produced and DLR assessing their thermodynamic parameters as heat transfer structures.

A final parameter that was analyzed and adapted in the design stage is the number of tubes. The tube length was set at the standard length of 6 m. Therefore, each tube has a set amount of PCM around its extruded fin and therefore a set thermal capacity, given the operation parameters for the application.

Table 1: Comparison of Fin Geometry in Various Storages

	Carboneras fins	Lab scale storage	TESIN fins
Fin type	radial	axial	axial
Tube spacing in mm	100	160	70
Fin fraction of total volume in %	7.94	14.1	16.7
PCM fraction of total volume in %	87.9	84.3	77.9
Steel tube fraction of total volume in %	1.94	0.62	2.54

2.3. Simulation methodology

The basic storage and fin design combined with nitrate salts as the storage material have been analyzed with simulation tools. In order to simulate the storage system by justifiable means, several simplifications are made. First of all, only a subsystem of the tube register is simulated. The simulation domain consists of one single tube with fins mounted on it and the surrounding PCM section. This simplification is justified due to the geometric symmetry of all the tube-fin-PCM subsystems. The result is then scaled to the number of tubes in the storage. Hence, it is assumed that the flow in the tubes as well as the heat transfer to the PCM is identical in all subsystems. This implies a uniform pressure distribution between the tubes and a uniform temperature distribution within the PCM. However, the header will lead to a slightly uneven pressure distribution and heat losses to the environment on the storage outer walls will lead to an uneven temperature distribution. Since with proper design considerations, these effects can be minimized, they are neglected. Natural convection in the liquid phase of the PCM is also neglected in this early design stage due to the complexity of a detailed simulation, the uncertainty of existing Nusselt correlations and the rather small effect due to the small gaps of the current fin design.

The subsystem of one tube, fin and PCM is a complex problem of conjugated heat transfer that is difficult to model. Different models for the two-phase flow of water inside the tube, the heat conduction in the tube and fin geometry and the heat conduction with phase change in the PCM are needed. Because of this complexity, the storage simulation is divided into three steps. In the first step, the detailed heat transfer in a two-dimensional section of the tube, fin and PCM is simulated to obtain the heat transfer characteristic of the specific fin design in conjunction with a specific PCM. The resulting fields of temperature and liquid phase fraction are shown in Fig. 2.

In a second step, from the resulting characteristic curve of the average PCM liquid phase fraction over time, a simplified model for the PCM and fin compound is derived. The model assumes a material that replaces the PCM and fins and that behaves in a similar fashion due to effective material properties. The heat capacity, density and latent heat are averaged and the heat conductivity is calculated from the analytical solution of melting in a shell-and-tube system without fins in such a way that the resulting melting time corresponds to that of the real system. The heat conduction problem in the tube, fin and PCM is then calculated again with a simplified one-dimensional model that uses the effective material. The results are then compared to the detailed two-dimensional simulation. Since the analytical solution only incorporates latent heat and neglects sensible heat, the heat conductivity may be further adjusted iteratively until both models have the same melting/solidification time in the results.
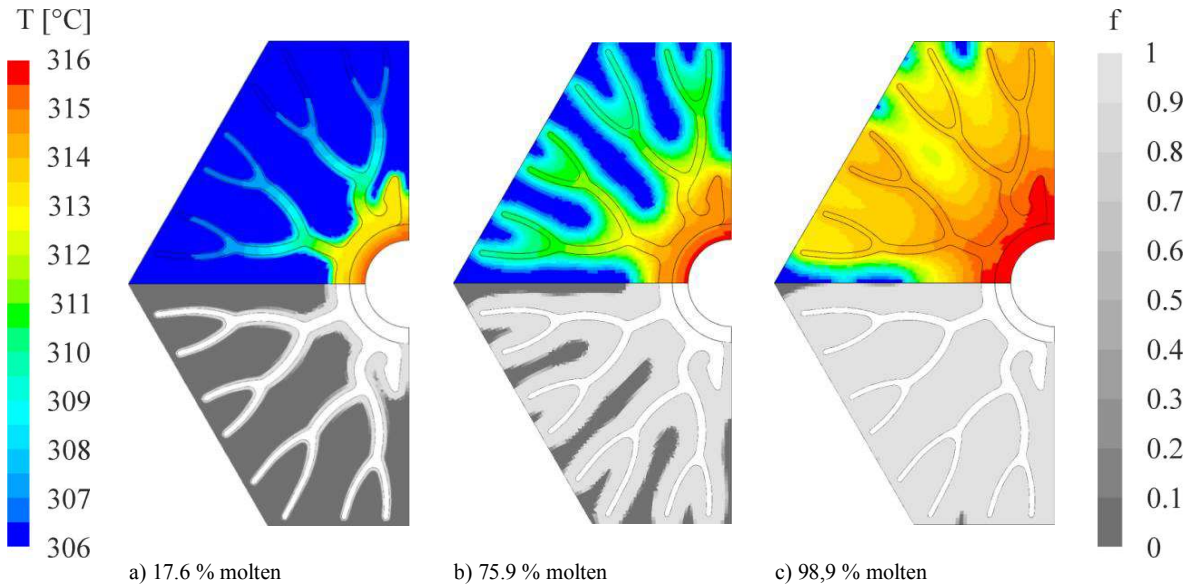
a) 17.6 % molten   b) 75.9 % molten   c) 98,9 % molten

Fig. 2: Temperature T and liquid phase fractionf from the detailed model at three different stages during melting.

In a third step, the effective model material properties are used in a simulation of the whole storage system including a simplified one-dimensional quasi-stationary two-phase flow in the heat transfer fluid and the two-dimensional-axissymmetric transient heat conduction in the tube, fin and PCM with phase change. In this last step, the cycle of charging and discharging the storage can be simulated. A modeling of the storage system behavior is possible only due to these simplifications from the detailed design to the simplified model. The model assumptions, especially the assumption for effective material properties, may lead to uncertainties. However, deviations are considered to be acceptable for the basic design stage. The numerical models have to be further improved and validated with results from the experimental storage unit.

3. Results and discussion

The iterative development of the fin design resulted in the following geometry in Fig. 3. Using this fin design, a storage unit has been planned. The storage unit has 852 tubes, ca. 32 t of storage material and internal dimensions for the storage material (excluding headers and insulation) of (length x width x height) 2.5 m x 1.5 m x 6 m.
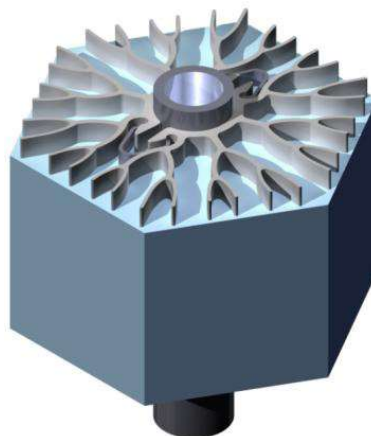

Fig. 3: Digital assembly with resulting fin design. Steel tube shown in dark grey, fin in light grey, PCM in blue.

The simulation results of discharging depicted in Fig. 4 show the inlet temperature of the feedwater at a constant 103 °C in a dashed black line and the outlet temperature of the storage unit during discharging as a solid black line. The outlet temperature decreases over time, so that the storage discharge is stopped after 28 minutes when the temperature reaches 300 °C.

The simulated temperature distribution for the top, middle and bottom level of the storage during discharging over time are also shown in Fig. 4. The simulation results are averaged over the cross-section of the storage, which is why a flat plateau for the phase change temperature is not visible. Temperatures in the upper level of the storage are significantly higher than the melting temperature of 306 °C, showing that the PCM is not fully discharged. Approximately 27 % of the PCM is still liquid at this point. However, the PCM at the lower end of the storage is cooled much below the solidification temperature of 306 °C to approximately 142 °C. This is due to the feedwater temperature of 103 °C and the high effective rate of heat conduction from the PCM through the fins to the heat transfer medium.

This design-point discharge time is significantly more than the required 15 minutes. Due to various assumptions in the design process and as the storage unit is providing steam to a critical production process, it was decided to overdesign the storage to ensure that the steam quality can be delivered the required minimum amount of time. Any time longer than the minimum provides the operating cogeneration plant with increased flexibility. The assumptions are, for example, that there is a good distribution of the heat transfer medium in both headers during both discharging and charging. The lower header, due to the sensible charging, is filled with water during discharging and steam during charging. It is therefore impossible to design for an optimum flow distribution in both cases.
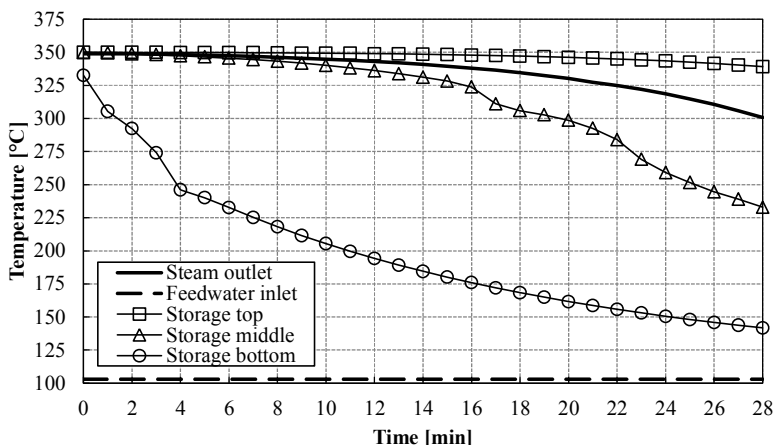

Fig. 4: Simulation results of the inlet and outlet temperatures of the heat transfer medium and the temperature distribution over the height of the storage unit during discharging over time.

The simulation results of temperatures during charging are shown in Fig. 5. For the first circa 30 minutes, condensate will leave the storage unit and will be disposed of. The water evaporates to steam at approximately 225 °C, shown as a plateau for approximately one hour after condensation ends. With the start of evaporation, the mixing of the bypass and storage outlet steam allows for a nearly constant steam temperature of 300 °C to the customer. Once all of the flow goes through the storage, the outlet temperature of the storage and therefore the mixed temperature begin to climb. At this point, water injection will reduce the temperature of the steam to 300 °C for the customer.

The mass flow rates of the storage system during charging over time are also shown in Fig. 5. The division of the flow rate into the bypass and through the storage is controlled based on the temperature at the mixing point and increases over time until the entire flow rate goes through the storage. The controls in the simulation are ideal. The adjustment of the bypass flow rate over time for the physical storage system will be adapted based on the temperature measurements during commissioning. The sensible charging results in a longer charging than discharging duration by a factor of about 50. As the steam can be used for the customer for the duration of charging, this long charging time is insignificant.
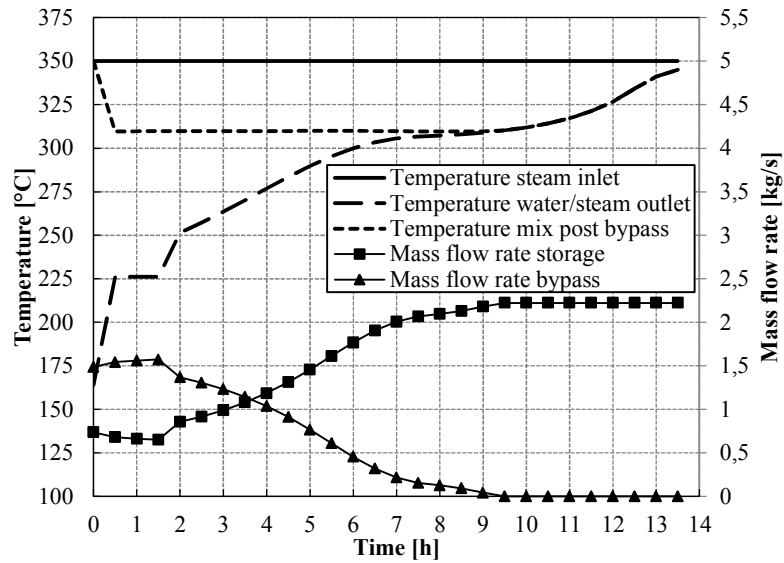
Fig. 5: Simulation results of the steam inlet and water / steam outlet temperatures, the mixed temperature post-bypass and the storage and bypass mass flow rates during charging over time.

Fig. 6 shows the top, middle and bottom averaged temperatures in the PCM. Here, the phase change plateau for both the evaporation on the HTF side at the bottom of the storage and the phase change temperature of the storage material are visible. The storage material at the top of the storage barely changes temperature at all. However, this energy is necessary for superheating the steam to 300 °C for the entire discharge.
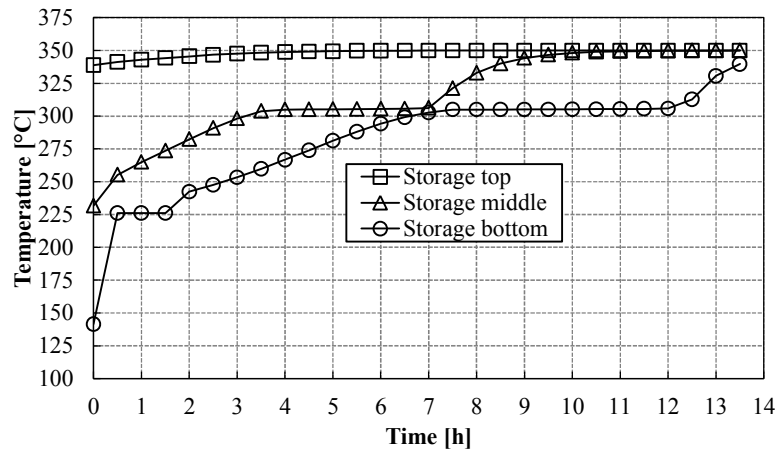
Fig. 6: Simulation results of the temperatures in the storage material at the top, middle and bottom of the storage unit during charging over time.

4. Conclusion andoutlook

This paper describes the simulation and design methodology for designing a latent heat thermal energy storage unit for a specific application and its requirements. Also, the various design considerations for designing a storage unit for a running production unit are discussed. The methodology has several steps for reaching a design result. This methodology will be optimized for future design processes to reduce the necessary number of steps. The operating requirements for the storage unit have been met with the design detailed here. With this critical step having been achieved, the detailed design and build can occur.

The storage unit design is currently in the detailed engineering phase, in which the headers are being dimensioned, the welds engineered and the flange and valve connections to the plant analyzed. The permitting process for the storage unit is currently in process, so that the process engineering and possibly the storage design may need adjustments after this process. Once the detailed design is set, the thermocouple and other sensory equipment can be planned. This will allow for a verification of the simulation models used to design this storage unit.

Acknowledgements

References

[1]   Kenisarin MM. High-temperature phase change materials for thermal energy storage. Renew Sustain Energy Rev 2010;14:955–70. doi:10.1016/j.rser.2009.11.011.

[2]   Mehling, Cabeza LF. Heat and cold storage with PCM. Heidelberg: Springer Verlag; 2008. doi:10.1007/978-3-540-68557-9.

[3]   Steinmann W-D, Laing D, Tamme R. Development of PCM Storage for Process Heat and Power Generation. J Sol Energy Eng 2009;131:041009. doi:10.1115/1.3197834.

[4]   Laing D, Bauer T, Breidenbach N, Hachmann B, Johnson M. Development of High Temperature Phase-Change-Material Storages. Appl Energy 2013;109:497–504. doi:http://dx.doi.org/10.1016/j.apenergy.2012.11.063.

[5]   Laing D, Eck M, Hempel M, Johnson M, Steinmann W, Meyer- M, et al. High Temperature PCM Storage for DSG Solar Thermal Power Plants Tested in Various Operating Modes of Water / Steam Flow. SolarPACES, 2012.

[6]   Johnson M, Breidenbach N, Laing D, Hachmann B. Experimental and numerical analysis of a phase change storage. Sol. 2013, Baltimore, MD, USA: 2013, p. 1–8.

2.7.   Paper VI: Experimental results

This article, entitled "Superheated steam production from a large-scale latent heat storage system within a cogeneration plant," was published in *Communications Engineering* in 2023. It was co-authored by Michael Fiss and this author is the first author.

The data from commissioning and filling of the storage system, followed by operation of the storage system is presented and analyzed here. This paper provides an analysis of the operation results, showing the initial operation and feasibility of production of superheated steam at the megawatt scale.

The author is responsible for the conceptualization, data analysis, funding acquisition, methodology, project administration, validation, visualization and writing of this paper. Michael Fiss assisted in the formal analysis and discussion of methodology.

ARTICLE

Check for updates

Superheated steam production from a large-scale latent heat storage system within a cogeneration plant

Maike Johnson [1]✉ & Michael Fiss[1]

During phase change, phase change materials absorb or release latent heat at a nearly constant temperature. Latent heat thus can be stored and integrated with evaporation/condensation systems such as steam generators within a relatively narrow range of operating temperature. Storage units and systems have been proven at pilot scale but none to-date have been integrated in industrial processes. This remains a challenge, due to the size of the systems and to hurdles in design, permission and build. Here we integrate a megawatt-scale latent heat storage into a cogeneration power plant in Wellesweiler-Neunkirchen, Saarland, Germany. The storage produced superheated steam for at least 15 min at more than 300 °C at a mass flow rate of 8 tonnes per hour. This provided thermal power at 5.46 MW and results in 1.9 MWh thermal capacity. Our study demonstrates the feasibility of using latent heat storage in the industrial production of superheated steam.

[1] DLR, Institute of Engineering Thermodynamics, Pfaffenwaldring 38-40, 70569 Stuttgart, Germany. ✉email: maike.johnson@dlr.de

Thermal energy is used for residential purposes, but also for processing steam and other production needs in industrial processes. Thermal energy storage can be used in industrial processes and power plant systems to increase system flexibility, allowing for a time shift between energy demand and availability[1]. To this end, various types of thermal energy storage have been developed, from thermo-chemical systems to molten salt, solid matter, or latent heat, as discussed in depth by Steinmann[2].

In latent-heat storages, the storage material changes phase from solid to liquid during the charging or energy absorption phase of operation, and from liquid to solid during discharging, or energy release. During phase change, the phase change enthalpy or latent heat is absorbed or released at a nearly constant temperature. Due to this, latent-heat storage integrated into evaporation/condensation systems such as steam generators provide or store relatively large amounts of energy per unit volume within the narrow temperature range of evaporation/condensation. The systems can be cooled to ambient temperatures, as solidification is integral to the system, as opposed to in molten salt thermal energy storage systems. Thermo-chemical storage concepts are in an earlier stage of development; currently, material development for the movability of reactants is still an issue[3].

To date, latent-heat storages tested with evaporation in the heat transfer fluid (HTF) at up to 700 kW$_{th}$ power have been tested and published, among others, by Laing et al.[4], Garcia et al.[5], and Weller et al.[6], but none of these systems produces superheated steam, and were not integrated into operating industrial processes. In Garcia et al.[5], an extensive listing and discussion of the existing high-temperature latent-heat storages are well documented; this listing shows developmental steps in the technology but no integration outside of the laboratory environment.

In this article, the commissioning of a latent-heat thermal energy storage system for the production of superheated steam in an industrial setting is discussed. This was developed, built, and integrated into a cogeneration power plant in Welleweiler-Neunkirchen, Saarland, Germany. The design of the system and the method including the simulation results are discussed in detail in ref. [7], and the build and integration in the plant in ref. [8].

Methods

System requirements. The requirements of this specific integration are for standby operation, resulting in a needs-driven (as opposed to scheduled) discharging at full load for at least 15 min, which is followed by a non-critical charging. While standby operation is not uncommon, these requirements are likely rare enough to not lead to the development of a specific decarbonization technology for this field. This type of storage system can, however, be introduced for waste heat integration or peak-shaving operation in, for example, autoclave processes[2]. This can be as a solo-unit or with a modular design, allowing for serial or parallel operation of multiple storage units within one system. Specific markets are being researched in parallel to the technology development[9,10]. Current price developments for both manufacturing, energy, and materials make cost estimations for such a new technology difficult and should be carried out by industrial process owners and storage system manufacturers.

The power plant in Wellesweiler-Neunkirchen is a cogeneration plant, producing steam for industrial customers for process and heating purposes, as well as electricity for the grid. The plant is heat-driven and the primary steam generator is a gas turbine (GT), with 5.2 MW$_{el}$ and 8.5 MW$_{th}$ nominal powers, connected to a downstream heat recovery steam generator (HRSG). The HRSG feeds steam mains, supplying steam to several industrial customers. The steam directly emitted from the HRSG has a temperature of 350 °C; water injection reduces the temperature to just above 300 °C. The GT burns mine damp from the mine-damp network in Saarland[11]. A basic schematic of the power plant, showing the integrated storage system, is depicted in Fig. 1.

The customers require constant specific parameters of steam with a minimum of 300 °C, 25 bar, and at least 8 t h^{-1}. When the GT and HRSG cannot supply this, the standby system must assume steam supply. This is often due to fluctuations in mine damp quality or quantity. The steam must be provided by the standby system within the time that the HRSG produces steam
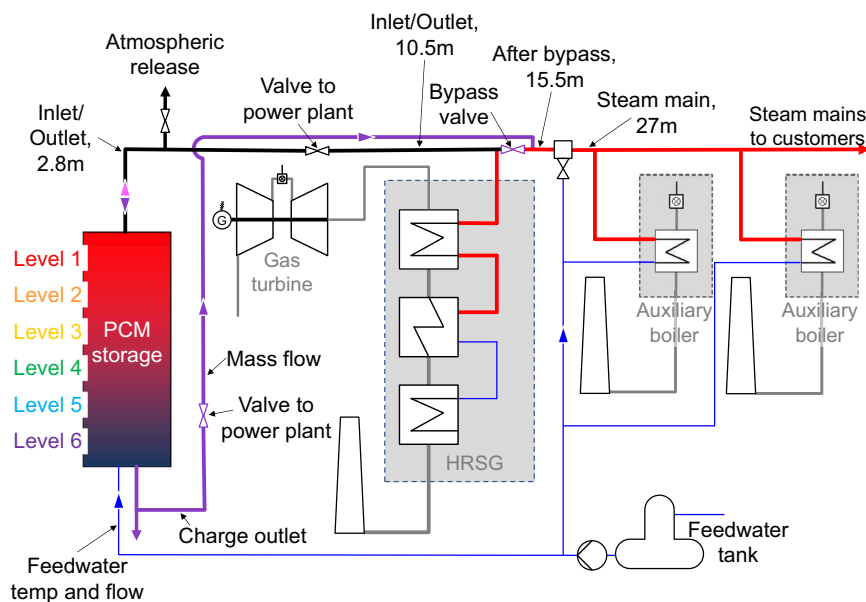
Fig. 1 Simplified schematic of the integration of the storage. The storage is in parallel to the heat recovery steam generator (HRSG) and auxiliary boilers with locations of the system and storage measurements denoted. Blue denotes feedwater and red denotes steam. Charging piping is shown in purple and discharging in pink.

after a GT-trip in lag-time, which is 2 min, as determined by experience from the power plant operator and discussed in ref. [7]. This ensures a constant steam quality in the steam mains.

Two auxiliary boilers, each with a nominal power rating of 13 MW$_{th}$, also feed the steam mains. The auxiliary boilers are used, depending on the season and related steam demand, either solely in standby or also to augment steam production. These auxiliary boilers can burn either mine damp or light fuel oil. In order to ensure high steam quality in the steam mains, an auxiliary boiler is held at least at minimal load. Minimal load is the lowest load at which fossil fuels are burned. Below this load, the component can be kept in so-called heat maintenance state; here, steam from another process (i.e., HRSG) flows through the auxiliary boiler to keep the component warm. From minimal load, full steam production can be attained in 2 min; from heat maintenance, 15 min are needed.

The thermal energy storage system is integrated into the power plant in order to reduce the minimal load operation of the auxiliary boilers. The fully charged storage can assume standby operation, which was to-date the operation in the minimal load of an auxiliary boiler. With the storage integrated, the auxiliary boilers are reduced from minimal load to heat maintenance.

The storage is, therefore, integrated in parallel to the HRSG and the auxiliary boilers (Fig. 1). When required, the storage is discharged and thereby evaporates feedwater to superheated steam. This steam flows past the water injection point to regulate the temperature to just over 300 °C and from there on to the steam mains. During this time, an auxiliary boiler is ramped-up from heat maintenance to full load.

The storage is discharged with 103 °C feedwater. The outlet parameter as required by the customers is steam at 300 °C, as stated. The saturation temperature at the system pressure of 25 bar is about 224 °C; the steam in the steam mains is, therefore, superheated by at least 76 °C. Using mass flow rates and enthalpy calculated with XSteam[12], which is based on IAPWS-IF97, the required minimum discharging parameters equate to a thermal power of 5.72 MW$_{th}$ using Eq. (1) and are summed to a thermal capacity of at least 1.43 MWh$_{th}$.

$$\dot{\mathbf{Q}}(t) = \dot{\mathbf{m}}(t) * \left(\mathbf{h}_{out}(t, p, T) - \mathbf{h}_{in}(t, p, T)\right) \quad (1)$$

Once the GT and HRSG are back in operation, the storage is charged, thereby returning it to standby conditions. During this time, an auxiliary boiler remains in minimal load operation, providing a standby for the HRSG/GT system until the storage system is again ready for operation. The storage is charged using steam directly from the HRSG. The steam can bypass the storage in total, which is normal operation, or in part (Fig. 1, purple), which is controlled by the bypass valve.

Steam flows downwards through the storage from the top to the bottom. At the beginning of charging, steam condenses. At the outlet of the lower header, the piping splits, with one part leading to a pressure release valve and a cooling pool for the condensate, and the other to the power plant system. Both of these piping sections are valve-controlled. The exiting steam temperature increases with the state-of-charge of the storage. Once the saturation temperature (~224 °C) is reached, the steam can be used by the power plant system; until this time, it is disposed of in the cooling pool. The mass flow rate going through the storage system is ramped-up during charging via a controlled bypass valve in order to maximize the steam used by the system. For most of the charging cycle, the steam cools in the storage but does not condense and is passed on to the customer. Because there is no phase change in the HTF during this time, comparatively little energy can be transferred, and charging, therefore, takes notably longer than discharging; the steam supply system continues operating while charging.

Storage design. In order to produce this superheated steam for these requirements, a thermal energy storage was developed. The development, detailed in ref. [7], resulted in a finned-tube shell-and-tube style latent-heat storage. The fins are assembled on the tubes with the clipping method studied by Johnson et al. in ref. [13]. Figure 2 shows the resulting hexagonal fin-tube assembly design. These fins are integrated to increase the heat transfer surface to the phase change material (PCM), which has a low thermal conductivity, especially when heat transfer is limited to conduction after solidification. The fin design results from a combination of two-dimensional simulations of heat transfer, empirical experience in manufacturing extruded aluminum, and experience with previous fin designs; the tube spacing in this storage is very dense at 70 mm.

Due to its melting temperature between the system limitations of 300 °C and 350 °C, as well as proven thermal stability as a PCM[14], sodium nitrate is used. The relevant material properties, as discussed by[14], are a theoretical melting temperature of 306 °C, a specific heat capacity of 1655 J (kg K)$^{-1}$, a heat conductivity of 0.55 W (m K)$^{-1}$, and a latent heat of 178 kJ kg^{-1}. The melting temperature of the actual salt inventory was measured using differential scanning calorimetry at about 304 °C (shown in the Supplementary Methods: Materials analysis, Supplementary
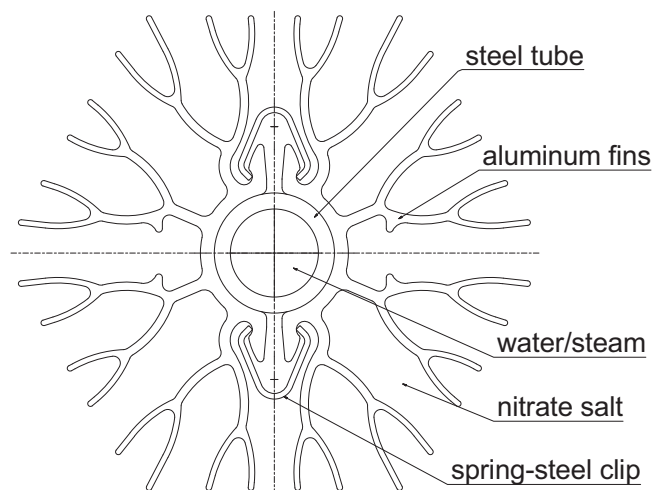
Fig. 2 Diagram of fin-tube assembly. Tree-like aluminum fins are held together by two spring-steel clips around a central steel tube.
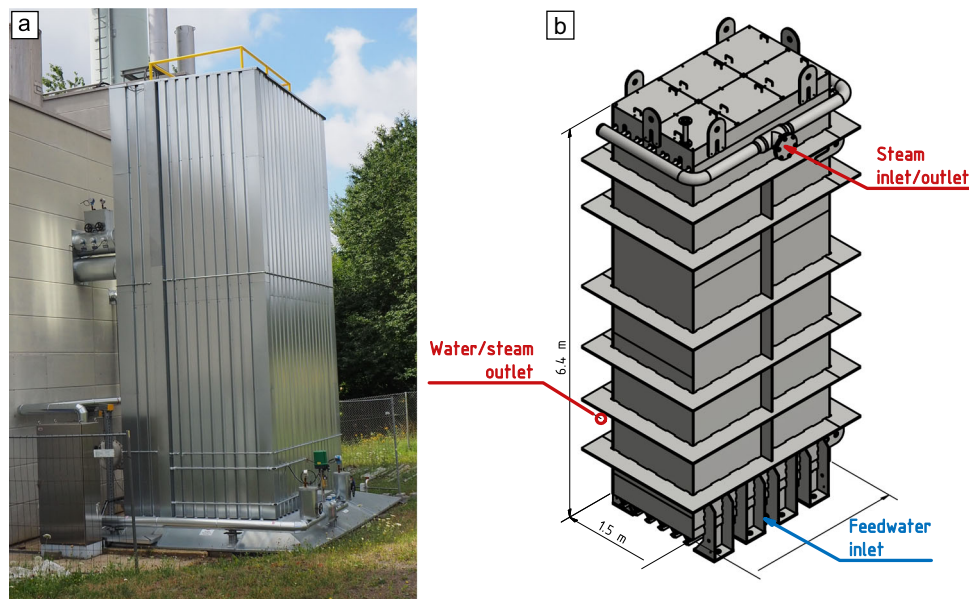
Fig. 3 Cogeneration plant with integrated storage. a A picture and **b** a schematic diagram. For reference: the control cabinet at the bottom left is 2 m tall.

Filling iteration	Empty volume at 25 °C, in m³	Salt mass at 350 °C in this volume, theoretical in t	Salt mass in storage, in t	Fill level, in %
Table 1 Volume and fill level of the storage during iterative filling.				
Empty	16.9	31.8	0	0
After 1st	8.9	13.8	18	57
After 2nd	4.7	4.2	27.6	87
After 3rd	3.5	1.5	30.3	95

Fig. 1). The ca. 32 t of storage material is on the shell side of the storage, directly contacting the fins. Figure 3 shows the storage installed, connected, and thermally insulated at the cogeneration plant, both as (a) a picture and (b) as a schematic diagram giving the basic dimensions.

Storage filling. Technical-grade sodium nitrate is the storage material in this system. This salt has a melting temperature of approximately 306 °C [14, and literature cited therein]. Due to the density differences in the salt depending on its temperature and form (Supplementary Methods: Materials analysis, Supplementary Table 2), filling is an iterative process. The iteration steps include manual filling, heating above the melting temperature, and active cooling as low as the system allows, followed by passive cooling down to safe working conditions.

After an initial filling of the storage, the system is heated above the melting temperature of the salt. For the heating step, the storage is heated from ambient temperature; during later normal operation, a return to ambient temperature is not planned. With the thermocouples dispersed in the salt volume of the storage, it is possible to measure the salt temperature at these points, but not globally throughout the storage. The storage was therefore heated with a low mass flow rate to slowly heat the system, and heated to well above the melting temperature. This is to ensure that all of the salt pellets melt. Due to the low thermal conductivity resulting from the point-form contact between the salt pellets, this process took several days for each iteration.

The heating of the storage was directly followed by an active cooling of the system. The active cooling is conducted by sending steam to the steam mains until the temperature is too low, and thereafter emitting the HTF to the atmosphere until the HTF

coming out of the roof expansion valve is in the liquid state. Thereafter, the system cools passively until safe working conditions are achieved; this passive cooling time increases with increasing fill level and takes 3–5 weeks.

Geometric calculations of the design of the storage results in a fill volume of 16.9 m³ of sodium nitrate, which results in a salt mass of approximately 32 t. However, considering the storage size, manufacturing tolerances and possible bowing of the side walls of the storage can change the ultimate fill level or amount. The iterative filling process has been conducted three times, and the storage attained approximately 95% fill level with the third filling, as detailed in Table 1.

Data acquisition. To analyze this storage system, both system data as well as detailed storage data are relevant. The system data measures the input-output of the storage system, including the flow parameters in different parts of the system but considering the storage itself more as a black-box. These results give insight into the performance of the whole system.

The storage measurements are used in order to better compare the design to the build of this storage. With this, it is possible to analyze solidification around the fins and at different points within the storage unit.

System measurements. The storage is integrated with two flanges at the bottom of the storage and one at the top, as shown schematically in Fig. 3b. At the bottom, one flange is an inlet for feedwater during discharging and the other is an outlet for water/steam during charging. The upper flange is a steam inlet/outlet for charging/discharging, respectively.

For the system analysis, the temperatures and pressures of the water/steam used as the HTF are measured near the flanges of the storage. The HTF temperatures are measured via 6 mm PT-100 type TR88, in 24 mm immersion sleeves type TW15, both from Endress and Hauser. The mass flow rate of the feedwater into the storage as well as the superheated steam in the steam main are measured. The feedwater flow is measured with an ultrasonic volumetric flow meter from Metra, type ultrakon®. In the steam main, the flow rate is measured via an orifice plate, and the temperature is measured via PT-100; these are components of an energy measurement unit from Metra, type autarkon® EWZ, coupled with a Danfoss IWK control unit. In addition, the ambient temperature is measured.

Storage measurements. For a detailed analysis of the storage, temperature measurements throughout the storage unit are used in combination with the system measurements. To this end, thermocouples are positioned throughout the PCM. In addition, thermocouples are affixed on the outside of the container walls, headers, and the outside of the insulation. The thermocouples are NiCr-Ni type K class 1 according to DIN EN 60584, with a 1.5 mm diameter Inconel sheath. Three lengths of thermocouple sheath were used in the system: 1.5, 6, and 9 m.

During the cycle analyzed here, 80 thermocouples were used for measurement. Of these thermocouples, 18 were calibrated according to DIN 55350-18-4.2.2 at the reference temperatures 103, 305, and 350 °C, correlating to the feedwater inlet temperature, the approximate melting temperature of the salt and the maximum steam inlet temperature, respectively. These calibrations showed an absolute minimum, maximum, and average deviation of respectively 0.01, 1.81, and 1.01 K.

The distribution of the thermocouples over the cross-section of the storage is shown in Fig. 4. Other thermocouples will be mounted during the finalization of the insulation. The thermocouples are affixed at six measurement levels. Some redundancy between the thermocouples exists, though not all measurements are fully redundant.

Thermocouples at the edges and corner of the storage—L02, B18, W18, M34, and W01—give insight into thermal losses over the large surface area of the storage and will assist in determining the necessity of recharging the storage if the standby time is long. In addition, there are thermocouples located between the edge and the center—L05 and S18—to also better understand thermal losses and temperature distribution throughout this large storage.

Most thermocouples are located in a central area around two central tubes. These are spaced so that the compromise between introducing an error by inserting a measurement device and needing the information is best met. The tube labels are those between columns I and N and rows 17 and 23, and are discussed in the Supplementary Discussion: Thermocouple results. A group of thermocouples near tube S5 is mounted specifically for an additional analysis of the state of charge, which will be conducted with further cycles.

The measurements are collected in a control cabinet next to the storage and are communicated from there to the power plant controls via a bus system. The control cabinet is on the north side of the storage, thereby having little temperature variation due to direct sun. The thermocouples are coupled into modules in the control cabinet of the multi-use type AI 731F from ABB with activated internal temperature compensation.

The data set and further analyses showed a residual current in the control cabinet that could not be adjusted for by the multi-use data acquisition modules used. These are not optimized specifically for thermocouples. As the measurement principle behind thermocouples is based on changes in voltage differences, the influence of the residual current has an influence on the data acquisition. To account for this, a length-dependent reductive shift was calculated into the thermocouple data. To determine the temperature-shift, the temperatures were measured with two thermocouples for each of the lengths with a calibrated hand-held measuring device and with the data acquisition system. The average difference between these two values was then subtracted from all thermocouple results according to their length.

The data for the specific storage system components is written for each data point every 30 s and transferred to files once a day. In the rest of the power plant, data is written to file when the value changes. The data analysis was conducted using Matlab® R2020a. Data for the thermocouple measurements is shown in the Supplementary Discussion: Thermocouple results.

Results and discussion

Charging. These charging results were gained during commissioning, after the third filling of the storage with pelleted salt. It brings the storage system from ambient conditions to a charged state. The salt inventory is partially pelleted, meaning that a part of the inventory has only point-contact with other particles.

The charging data, shown in Fig. 5, show that charging was started at 9:33 on Nov. 26, and continued until 9:55 on Nov. 29, meaning the storage was charged for 72 h. Figure 5a shows the mass flow from the storage and the valve setting controlling flow to the storage. Figure 5b shows the temperature measurements at the storage inlet and outlet as well as after the bypass. Charging was started with an average temperature, measured by the thermocouples in the PCM, of 19.6 °C. The lowest measured temperature in the PCM was 17.3 °C, and the highest 22.3 °C. Steam was produced after about 3 h and after about 44 h, at 5:18 on Nov. 28, the outlet temperature was more than 300 °C, the required temperature for sending the steam directly to the steam mains without mixing. The mass flow rate during charging was about 4 t h^{-1}.

During charging, the storage is heated to well above 306 °C, the melting temperature of the sodium nitrate. Charging was completed with an average temperature measured by the thermocouples in the PCM of 327.9 °C. The highest measured PCM temperature was 331.5 °C and the lowest was 324.8 °C. This allows for a high driving temperature difference between the PCM and the feedwater during discharging.

Discharging. The storage is discharged using feedwater, which evaporates and is superheated, as shown schematically in Fig. 1 in blue and pink. The main system data results are shown in Fig. 6. Here, the feedwater mass flow (a, blue dashes) and the steam main mass flow rate (a, black line) are shown. The feedwater flow rate is an input to the system, and is a variable that is always varied by the operator according to power plant needs and operating conditions; for these initial tests, it is controlled manually. The five valves controlling flow to and from the storage in the different connections also are adjusted, leading to temperature reactions in the system, shown in Fig. 6b. With more operation experience and increasing automation of the discharge, the input flow rate will become more constant.

The steam temperature data is shown for several positions in Fig. 6b. Shown are the temperature measurements 2.8 m after the outlet of the storage, the temperature past the bypass, located about 15.5 m from the outlet of the storage and inside the GT-Building, and past the water injection site at the entrance to the steam mains, 27 m from the storage flange. These distances are given to assist in understanding differences in temperatures as well as shifts over time, considering the ambient temperatures (0.2 °C at the beginning of discharging).

For the discharging of the system after the third filling, discharging began at 10:11, at which time mass flow into the storage started and the valves to the storage and from the storage
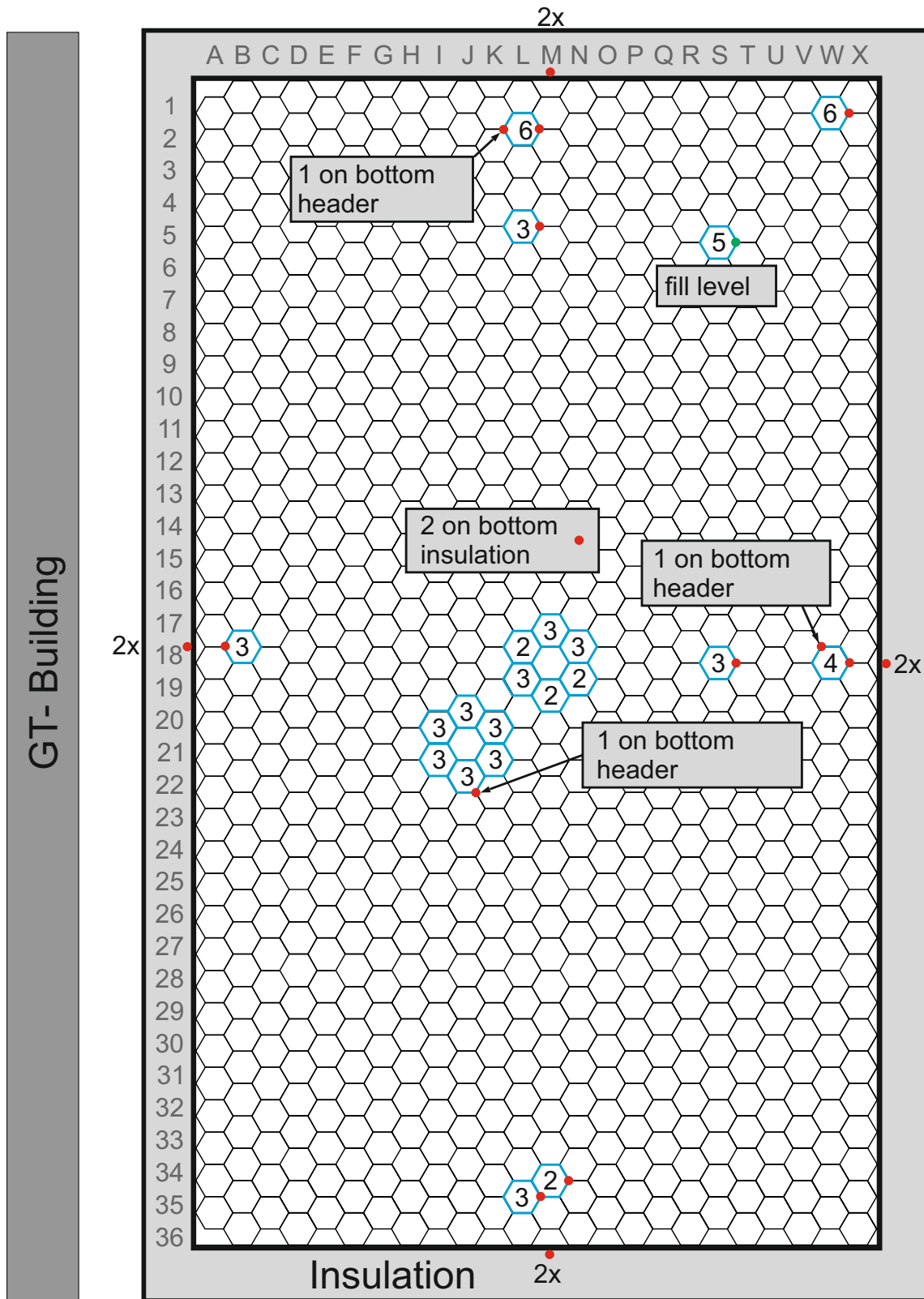
Fig. 4 Schematic location of thermocouples. Shown from above is a cross-section of the storage, with row numbers and column letters for location, and finned-tubes denoted by hexagons. Numbers in hexagons denote how many vertical levels are equipped with thermocouples. Thermocouples are mounted around two central tubes for redundancy, as well as at the middle, edges, and corners. Red dots denote thermocouple locations, also on the container wall at two heights.
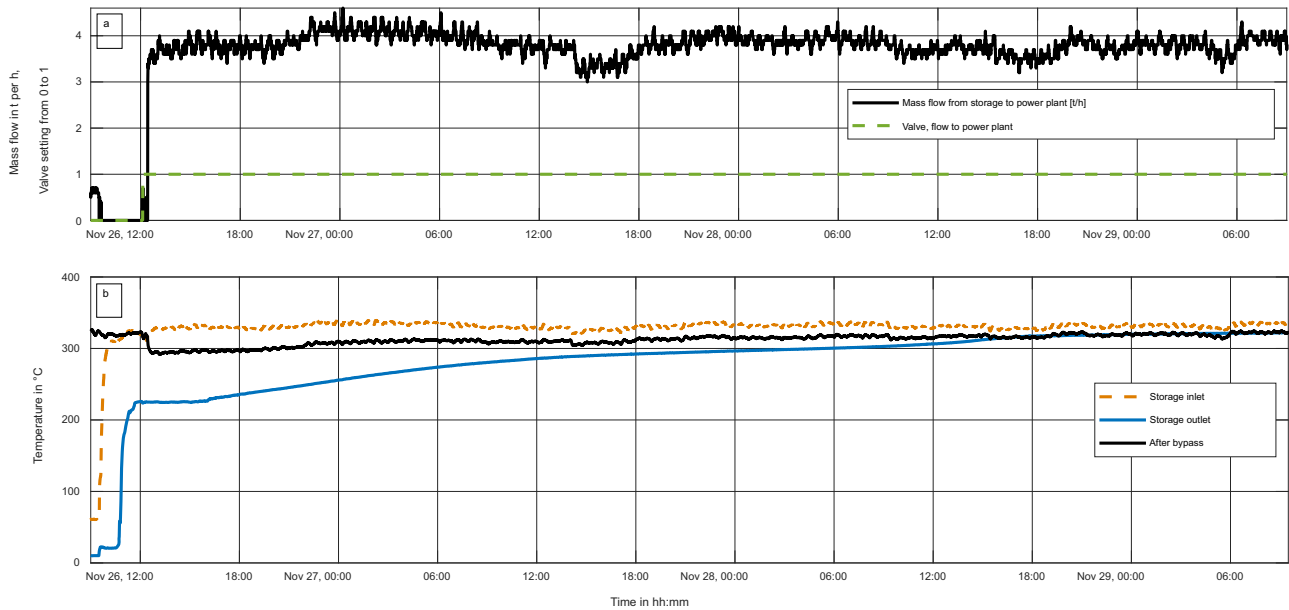
Fig. 5 Plot of charging data of the storage system. Shown from ambient conditions, showing **a** mass flow rate through the system and the valve setting denoting when the flow through the storage system flowed to the steam mains and was no longer emptied to the condensate outlet as well as **b** temperatures of the storage inlet and outlet near the top and bottom flanges, respectively, and after the system bypass.
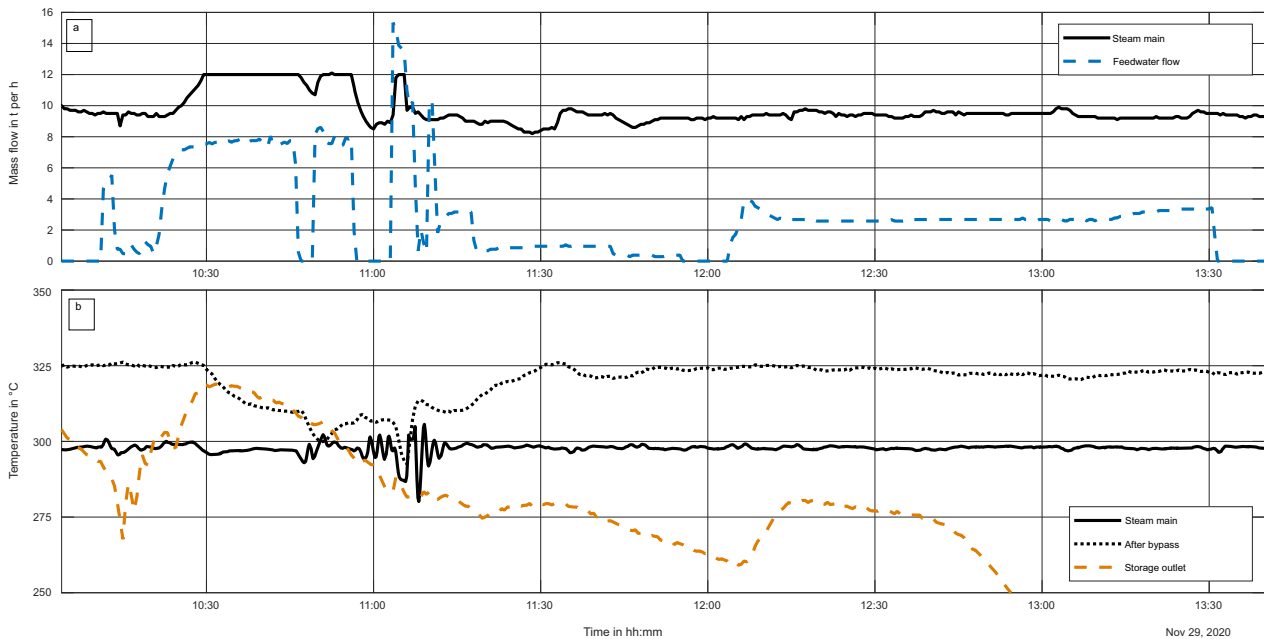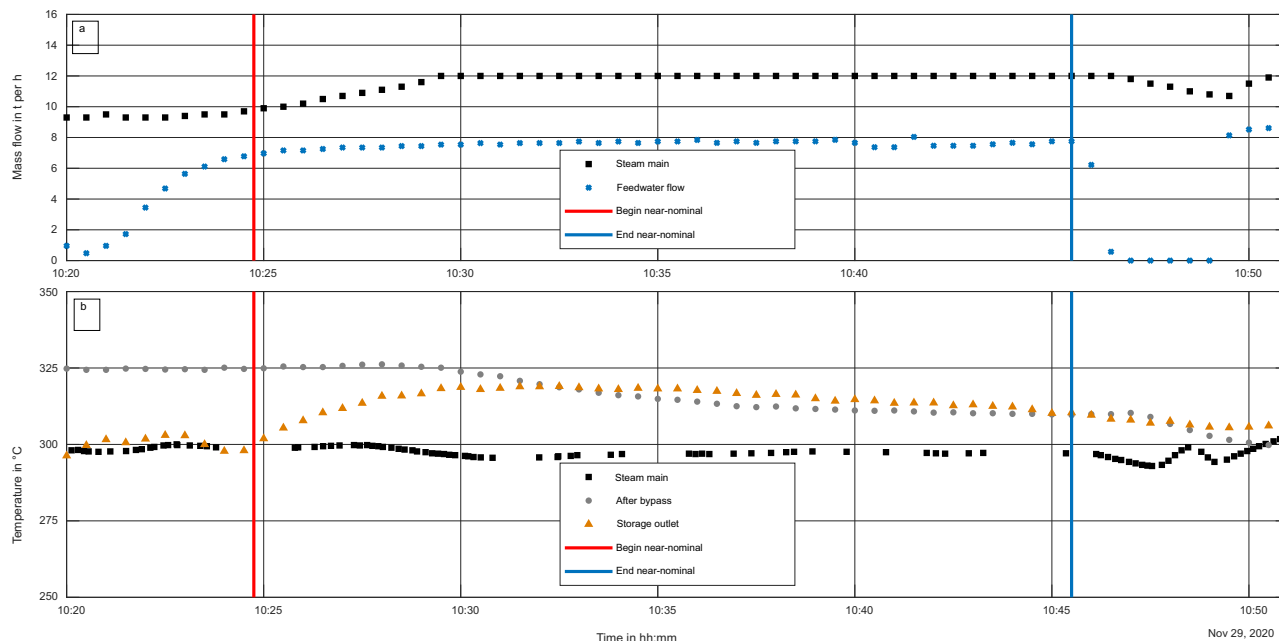

Fig. 6 Plot of full discharging of the storage system. Showing **a** mass flow rate through the storage system and in the steam main and **b** temperatures of the steam past the outlet of the storage, just after the system bypass and in the steam main.

to the power plant were opened. At 13:33, feedwater flow into the storage system was stopped.

The minimum required temperature for stable operation of the steam mains is 300 °C. In a real operation of the system, the HRSG would not be in operation, so this requirement must be met by the storage system. This temperature was maintained for 28 min (from 10:25 until 10:53). The first 20 min (from 10:25 until 10:45), the mass flow rate through the storage was approximately the nominal rate of 8 t h^{-1}; this means that during this timeframe, the storage was discharged under nearly nominal conditions.

The measurement position for the mass flow rate in the steam main measures the combined flow from the storage and the HRSG. During this initial operation, the HRSG was also in operation, so that the mass flow rate in the steam mains is augmented by the steam from the storage system; steam production by the HRSG was manually adjusted to match the demand parameters.

The steam from the storage system was fed into the main from 10:22 until 11:04. At 11:04, the steam temperature after the bypass sunk to 300 °C. At this point, the valve to the main was closed and the flow was emitted to the atmosphere. Discharging continued in

Fig. 7 Plot of discharging of the storage system for near-nominal conditions. Near-nominal conditions are denoted by vertical lines, from 10:20 to 10:50, showing **a** mass flow through the storage system and in the steam main and **b** temperatures of the steam past the outlet of the storage, just after the system bypass and in the steam main.

order to cool the storage as much as possible for further commissioning, as described in the methods section.

The system requirement for the storage system is the production of superheated steam for at least 15 min; during this discharging, steam of sufficient quality (>300 °C, >25 bar) was produced for 43 min, showing a much better performance than necessary.

Thermal power and capacity. The discharging of the storage system is the more critical of the two processes. It requires high thermal power from the component, and only with this thermal power can the system parameters be reached and the storage be useful for the power plant once the testing phase is completed. This high thermal power level requires a very fast heat transfer from the PCM to the HTF.

To assess the capabilities of the storage system, the results were analyzed for the time during which the outlet temperature of the storage was greater than 300 °C and the mass flow rate close to $8 \, \text{t h}^{-1}$. During this timeframe, the average mass flow rate of feedwater into the storage was $7.6 \, \text{t h}^{-1}$, with a minimum of $7.0 \, \text{t h}^{-1}$ and a maximum of $8.0 \, \text{t h}^{-1}$. The timeframe for these near-nominal conditions was 10:25 and 10:45. The details for this timeframe are shown in Fig. 7 in (a) for the mass flow rates and (b) for the temperatures.

From the measurements, the thermal power transferred to the HTF is calculated using Eq. (1). For each time step of 30 s, using the temperature and pressure data, enthalpy is calculated at the inlet and outlet of the storage using XSteam[12]. With this and the mass flow rate, thermal power is calculated and summed to thermal capacity.

These results are plotted in Fig. 8. The timeframe for capacity summation, shown in (c), begins with the temperature meeting the 300 °C criterion (orange vertical line, temperature shown in (b)) and ends when the power plant operator down-regulated the mass flow rate (blue vertical line, mass flow shown in (a)).

The average discharging power during this time was $5.46 \, \text{MW}_{\text{th}}$; the energy discharged was $1.9 \, \text{MWh}_{\text{th}}$. As discussed earlier, the operating requirements lead to a necessary power of

$5.72 \, \text{MW}_{\text{th}}$ and a capacity with a 15-min discharge of $1.43 \, \text{MWh}_{\text{th}}$. This thermal power level was not quite attained; however, with a mass flow rate of $8 \, \text{t h}^{-1}$ and not just $7.6 \, \text{t h}^{-1}$, the requirements will be met.

Conclusions

The storage system analyzed here is integrated into an operating cogeneration plant, mostly providing steam to critical customers. This gives insight into the entire process of design, permitting, build, and integration into a real system. However, the parameters with which the system can be commissioned and tested are limited by both power plant system limitations as well as operating restrictions, as the steam demand has to be met constantly.

Within this work, a storage system for the production of superheated steam for an industrial system was operated. This process is a cogeneration plant requiring steam with at least a temperature of 300 °C and a pressure of 25 bar. In order to maintain steam quality in the steam mains for the industrial processes, this storage is integrated as a standby for the GT and HRSG, providing the full steam load of $8 \, \text{t h}^{-1}$ within 2 min if the GT trips, and providing this steam for at least 15 min while an auxiliary boiler increases load from heat maintenance to full load. This integration allows for a load reduction in the auxiliary boilers from minimal load, which burns fossil fuels, to heat maintenance, reducing the use of oil as a primary energy source.

The results from an initial operation are discussed. Charging of the storage took about 44 h from ambient conditions with pelleted salt. According to the design, from normal operating conditions post-commissioning, charging takes about 14 h. This is because charging is conducted using the sensible heat from steam, and that steam is used by the customer. Therefore, the system continues to operate during charging. In other integrations in which the condensate can be integrated into the industrial system, faster charging with phase change in the HTF would be possible.
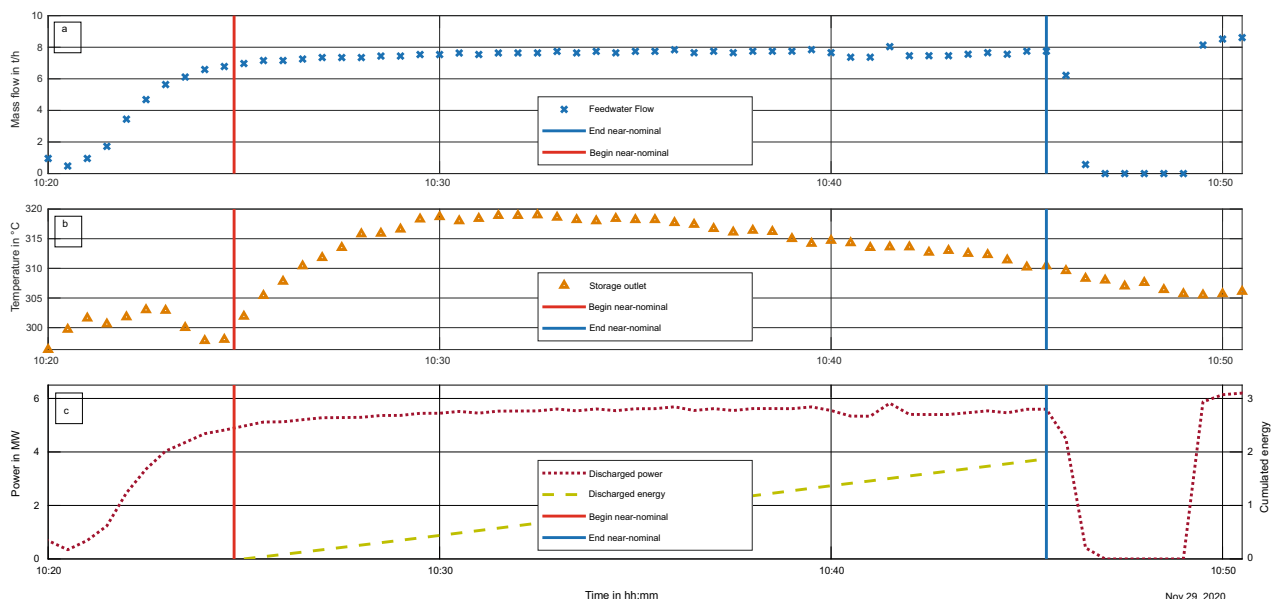
Fig. 8 Plot of discharging of the storage system for near-nominal conditions from 10:20 to 10:50. Near-nominal conditions denoted by vertical lines, limited by mass flow averaging 7.6 t h^{-1} (shown in **a**) and an outlet temperature >300 °C (shown in **b**). These are calculated to power and energy (shown in **c**). Energy is cumulated during the near-nominal conditions.

The discharging process analyzed here directly followed a charging process. During commissioning, the method for recharging the storage is determined—either constantly recharged with a minimal flow or periodically. Both are possible during standby operations.

During this discharging, near-nominal conditions were attained for 20 min, with an average superheated steam mass flow rate of 7.6 t h^{-1} to the industrial customers produced by the storage system. This exceeds the minimum requirement by 5 min, respectively, 33%. During this time, an average power of 5.46 MW$_{th}$ was discharged, resulting in an energy discharge of 1.9 MWh$_{th}$. The design goals were 5.72 MW$_{th}$ and 1.43 MWh$_{th}$, respectively; the flow rate used in this discharge was somewhat under the nominal flow rate of 8 t h^{-1}.

These results show that the high thermal power rates required in industrial processes are possible, overcoming the hurdle of heat transfer into PCMs. In addition, with more trust in the design methods used, smaller storages can be built to meet these same requirements; simply said, this storage is larger than necessary. However, as this was the first such storage system integrated into an operating system, safety factors were planned into the design.

Due to complications with the system integration, commissioning has been paused. Once commenced, it will embody a full testing regime of further charging and discharging cycles and tests at partial load, analysis of environmental losses, and more detailed comparisons of the thermocouple data with design results.

Although the integration goal of serving as a standby, and amortizing through the reduced use in fossil fuel use is less common, the need for peak shaving and other similar needs for steam delivery are more common. This first installation in an industrial setting can be used to reduce costs in future installations and better trust design methods for future storage systems specifically for different processes.

This storage system will not only provide system flexibility and fuel savings for this specific power plant system but, as the world's largest evaporative latent-heat storage system, it also shows that the feasibility of both upscaling, production of superheated steam and megawatt-scale heat transfer rates, as well as permitting a real system.

Data availability

Data sets generated during the current study are available from the corresponding author upon reasonable request.

References

1. IRENA. *Innovation Outlook: Thermal Energy Storage.* (International Renewable Energy Agency, Abu Dhabi, 2020).
2. Steinmann, W.-D. *Thermal Energy Storage for Medium and High Temperatures.* https://doi.org/10.1007/978-3-658-02004-0. ISBN 978-3-658-02003-3 (Springer, Wiesbaden, 2022).
3. Linder, M. Gas-solid reactions for energy storage and conversion, University of Stuttgart. *Habilitation Thesis.* url: https://elib.dlr.de/192363/ (2022).
4. Laing, D., Bauer, T., Breidenbach, N., Hachmann, B. & Johnson, M. Development of high temperature phase-change-material storages. *Appl. Energy* **109**, 497–504 (2013).
5. Garcia, P. & Largiller, G. Performances and control aspects of steam storage systes with PCM: Key learnings from a pilot-scale prototype. *Appl. Energy* **325**, 119817 (2022).
6. Weller, T., Johnson, M., Trebilcock, F., Lecompte, S. & Bauer, D. (2021) Design, build and initial testing of a novel energy management system. *Heat Powered Cycles Conference.* Bilbao, Spain, Sept. 2021 (2021).
7. Johnson, M., Vogel, J., Hempel, M., Hachmann, B. & Dengel, A. Design of high temperature thermal energy storage for high power levels. *Sustain. Cities Soc.* **35**, 758–763 (2017).
8. Johnson, M. et al (2018) Design and integration of high temperature latent heat thermal energy storage for high power levels. *Proceedings of the ASME IMECE, IMECE2018-86281.* Pittsburgh, USA, Nov. 2018 (2018). https://doi.org/10.1115/IMECE2018-86281.
9. Mehling, H., Brütting, M. & Haussmann, T. PCM products and their fields of application—An overview of the state in 2020/2021. *J. Energy Storage* **51**, 104354 (2022).
10. Du, K., Calauti, J., Wang, Z., Wu, Y. & Liu, H. A review of the applications of phase change materials in cooling, heating and power generation in different temperature ranges. *Appl. Energy* **220**, 242–273 (2018).
11. Steag New Energies GmbH, Saarbrücken. Grubengas verwerten bedeutet Klimaschutz, Sicherheit, Energieeffizienz. https://www.steag-newenergies.com/fileadmin/user_upload/FM_SNE/Leistungen/Grubengas/Artikel_Grubengas_Ruhr_Saar_2014.doc.pdf. Retrieved 25.04.2022 (2014).
12. Holmgren, M. X Steam, Thermodynamic properties of water and steam. (https://www.mathworks.com/matlabcentral/fileexchange/9817-x-steam-thermodynamic-properties-of-water-and-steam), MATLAB Central File Exchange. Retrieved 03.02.2021 (2021).
13. Johnson, M. et al. Assembly and attachment methods for extended aluminum fins onto steel tubes for high temperature latent heat storage units. *Appl. Therm. Eng.* **144**, 96–105 (2018).

14. Bauer, T., Laing, D. & Tamme, R. Characterization of sodium nitrate as phase change material. *Int. J. Thermophys.* **33**, 91–104 (2012).

Author contributions

M.J. is responsible for the conceptualization, data analysis, funding acquisition, methodology, project administration, validation, visualization, and writing of this paper. M.F. assisted in the formal analysis and discussion of methodology.

Competing interests

The authors declare no competing interests.

Additional information

Supplementary information The online version contains supplementary material available at https://doi.org/10.1038/s44172-023-00120-0.

Correspondence and requests for materials should be addressed to Maike Johnson.

Peer review information *Communications Engineering* thanks Ehsan Baniasadi and the other anonymous, reviewer for their contribution to the peer review of this work. Primary handling editors: Rosamund Daw, Mengying Su. A peer review file is available.

Reprints and permission information is available at http://www.nature.com/reprints

Publisher's note Springer Nature remains neutral with regard to jurisdictional claims in published maps and institutional affiliations.

Superheated steam production from a large-scale latent heat storage system within a cogeneration plant
# Supplementary information

Maike Johnson, Michael Fiss

Supplementary Methods: Materials analysis

Analysis of the storage material was conducted both with differential scanning calorimetry (DSC) as well as ion chromatography (IC). The DSC was conducted using a DSC 204 F1 Phoenix from Netsch, using perforated and cold-pressed standard aluminum crucibles and approximately 10 mg samples. The inert atmosphere was nitrogen at a flow rate of 40 mL min^{-1} and the heating rate 10 K min^{-1}. The DSC results are shown in Supplementary Figure 1. The melting onset temperatures were measured at 304.2 °C - 304.5 °C.

The IC was done with an 883 Basic IC plus from Metrohm using a Metrosep C4-150/4.0 cation column and 2.0 mmol HNO$_3$ + 0.3 mmol oxalic acid eluent. The anion column is Metrosep A Supp 5-250/4.0 and contains an eluent of 4 mmol Na$_2$CO$_3$ + 1 mmol NaHCO$_3$. The IC results are shown in Supplementary Table 1. Two probes were measured using a dilution of 1:10 and one with a dilution of 1:50, and the three probes show consistent results of the composition. The average nitrate in the anion is 70.7% and sodium in the cation is 26.1%.

For reference, the density of sodium nitrate in various states according to various sources is given in Supplementary Table 2.
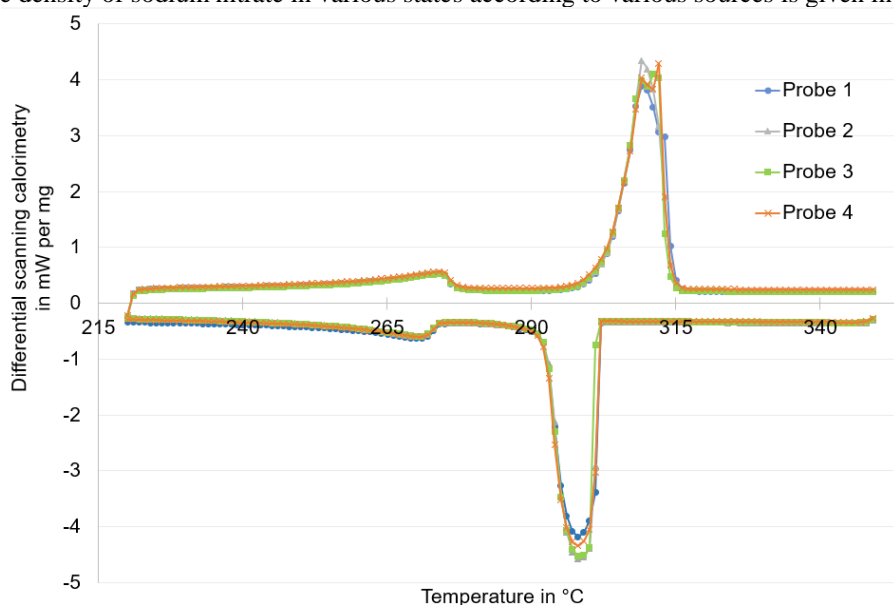
Supplementary Figure 1. DSC results for the technical grade sodium nitrate in the storage unit measuring a melting onset temperature of 304.2-304.5 °C.

Supplementary Table 1. IC measurements of probes of the pelleted sodium nitrate used in the storage unit.

Probe	Weight [mg]	Solution volume [mL]	Dilution [1:x]	Anion				Cation			
				Concentration [mg L^{-1}]		Amount [%]		Concentration [mg L^{-1}]		Amount [%]	
				Nitrate	Sulfate	Nitrate	Sulfate	Na	K	Na	K
1	1212.4	500	10	1732.32	2.94	71.44	0.12	641.67	4.79	26.46	0.20
2	1251.9	500	10	1789.51	3.03	71.47	0.12	661.63	5.06	26.43	0.20
3	6066.4	500	50	8404.95	14.39	69.27	0.12	3092.46	23.12	25.49	0.19

Supplementary Table 2. Temperature and state-dependent densities of sodium nitrate.

States	Temperature in °C	Density in kg (m³)$^{-1}$
Solid pellets [1]	25	1230
Solid block [2]	25	2260
Liquid [2]	306	1908
Liquid [3]	350	1879

Supplementary Discussion: Thermocouple results

In addition to system data during discharging, temperature measurements using thermocouples immersed in the PCM, as shown in Figure 8, main article, were also collected. The PCM temperature during charging around the central tubes are shown with the inlet and outlet temperatures of the HTF in Supplementary Figure 2. The evaporation temperature in the HTF at 225 °C is shown by a plateau in the PCM temperature measurements, and a plateau or slope change around the melting temperature of the PCM around 306 °C is also visible. The phase change front through the measurement levels (rainbow from top to bottom) is also clearly visible.
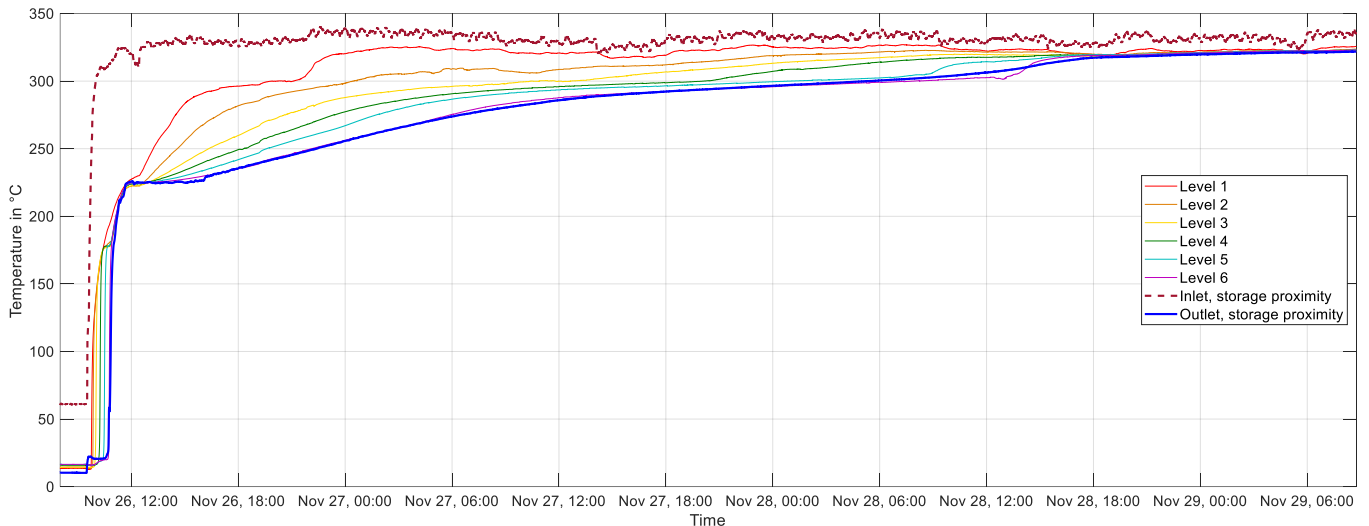
Supplementary Figure 2. Charging of the storage system, showing temperatures of the storage inlet and outlet as well as temperatures around the central tubes in the PCM, where each color shows a measurement level, 1 being near the top and 6 near the bottom of the storage.

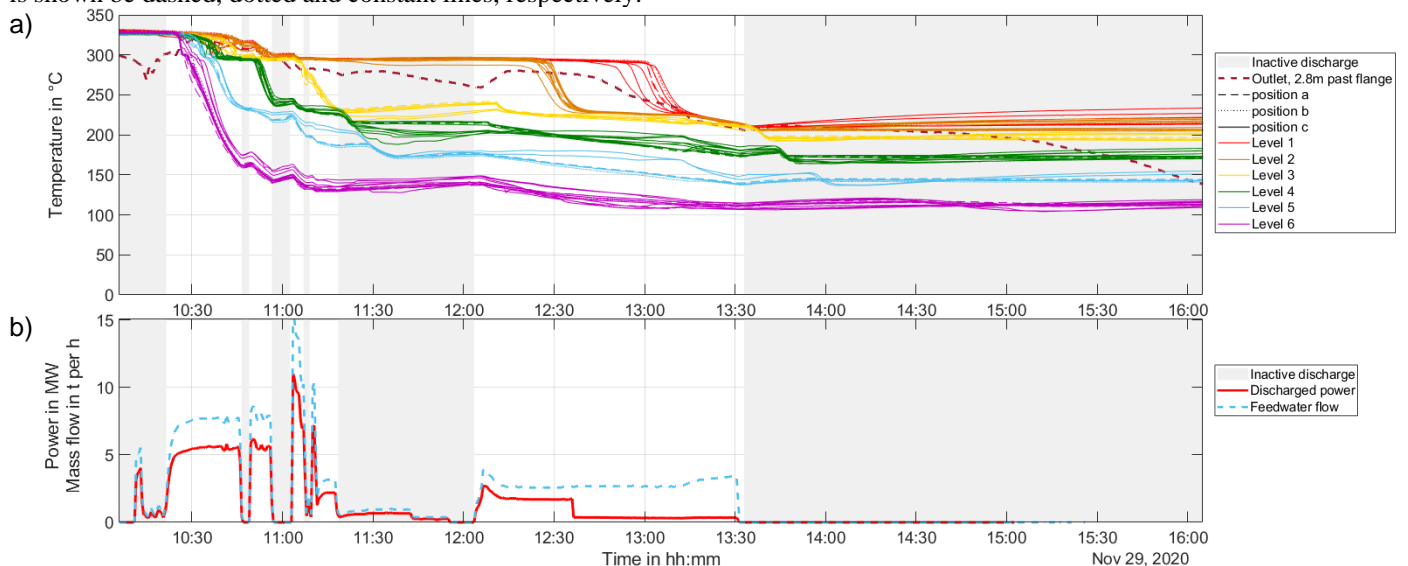Supplementary Figure 3 shows the thermocouple measurements during discharging for all of the central thermocouples. The feedwater flow rate, outlet temperature and calculated thermal power are also shown, and the timeframes during which the feedwater flow rate was zero, as in discharge paused or stopped, are greyed out in order to better show the phases of active discharging.

In the central tubes, the thermocouples are located in 'a', 'b' and 'c' positions, as shown in Supplementary Figure 4. These positions are to help compare the data with the design of the storage unit. To that end, a qualitative comparison is possible with the overlay of the positions and the FEM data from the design phase, shown in Supplementary Figure 4. The simulations in the design phase used for this overlay are discussed by Johnson et al. [4]. In Supplementary Figure 3, the 'a', 'b' and 'c' position data is shown be dashed, dotted and constant lines, respectively.

Supplementary Figure 3. Discharging of the storage unit as depicted by the thermocouple data. a) Thermocouples in the PCM during discharge, with greyed-out areas denoting inactive discharging phases and 'a', 'b' and 'c' position data is shown be dashed, dotted and constant lines, respectively. Temperature past the outlet shown in bold dashed. b) The accompanying mass flow rate and calculated heat transfer power.
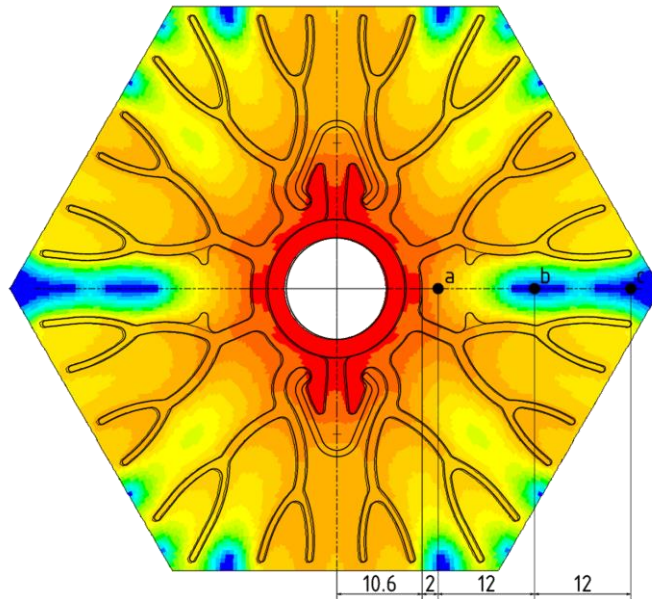
Supplementary Figure 4. Qualitative comparison of thermocouple positions on central tubes (see Figure 8, main article) located at 'a', 'b' and 'c' positions overlaid with design FEM analysis data for charging.

Supplementary Figure 5 shows an overview of the temperatures in the center tubes (columns I-N and rows 17-23 in Figure 8, main article). A clear front through the storage unit is visible from bottom (L6) to top (L1). The phase change plateau just below 300 °C is visible for each of the measurement levels, although it is unclear why this plateau is below the measured phase change temperature of about 304 °C. Level 6 (L6, purple) is about 20 cm from the bottom of the 5.5 m long fins and is deeply discharged past solidification at the end of this active discharging phase. The water inlet temperature is 103 °C during discharging. Levels 1 and 2 (red, orange, resp.) are still solidifying at this point in time.
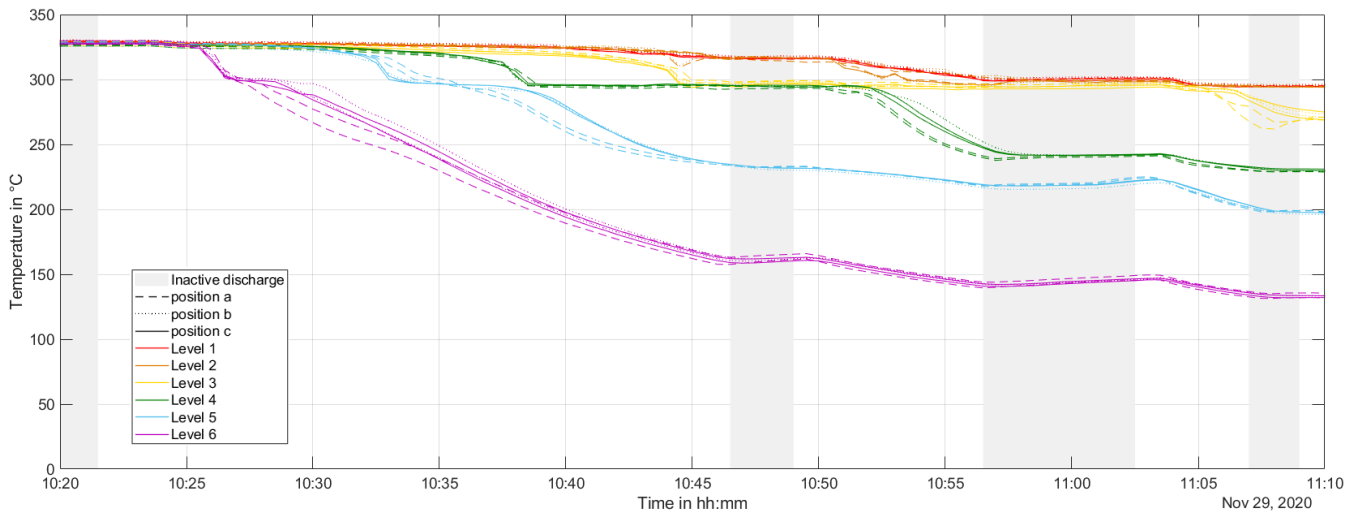
Supplementary Figure 5. Thermocouple measurement data in PCM during discharging with levels L1-L6 in red-purple rainbow, and position a (dashed), b (triangle, dotted) and c (solid) of the center tubes. During greyed-out times, there was no flow through the unit.

The analyses of the temperature distributions conducted during the design of the storage unit and system, discussed in [4], showed that, as expected, the temperature of the 'a'-located thermocouples should react fastest to the temperature changes. The 'b' and 'c' temperatures, however, react very similarly, due to the dense fin structure. The simulation results are overlaid with these positions in Supplementary Figure 4 to give a qualitative view of the expected results. A comparison of the expected temperature distribution and those measured during active discharging shows a correlation – the 'a'-located thermocouples in dashed lines in Supplementary Figure 5 discharge more quickly and the 'b' and 'c' thermocouples are more similar in temperature. Further analyses comparing these data to the design data will be conducted when more experiments have been conducted.

Supplementary Figure 6 shows the measurements during discharging of measurement level 4, showing both the center tube measurements (in green) and the middle and edge measurements, both close and far from the inlet headers. These measurements show that there is no great discrepancy over the cross-section of the storage in the active discharging of the unit. An even flow distribution through the headers at nominal flow rates can be assumed. A discrepancy due to thermal losses is expected during hot standby operation, which will be analyzed in future experiments.

3
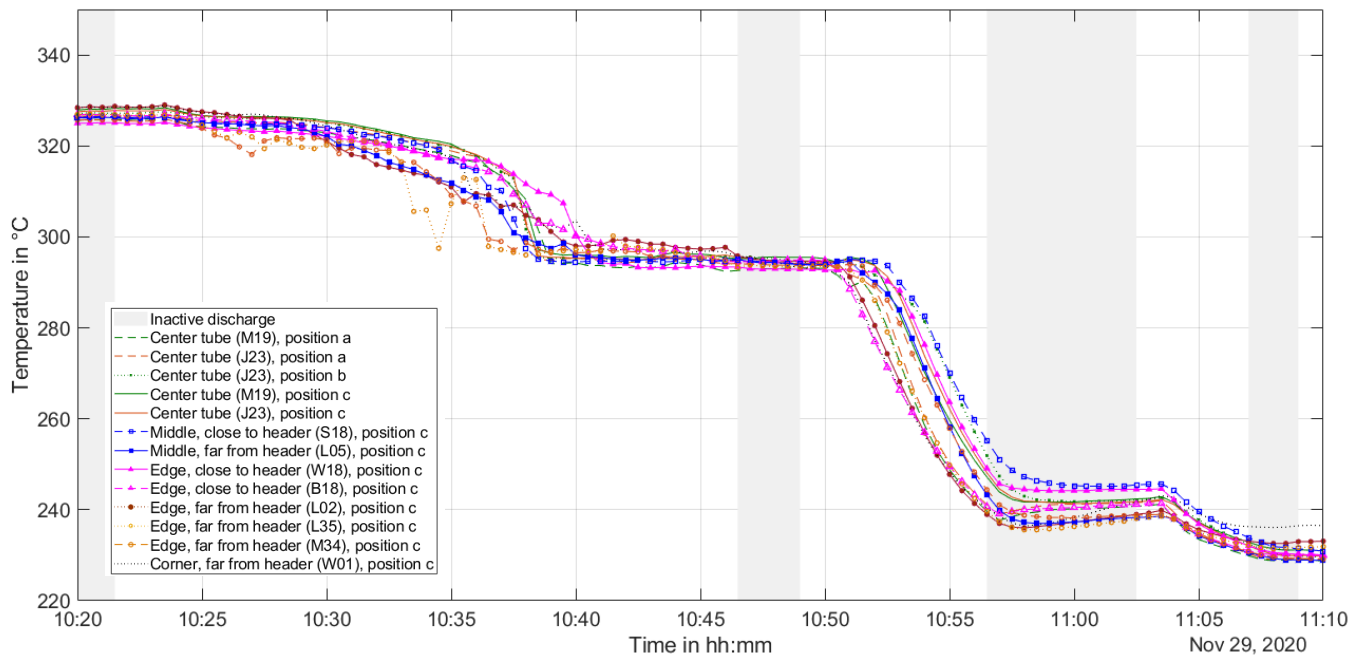
Supplementary Figure 6. Measurements at various positions in the cross-section in measurement level 4. During greyed-out times, there was no mass flow through the unit.

Supplementary References

[1] Sodium Nitrate prilled datasheet rev. 1 Cofermin

[2] Bauer T, Laing D, Tamme R. (2012) Characterization of sodium nitrate as phase change material. International Journal of Thermophysics; 33:91-104. doi: 10.1007/s10765-011-1113-9.

[3] Byrne, J., Fleming, H. and Wetmore, F. E. W. (1952) Molten salts electrical conductivity in the system silver nitrate-sodium nitrat. Canadian Journal of Chemistry. 30(12): 922-923. doi:10.1139/v52-111.

[4] Johnson, M, Vogel, J, Hempel, M, Hachmann, B, Dengel, A, (2017) Design of high temperature thermal energy storage for high power levels. Sustainable Cities and Society, 35: 758-763. doi: 10.1016/j.scs.2017.09.007

3. Discussion and relation to scientific context

The core of this thesis is the further development of the high-temperature latent heat storage technology to determine how a PCM storage can supply superheated steam at specific parameters in an operating system, thereby raising the technology readiness level from 4 to 5. Within that work, the first megawatt-scale unit was integrated in an operating industrial process, producing superheated steam in once-through operation, showing feasibility. The work encompasses the determination of design parameters, scale-up from ca. 700 kWh and 480 kW to 1500 kWh and 6000 kW thermal capacity and power, integration and permitting in an operating process and initial operation.

In other sectors, such as electrochemical batteries, some processes are very standardized and the focus is on AA or AAA batteries and how many of these, but even within this very well-developed field, the range of button or coin batteries is immense. As high temperature thermal energy storages are by all arguments at a lower technology readiness level, the integration of a thermal energy storage system first begins with the determination of relevant parameters, and from there progresses to the design, adaptation, integration, etc. The development of guidelines for the determination of relevant parameters, published in **Paper I**, will assist other researchers making the leap from the lab to the industrial environment.

The design method developed within this work, coordinated and managed by the author but created in parts by Matthias Hempel and Julian Vogel, allows for the design of a storage unit based on a number of tubes with a tube length. The tubes can have differing parameters, to simulate non-ideal flow patterns through the headers as well as thermal losses. The modeling of the full black-box unit is conducted in the Dymola© environment, so that dynamic input data can be used. The model is limited, in that experience with the pre-existing fin-design is needed as a starting block for adaptation for a new application.

In **Paper III**, a brief comparison of three fin designs is conducted. The fins from this thesis, discussed in **Papers II** and **IV**, are compared with the plate-like fin from [64], [72] and

an initial axial fin design, also discussed in [72]. Vogel and Johnson [77] deepen that comparison and include a fourth fin, discussed in [61]. The high-density fin used in this high-power storage unit is shown to have a significantly higher rate of heat transfer than the other three fins studied. Three of these are axially mounted extruded aluminum fins; one is the plate-like fin used in the storage studied in [64, 72]. Currently, more work has been done on axial fins, as they allow for more natural convection in the liquefied salt. However, the plate-like fins are advantageous in their use of material, as a thicker core around the tube is not mechanically necessary. Table 1 shows a summary of the fin design parameters discussed here, and Figure 3 compares the development of the liquid phase fraction for each of these designs, where *Organic* denotes the fin that is developed within this thesis, *Plate* studied in [64, 72], *Snowflake* in [72], and *Eco* in [61] and **Paper II**. These fins were simulated with a height of 100 mm, and two additional heights for the *Eco* fin.

Table 1: Fin design definition parameters [77].

Parameter	Organic	Plate	Snowflake	Eco
Type	Axial	Radial	Axial	Axial
Tube spacing Dt/mm	70	100	160	230
Height H/mm	100	100	100	50, 100, 200
Inner tube diameter d_i/mm	12.6	15.8	16.7	22.3
Fin fraction f_{fin}/%	17.9	8.2	14.3	9.0
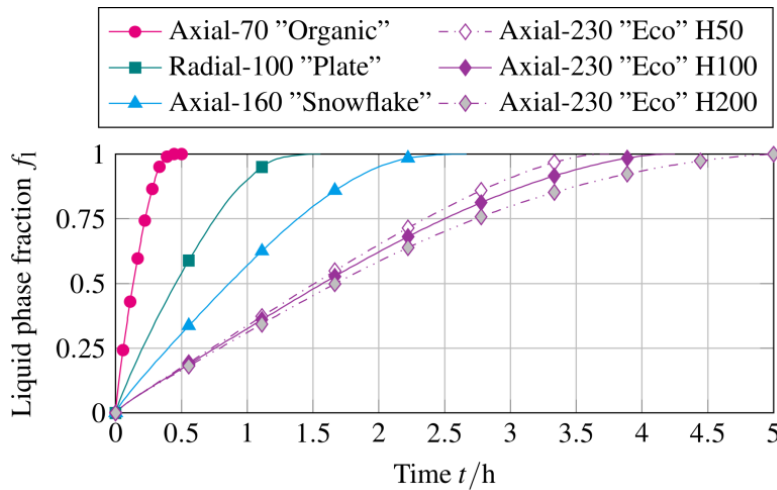
Figure 3: Liquid phase fraction plotted for each of the six parameters over time.

With the comparable parameters used in these simulations, the development of the liquid phase fraction is analogous to the rate of heat transfer. These simulations are for charging and therefore melting of the PCM. The critical portion of the charging-discharging cycle in the work discussed in this thesis and in other applications known to the author is the discharging and therefore solidification portion. However, the comparison is helpful for understanding the relationship between the various parameters fin fraction and tube spacing. Simply comparing the fin fraction and the development of the liquid phase fraction, it is clear that *Organic*, with

a fin fraction of 17.9% has the highest rate of heat transfer during charging, but *Plate*, with 8.2% has the lowest fin fraction and the second fastest increase in liquid phase fraction. The *Plate* fin has a tube spacing of 100 mm. Significantly larger tube spacings and therefore fin radii are considered mechanically challenging for a plate-like fin, as the aluminum at higher temperatures is not as hard, and the influence of gravity, likely combined with PCM movement due to natural convection, would result in an instable structure in high-temperature thermal cycling. This discussion, as well as the fin optimization work conducted by Hübner [61] and Pizzolato et al. [62], show that the design and optimization of functional, feasible and efficient heat transfer structures remains a challenging topic. Recent work by Pizzolato et al. [78] has shown that through the development of modern manufacturing methods – specifically 3-D printing – the theoretically optimized fin structures can now also be produced. Production at a large scale combined with attachment to steel tubes that can withstand higher pressures than aluminum still needs to be analyzed.

Within this thesis, a storage unit was developed for a short duration discharging (>15 minutes). As the storage unit needs to produce a minimum temperature (>300 °C), and as latent heat storage units without active PCM removal from the heat transfer surface inherently cannot produce constant heat transfer rates, this resulted in a systematic over-design. The heat transfer at the beginning of discharging is higher than necessary, resulting in a too-high temperature for the steam customer at the outlet, as shown in Figure 4 (red line slowly sinking to the minimum temperature), from **Paper III**. This temperature is then reduced through a system integration using water injection to reduce the initially too-high temperature, reducing use of water injection over the course of the discharging of the unit. This essentially means that the heat transfer surface at the beginning is too high, and the storage is too large. From the full discharging and system integration perspective, however, it is designed correctly.

This sizing could be optimized in future developments, allowing for a smaller overall system. One method for this is the cascading of storage units. This was analyzed by Michels et al. [79] in 2007, showing that the idea is not new, and was considered promising then. The concatenation of physically separated storage units requires headers and pipework at the inlet and outlet of each unit. As discussed by Hübner et al. [70], the headers result in a significant cost fraction of a storage unit, due to the number of welds necessary. A further development of the concatenation has been discussed by Mahdi et al. [80]. Here, metal foams of differing densities were stacked over the height of a storage unit, thereby altering the heat transfer enhancement over the height. Through this variation, an optimization of the size is possible.

With the topology-optimized and 3-D printable designs researched by Pizzolato et al. [78], this may also be possible in the future with a smooth transition over height.
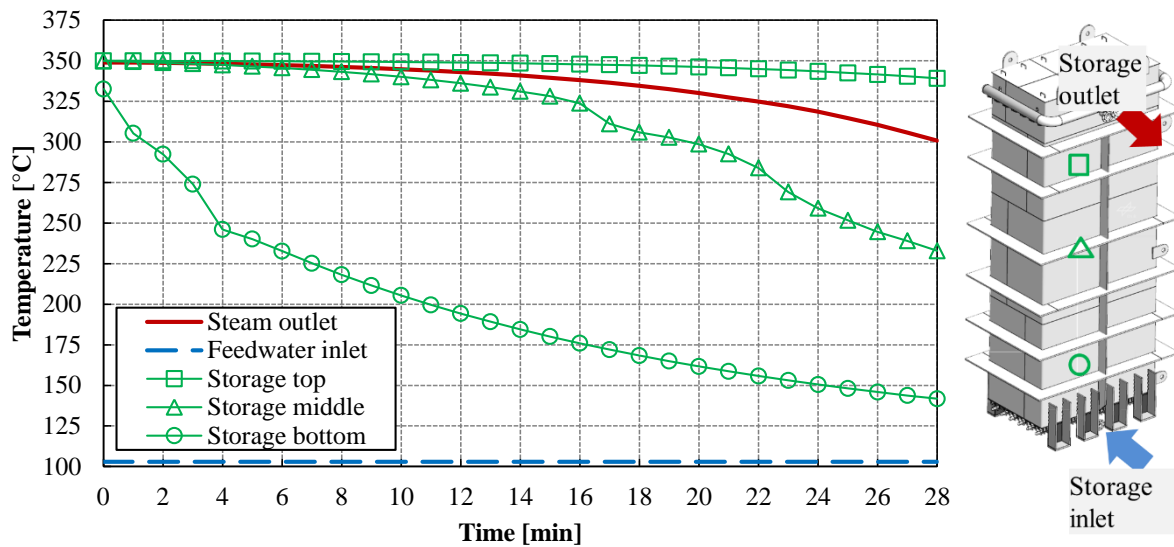

Figure 4: Simulation results during discharging of the inlet and outlet temperatures of the HTF and the temperature distribution over the height of the storage unit, with the schematic at the right showing the approximate positions in relation to the storage unit. **Paper III**

In **Paper VI**, the results from commissioning and operation of the storage unit are discussed. Here, we see the results from a discharging cycle conducted at the end of the third filling of the storage unit. At this point, it was 95% filled, containing over 30 t of sodium nitrate. This discharging occurred at close to nominal conditions, showing that the necessary high heat transfer rate close to 6 MW_{th} is possible. It discharged at nearly nominal conditions for more than 20 minutes, showing that the dimensioning is somewhat overdesigned for the application (>15 minutes), but not quite matching the design discharge of 28 minutes (shown in Figure 4). In this paper, only the discharging is discussed, as discharging has very critical parameters.

Charging is planned to occur very slowly – over 13 hours –, using a bypass to slowly increase the mass flow in the storage unit, thereby emitting superheated steam from the storage, usable in the steam mains, for a significant portion of the charging. This is discussed in **Paper III** and **Paper IV**. This method of charging is an example of the necessity of developing storage systems for real integration. In lab settings, storage systems are often cycled between a fully "charged" and "discharged" state, meaning a fully molten or solidified state. In a real integration, these parameters may be significantly shifted, as the discharged and charged states are determined by the system parameters. These aspects – parameters for performance indicators in an application – are discussed in **Paper I**.

In this case, the storage is considered "charged" when as much of the PCM nears 350 °C and is at least over 340 °C in temperature – well over the melting temperature of around 305 °C. It is considered "discharged" when the exit temperature reaches 300 °C. At this point, less than 75% of the PCM is solidified, as shown in **Paper III** and discussed in **Paper IV**.

Paper VI discusses the nominal discharging during the iterative filling process. As is clear in the paper, it only discusses one discharging. This is because the lower header was not designed correctly by the contracted company, and cracks developed. Due to corrosion issues occurring due to the unexpectedly long time the storage unit was kept at ambient temperatures; the header has not yet been rebuilt. Because of this, the charging regimen and discharging at various parameter variations have not yet been evaluated. This will be a part of future development work.

As discussed in **Paper VI**, the design goal of the storage unit is to produce superheated steam for at least 15 minutes. During discharging, steam of sufficient quality (>300 °C, >21 bar) was produced for 43 minutes. For 20 minutes, close to nominal conditions were attained with an average mass flow rate of 7.6 t/h. During this time, an average heat transfer rate of 5.46 MW$_{th}$ was discharged, resulting in an energy discharge of 1.9 MWh. The design goal was 5.72 MW$_{th}$ and 1.43 MWh; the flow rate used in this discharge was below the nominal flow rate of 8 t/h.

The core of this thesis is the development and integration of a megawatt-scale high-temperature latent heat thermal energy storage in an operating industrial process, bringing the technology from readiness level 4 to 5 [2]. The work and results are shown in parts of six papers, due to the nature of the work. Looking at the publishing dates of the papers, it becomes noticeable that the work took a long time. Due to the scale of the project, delays and unforeseen problems that have nothing to do with research occurred – permitting delays, company bankruptcies, etc. These do not need to be discussed here, but suffice it to say that this scale of project is difficult to carry out in the research environment. At the same time, experience with real environments and large-scale units is critical to the technology development. The market for such storage technologies will only develop with their availability, as an integrated energy storage unit is a puzzle piece designed to meet system parameters. Policy changes and pushes towards decarbonization make the technology more attractive, but without critical developments overcoming hurdles in upscaling, the benefits of research development are not integrable in industrial processes. It is of critical importance that policy makers understand the value of thermal energy storages for meeting decarbonization goals, and adapt policies to motivate market deployment.

4. Summary

In this thesis, the development and integration of a megawatt-scale high-temperature latent heat thermal energy storage in an operating industrial process was conducted, starting from the idea of an integration in an industrial process and the work conducted in the lab with axially mounted fins [72] and previous experience with a radially finned evaporator. The investigation at hand spans research results along the development path from the methods for determining appropriate integration parameters to the development of design methods for large-scale integrations up to the integration and initial results of a high-temperature and - power superheated-steam-producing latent heat thermal energy storage unit.

- Retrofitting a thermal energy storage system into an operating system is a six step processes, beginning with the determination of integration goals, defining the process and boundaries of the process to be analyzed, identification of energy sinks and sources within that process followed by the quantification of these, determination of overarching factors, all resulting in a set of process requirements for the storage. The method becomes somewhat more iterative for a greenfield application, as some parameters in the process, sink and source can be adjusted, allowing for more flexibility in design. In addition, with changing markets and prices, the overarching factors may in the future lead to the possibilities for hitherto uninteresting sinks or sources, such as the current development of power-to-heat as a source.

- Both the clipping and crimping methods allow for a good axial attachment of the fins to the tubes, both allowing for a good differential expansion. The crimping method, however, did not acceptably hold the fins on the tubes radially on the one-meter tubes tested here. A combination of these methods would likely result in a cost reduction, but needs to be further developed. Cycling testing showed that, once a minimal temperature of 220 °C was attained and the hardening of the aluminum was relaxed, even very low numbers of clips, as low as 9.5%, can maintain the fins on the tubes. In the storage tested,

which was built in parallel to this testing due to time constraints, 50% of the tube length had clips; a reduction in future storage units is possible.

- A method for the thermal design of latent heat storage units was developed, and is comprised of several steps: a 2-dimensional heat transfer analysis of the cross-section of one tube without modeling the heat transfer fluid using Ansys Fluent, a transfer from the cross-section to a simplified one-dimensional radial model using Dymola and effective material properties, followed by a two-dimensional axial and radial analysis coupling the axial flow of the heat transfer fluid and the radial heat transfer into the storage, also using Dymola. This method allows for a dynamic application of the input parameters, and through coupling of smaller storage units, can also simulate uneven flow rates through the headers or thermal losses at exterior tubes.

- Using the parameter determination and design method, a storage unit using sodium nitrate was thermally designed and a fin design iteratively determined. The fin design derives from a combination of empirical knowledge on the manufacturing side and thermodynamic simulations and experience on the design side. With this fin, having a 70 mm side-to-side hexagonal form for a good packing density in and with manufacturability of the storage, and a basic length of 5.6 m for transportability on standard roads and trucks, a storage unit consisting of 852 finned-tubes was designed. This allows for at least the minimal 15 minutes of steam production with a temperature of at least 300 °C and at a pressure of 25 bar. The system integration allows for discharging using feedwater from preexisting feedwater pumps and container, with a water injection allowing for temperature control after the storage outlet. According to the design, discharging should last about 28 minutes.

- At the end of discharging, the exit temperature is 300 °C. Approximately 27% of the storage material remains liquid throughout the charging and discharging cycles, providing energy for the sensible superheating of the steam. The storage material at the bottom of the storage unit, on the other hand, is discharged to approximately 132 °C.

- The storage is charged using steam directly from the heat recovery steam generator and a three-way-valve-controlled bypass method. With this method, the exit flow from the storage system is condensate that is rejected from the system for less than two minutes. Once steam exits the system allowing for a temperature of 300 °C after mixing with the main flow, the flow rate is steadily increased until the full flow goes through the storage unit and the storage material is heated to above 340 °C at all thermocouples, after about 800 minutes. This allows for an integration in a setting that cannot make use of

condensate, providing a sensible charging over a period of about 13.3 hours but emitting usable superheated steam for the majority of this time period.

- The storage unit has approximate dimensions of 1.67x2.38x6.72 meters without thermal insulation and contains about 32 tons of sodium nitrate. The upper header design allows for maximum possible spacing between headers by stacking sub-header levels. This aspect allows for the initial filling of the storage unit with the sodium nitrate inventory.

- Semi-automatic assembly of fins and tubes can be further automated in future systems, allowing for time and cost reductions. This semi-automation shows this possibility, and as such allowed for a consistent quality of attachment between the more than 4.7 km of fins and tubes within this storage unit.

- The system integration includes a storage unit foundation with a catchment basin below the storage unit large enough for the full inventory of sodium nitrate in the case of a leakage.

- During commissioning, the storage unit discharged at a mass flow rate of 7.6 t/h, at least 25 bar and 300 °C for more than 20 minutes. This production of superheated steam for an operating system was at a heat transfer rate of 5.46 MW and discharged 1.9 MWh from the storage unit.

 The author is convinced that the data from this system is extremely important for the research community due to the scale of the storage unit as well as the real operating characteristics. The goal of integrating thermal energy storages into industrial processes has been brought a significant step closer by having a first high-temperature latent heat storage unit in an operating process. Future work includes the full analysis and testing of the storage system, development of modular and cost-effective designs as a product for a manufacturer, development of power-to-heat integration for a higher degree of decarbonization, analysis of the benefits of changing the heat exchanger surface over the height of the storage and the development of a dual-tube heat exchanger system, allowing for independent charging and discharging parameters.

References

[1] Presse- und Informationsamt der Bundesregierung, "Climate Change Act 2021," 25 06 2021. [Online]. Available: https://www.bundesregierung.de/breg-de/themen/klimaschutz/climate-change-act-2021-1936846. [Accessed 06 05 2023].

[2] European Commission, "EN Horizon 2020 Work Programme 2016-2017 20. General Annexes, p. 29," 24 04 2017. [Online]. Available: https://ec.europa.eu/research/participants/data/ref/h2020/other/wp/2016-2017/annexes/h2020-wp1617-annex-ga_en.pdf. [Accessed 30 05 2023].

[3] T. Nägler, S. Simon, M. Klein and H. C. Gils, "Quantification of the European industrial heat demand by branch and temperature level," *International Journal of Energy Research,* vol. 39, no. 15, pp. 2019-2030, 2015. doi:10.1002/er.3436.

[4] M. Rehfeldt, T. Fleiter and F. Toro, "A bottom-up estimation of the heating and cooling demand in European industry," *Energy Efficiency,* vol. 11, pp. 1057-1082, 2017. doi:10.1007/s12053-017-9571-y.

[5] T. Fleiter, R. Elsland, M. Rehfeldt, J. Steinbach, U. Reiter, G. Catenazzi, M. Jakob, C. Rutten, R. Harmsen, F. Dittmann, P. Riviére and P. Stabat, "Heat Roadmap Europe: Profile of heating and cooling demand in 2015," Horizon 2020 No. 695989, 2017. https://heatroadmap.eu/wp-content/uploads/2018/11/HRE4_D3.1.pdf.

[6] DMT, "Ministry of Economic Affairs, Industry, Climate Action and Energy of the State of North Rhine-Westphalia," 06 2020. [Online]. Available: https://www.wirtschaft.nrw/sites/default/files/documents/2020-06-0029877.pdf. [Accessed 09 08 2023].

[7] T. Tawitpat, „Analyse des Einsatzes eines Latentwärmespeichers in einem Heizkraftwerk," 2022.

[8] H. Mehling and L. F. Cabeza, Heat and cold storage with PCM, Heidelberg: Springer Verlag Berlin, 2008.

[9] W.-D. Steinmann, Thermal Energy Storage for Medium and High Temperatures: Concepts and Applications, Wiesbaden: Springer Fachmedien, 2022.

[10] M. Krüger, S. Muslabas, T. Loeper, F. Klasing, P. Knödler and C. Mielke, "Potentials of Thermal Energy Storage Integrated into Steam Power Plants," *Energies,* vol. 13, p. 2226, 2020. doi:10.3390/en13092226.

[11] T. Bauer, C. Odenthal and A. Bonk, "Molten Salt Storage for Power Generation," *Chemie Ingenieur Technik,* vol. 93, no. 4, pp. 534-546, 11 02 2021. doi:10.1002/cite.202000137.

[12] V. A. Sötz, A. Bonk and T. Bauer, "With a view to elevated operating temperatures in thermal energy storage - Reaction chemistry of Solar Salt up to 630°C," *Solar Energy Materials and Solar Cells,* vol. 212, p. 110577, 2020. doi:10.1016/j.solmat.2020.110577.

[13] V. A. Sötz, A. Bonk, J. Steinbrecher and T. Bauer, "Defined purge gas composition stabilizes molten nitrate salt - Experimental prove and thermodynamic calculations," *Solar Energy,* vol. 211, p. 453 – 462, 2020. doi:10.1016/j.solener.2020.09.041.

[14] V. M. Nunes, M. J. Laurenco, F. J. Santos and C. A. Nieto de Castro, "Molten alkali carbonates as alternative engineering fluids for high temperature applications," *Applied Energy,* vol. 242, pp. 1626-1633, 2019. doi:10.1016/j.apenergy.2019.03.190.

References

[15] Y. Zhao and J. Vidal, "Potential scalability of a cost-effective purification method for MgCl2-Containing salts for next-generation concentrating solar power technologies," *Solar Energy Materials and Solar Cells,* vol. 215, p. 110663, 2020. doi:10.1016/j.solmat.2020.110663.

[16] C. Odenthal, F. Klasing, P. Knödler, S. Zunft and T. Bauer, "Experimental and numerical investigation of a 4 MWh high temperature molten salt thermocline storage system with filler," *AIP Conference Proceedings,* vol. 2303, p. 190025, 2020. doi:10.1063/5.0028494.

[17] W. Lou, L. Luo, Y. Hua, Y. Fan and Z. Du, "A Review on the Performance Indicators and Influencing Factors for the Thermocline Thermal Energy Storage Systems," *Energies,* vol. 14, no. 24, 2021. doi:10.3390/en14248384.

[18] M. Krüger, J. Haunstetter, J. Hahn, P. Knödler and S. Zunft, "Development of Steelmaking Slag Based Solid Media Heat Storage for Solar Power Tower Using Air as Heat Transfer Fluid: The Results of the Project REslag," *Energies,* vol. 13, no. 22, 2020. doi:10.3390/en13226092.

[19] S. Belik, O. Khater and S. Zunft, "Induction Heating of a Fluidized Pebble Bed: Numerical and Experimental Analysis," *Applied Sciences,* vol. 13, no. 4, 2023. doi:10.3390/app13042311.

[20] A. Paul, F. Holy, M. Textor and S. Lechner, "High temperature sensible thermal energy storage as a crucial element of Carnot Batteries: Overall classification and technical review based on parameters and key figures," *Journal of Energy Storage,* vol. 56, p. 106015, 2022. doi:10.1016/j.est.2022.106015.

[21] H. Mehling, M. Brütting and T. Haussmann, "PCM products and their fields of application - An overview of the state in 2020/2021," *Journal of Energy Storage,* vol. 51, p. 104354, 2022. doi:10.1016/j.est.2022.104354.

[22] K. Du, J. Calauti, Z. Wang, Y. Wu and H. Liu, "A review of the applications of phase change materials in cooling, heating and power generation in different temperature ranges," *Applied Energy,* vol. 220, pp. 242-273, 2018. doi:10.1016/j.apenergy.2018.03.005.

[23] M. Linder, "Gas-Solid Reactions for Energy Storage and Conversion," Stuttgart, 2022. url: https://elib.dlr.de/192363/.

[24] H. Nazir, M. Batool, F. J. Bolivar Osorio, M. Isaza-Ruiz, X. Xu, K. Vignarooban, P. Phelan, Inamuddin and A. M. Kannan, "Recent developments in phase change materials for energy storage applications: A review," *International Journal of Heat and Mass Transfer,* vol. 129, pp. 491-523, 2019. doi:10.1016/j.ijheatmasstransfer.2018.09.126.

[25] T. Bauer, R. Tamme and D. Laing, "Overview of PCMs for Concentrated Solar Power in the Temperature Range 200 to 350°C," *Advances in Science and Technology,* vol. 74, pp. 272-277, 01 2011. doi:10.4028/www.scientific.net/AST.74.272.

[26] T. Bauer, D. Laing and R. Tamme, "Characterization of sodium nitrate as phase change material," *International Journal of Thermophysics,* vol. 33, no. 1, pp. 91-104, 2012. doi:10.1007/s10765-011-1113-9.

[27] Y. B. Tao and Y.-L. He, "A review of phase change material and performance enhancement method for latent heat storage system," *Renewable and Sustainable Energy Reviews,* vol. 93, pp. 245-259, 2018. doi:10.1016/j.rser.2018.05.028.

[28] R. Elarem, T. Alqahtani, S. Mellouli, F. Askri, A. Edacherian, T. Vineet, I. A. Badruddin and J. Abdelmajid, "A comprehensive review of heat transfer intensification methods for latent heat storage units," *Energy Storage,* vol. 3, no. 1, p. e127, 2021. doi:10.1002/est2.127.

[29] A. Sharma, V. V. Tyagi, C. Chen and D. Buddhi, "Review on thermal energy storage with phase change materials and applications," *Renewable and Sustainable Energy Reviews,* vol. 13, no. 2, pp. 318-345, 2009. doi:10.1016/j.rser.2007.10.005.

[30] X. Huang, C. Zhu, Y. Lin and G. Fang, "Thermal properties and applications of microencapsulated PCM for thermal energy storage: A review," *Applied Thermal Engineering,* vol. 147, pp. 841-855, 2019. doi:10.1016/j.applthermaleng.2018.11.007.

[31] J. Giro-Paloma, M. Martínez, L. F. Cabeza and A. I. Fernández, "Types, methods, techniques, and applications for microencapsulated phase change materials (MPCM): A review," *Renewable and Sustainable Energy Reviews,* vol. 53, pp. 1059-1075, 2016. doi:10.1016/j.rser.2015.09.040.

[32] M. A. Kibria, M. R. Anisur, M. Mahfuz, R. Saidur and I. H. S. C. Metselaar, "A review on thermophysical properties of nanoparticle dispersed phase change materials," *Energy Conversion and Management,* vol. 95, pp. 69-89, 2015. doi:10.1016/j.enconman.2015.02.028.

[33] S. L. Tariq, H. M. Ali, M. A. Akram, M. M. Janjua and M. Ahmadlouydarab, "Nanoparticles enhanced phase change materials (NePCMs)-A recent review," *Applied Thermal Engineering,* vol. 176, p. 115305, 2020. doi:10.1016/j.applthermaleng.2020.115305.

[34] Y. Jiang, M. Liu and Y. Sun, "Review on the development of high temperature phase change material composites for solar thermal energy storage," *Solar Energy Materials and Solar Cells,* vol. 203, p. 110164, 2019. doi: 10.1016/j.solmat.2019.110164.

[35] W.-D. Steinmann, D. Laing and R. Tamme, "Latent heat storage systems for solar thermal power plants and process heat applications," *Journal of Solar Energy Engineering,* vol. 132, no. 2, pp. 0210031-0210035, 2010. doi:10.1115/1.4001405.

[36] H. Zondag, G. Herder, M. van der Pal, S. Smeding, G. Elzinga and R. de Boer, "Development of an Industrial Heat Storage Using High-Temperature PCM-Graphite Composites," *Atlantis Press,* 2021. doi:10.2991/ahe.k.210202.015.

[37] H. Pointner and W.-D. Steinmann, "Experimental demonstration of an active latent heat storage concept," *Applied Energy,* vol. 168, pp. 661-671, 2016. doi:10.1016/j.apenergy.2016.01.113.

[38] J. Tombrink, H. Jockenhofer and D. Bauer, "Experimental investigation of a rotating drum heat exchanger for latent heat storage," *Applied Thermal Engineering,* vol. 183, p. 116221, 2021. doi:10.1016/j.applthermaleng.2020.116221.

[39] N. Maruoka, T. Tsutsumi, A. Ito, M. Hayasaka and H. Nogami, "Heat release characteristics of a latent heat storage heat exchanger by scraping the solidified phase change material layer," *Energy,* vol. 205, p. 118055, 2020. doi:10.1016/j.energy.2020.118055.

[40] A. Egea, A. García, R. Herrero-Martín and J. Pérez-García, "Preliminary thermal characterisation of an active latent thermal energy storage system using PCM," *Journal of Physics: Conference Series,* vol. 2116, no. 1, p. 012045, 2021. doi:10.1088/1742-6596/2116/1/012045.

[41] U. Nepustil, D. Laing-Nepustil, D. Lodemann, S. Rameesh and V. Hausmann, "High Temperature Latent Heat Storage with Direct Electrical Charging – Second Generation Design," *Energy Procedia,* vol. 99, pp. 314-320, 2016. doi:10.1016/j.egypro.2016.10.121.

[42] V. Zipf, D. Willert and A. Neuhäuser, "Active latent heat storage with a screw heat exchanger – experimental results for heat transfer and concept for high pressure steam," *AIP Conference Proceedings,* vol. 1734, no. 1, p. 050044, 2016. doi:10.1063/1.4949142.

[43] J. Alario, R. Kosson and R. Haslett, "Active heat exchange system development for latent heat thermal energy storage," DOE/NASA, Bethpage, NY, 1980. Report Nr. 0039-79/1.

[44] S. Höhlein, A. König-Haagen and D. Brüggemann, "Macro-encapsulation of inorganic phase-change materials (PCM) in metal capsules," *Materials,* vol. 11, no. 9, 2018. doi:10.3390/ma11091752.

References

[45] A. Raul, M. Jain, S. Gaikwad and S. K. Saha, "Modelling and experimental study of latent heat thermal energy storage with encapsulated PCMs for solar thermal applications," *Applied Therman Engineering,* vol. 143, pp. 415-428, 2018. doi: 10.1016/j.applthermaleng.2018.07.123.

[46] Z. Liu, Z. (. Yu, T. Yang, D. Qin, S. Li, G. Zhang, F. Haghighat and M. M. Joybari, "A review on macro-encapsulated phase change material for building envelope applications," *Building and Environment,* vol. 144, pp. 281-294, 2018. doi:10.1016/j.buildenv.2018.08.030.

[47] J. Lei, Y. Tian, D. Zhou, W. Ye, Y. Huang and Y. Zhang, "Heat transfer enhancement in latent heat thermal energy storage using copper foams with varying porosity," *Solar Energy,* vol. 221, pp. 75-86, 2012. doi:10.1016/j.solener.2021.04.013.

[48] M. Martinelli, F. Bentvoglio, A. Caron-Soupart, R. Couturier, J.-F. Formigue and P. Marty, "Experimental study of a phase change thermal energy storage with copper foam," *Applied Thermal Engineering,* vol. 101, no. Supplement C, pp. 247-261, 2016. doi:10.1016/j.applthermaleng.2016.02.095.

[49] T. Klemm, A. Hassabou, A. Abdallah and O. Andersen, "Thermal energy storage with phase change materials to increase the efficiency of solar photovoltaic modules," *Energy Procedia,* vol. 135, pp. 193-202, 2017. doi:10.1016/j.egypro.2017.09.502.

[50] A. Schlott, J. Hörstmann, K. Tittes, O. Andersen and J. Meinert, "High power latent heat storages with 3D wire structures – numerical evaluation of phase change behavior," *Energy Procedia,* vol. 135, pp. 75-81, 2017. doi:10.1016/j.egypro.2017.09.488.

[51] J. Gasia, J. M. Maldonado, F. Galati, M. de Simone and L. F. Cabeza, "Experimental evaluation of the use of fins and metal wool as heat transfer enhancement techniques in a latent heat thermal energy storage system," *Energy Conversion and Management,* vol. 184, pp. 530-538, 2019. doi:10.1016/j.enconman.2019.01.085.

[52] C. Prieto, C. Rubio and L. F. Cabeza, "New phase change material storage concept including metal wool as heat transfer enhancement method for solar heat use in industry," *Journal of Energy Storage,* vol. 33, p. 101926, 2021. doi:10.1016/j.est.2020.101926.

[53] M. Johnson, M. Fiss and T. Klemm, "Experimental testing of various heat transfer structures in a flat plate thermal energy storage unit," *AIP Conference Proceedings,* vol. 1734, no. 1, p. 050022, 2016. doi:10.1063/1.4949120.

[54] G. Diarce, Á. Campos-Celador, J. M. Sala and A. García-Romero, "A novel correlation for the direct determination of the discharging time of plate-based latent heat thermal energy storage systems," *Applied Thermal Engineering,* vol. 129, pp. 521-534, 2018. doi:10.1016/j.applthermaleng.2017.10.057.

[55] M. Liu, M. Belusko, N. Steven Tay and F. Bruno, "Impact of the heat transfer fluid in a flat plate phase change thermal storage unit for concentrated solar tower plants," *Solar Energy,* vol. 101, pp. 220-231, 2014. doi:10.1016/j.solener.2013.12.030.

[56] N. S. Dhaidan and J. M. Khodadadi, "Improved performance of latent heat energy storage systems utilizing high thermal conductivity fins: A review," *Journal of Renewable and Sustainable Energy,* vol. 9, no. 3, 2017. doi:10.1063/1.4989738.

[57] N. I. Ibrahim, F. A. Al-Sulaiman, S. Rahman, B. S. Yilbas and A. Z. Sahin, "Heat transfer enhancement of phase change materials for thermal energy storage applications: A critical review," *Renewable and Sustainable Energy Reviews,* vol. 74, pp. 26-50, 2017. doi:10.1016/j.rser.2017.01.169.

[58] Y. Lin, Y. Jia, G. Alva and G. Fang, "Review on thermal conductivity enhancement, thermal properties and applications of phase change materials in thermal energy storage," *Renewable and Sustainable Energy Reviews,* vol. 82, pp. 2730-2742, 2018. doi:10.1016/j.rser.2017.10.002.

[59] Q. Li, C. Li, Z. Du, F. Jiang and Y. Ding, "A review of performance investigation and enhancement of shell and tube thermal energy storage device containing molten salt based phase change materials for medium and high temperature applications," *Applied Energy,* vol. 255, p. 113806, 2019. doi:10.1016/j.apenergy.2019.113806.

[60] M. Eslami, F. Khosravi and H. R. Fallah Kohan, "Effects of fin parameters on performance of latent heat thermal energy storage systems: A comprehensive review," *Sustainable Energy Technologies and Assessments,* vol. 47, p. 101449, 2021. doi:10.1016/j.seta.2021.101449.

[61] S. Hübner, "Techno-ökonomische Optimierung eines Hochtemperatur-Latentwärmespeichers," Stuttgart, 2018.

[62] A. Pizzolato, A. Sharma, K. Maute, A. Sciacovelli and V. Verda, "Topology optimization for heat transfer enhancement in Latent Heat Thermal Energy Storage," *International Journal of Heat and Mass Transfer,* vol. 113, no. Supplement C, pp. 875-888, 2017. doi:10.1016/j.ijheatmasstransfer.2017.05.098.

[63] P. Garcia, G. Largiller, G. Matringe, L. Champelovier and S. Rougé, "Experimental results from a pilot scale latent heat thermal energy storage for DSG power plants – Advanced operating strategies," *AIP Conference Proceedings,* vol. 2445, p. 160008, 2022. doi:10.1063/5.0085753.

[64] D. Laing, T. Bauer, W.-D. Steinmann and D. Lehmann, "Advanced high temperature latent heat storage system - design and test results," in *11th International Conference on Thermal Energy Storage - Effstock*, Stockholm, Sweden, 2009.

[65] Wold Material, "Aluminium 6060 T5, T6, T4; Aluminum Alloy 6060 Properties," 15 06 2022. [Online]. Available: https://www.theworldmaterial.com/aluminum-6060/. [Accessed 25 05 2023].

[66] SteelGr - China steel suppliers, "China steel suppliers - Superior technology, Advanced equipment, Perfect procedure!," [Online]. Available: https://www.steelgr.com/Steel-Grades/High-Alloy/16mo3.html. [Accessed 23 05 2023].

[67] G. Urschitz, H. Walter and J. Brier, "Experimental investigation on bimetallic tube compositions for the use in latent heat thermal energy storage units," *Energy Conversion and Management,* vol. 125, pp. 368-378, 2016. doi:10.1016/j.enconman.2016.05.054.

[68] T. Bauer and B. Hachmann, "Heat Transfer Tube". world Patent WO2011069693A1, 16 06 2011.

[69] M. Fiß and M. Johnson, "Wärmeübertragungsrohranordnung sowie Wärmespeicher mit einer solchen". Germany Patent DE 10 2017 114 141 A1, 27 12 2018.

[70] S. Hübner, M. Eck, C. Stiller and M. Seitz, "Techno-economic heat transfer optimization of large scale latent heat energy storage systems in solar thermal power plants," *Applied Thermal Engineering,* vol. 98, pp. 483-491, 2016. doi:10.1016/j.applthermaleng.2015.11.026.

[71] D. Laing, T. Bauer, D. Lehmann and C. Bahl, "Development of a thermal energy storage system for parabolic trough power plants with direct steam generation," *Journal of Solar Energy Engineering, Transactions of the ASME,* vol. 132, no. 2, pp. 0210111-0210118, 2010. doi:10.1115/1.4001472.

[72] D. Laing, T. Bauer, N. Breidenbach, B. Hachmann and M. Johnson, "Development of high temperature phase-change-material storages," *Applied Energy,* vol. 109, pp. 497-504, 2013. doi:10.1016/j.apenergy.2012.11.063.

[73] V. Vuillerme, P. Garcia, P. Aubouin, A. Camus, E. Carnacina, M. Manzoni and E. Bregeard, "Experimental results of 2018 test campaign of the ALSOLEN 450 prototype for direct steam

References

generation and thermal storage," *AIP Conference Proceedings,* vol. 2303, no. 1, 2020. doi:10.1063/5.0028743.

[74] M. Johnson, A. Dengel, R. Hetzel, B. Hachmann, D. Bauer, M. Fiss, M. Hempel, R. Ortwein, M. Seitz and J. Vogel, "TESIN: Projektabschlussbericht," BMWK FKZ 03ESP011A/B/C, 2022. doi:10.2314/KXP:1820008215.

[75] NISO, "Contributor Roles Taxonomy," 2023. [Online]. Available: https://credit.niso.org/. [Accessed 20 04 2023].

[76] M. Johnson and L. Reinholdt, "IEA-ES," 02 05 2018. [Online]. Available: https://iea-es.org/wp-content/uploads/public/20180502_ProcessAnalysisGuidelines.pdf. [Accessed 05 05 2023].

[77] J. Vogel and M. Johnson, "Natural convection during melting in vertical finned tube latent thermal energy storage systems," *Applied Energy,* vol. 246, pp. 38-52, 2019. doi:10.1016/j.apenergy.2019.04.011.

[78] A. Pizzolato, A. Sharma, R. Ge, K. Maute, V. Verda and A. Sciacovelli, "Maximization of performance in multi-tube latent heat storage – Optimization of fins topology, effect of materials selection and flow arrangements," *Energy,* vol. 203, p. 114797, 10.1016/j.energy.2019.02.1552020. doi:.

[79] H. Michels and R. Pitz-Paal, "Cascaded latent heat storage for parabolic trough solar power plants," *Solar Energy,* vol. 81, no. 6, pp. 829-837, 2007. doi:10.1016/j.solener.2006.09.008.

[80] J. M. Mahdi and E. C. Nsofor, "Multiple-segment metal foam application in the shell-and-tube PCM thermal energy storage system," *Journal of Energy Storage,* vol. 20, pp. 529-541, 2018. doi:10.1016/j.est.2018.09.021.